

THESIS

DEVELOPMENT OF BIOPOLY[®] MATERIALS FOR USE IN
PROSTHETIC HEART VALVE REPLACEMENTS

Submitted by

Harold Dean IV

Department of Mechanical Engineering

In partial fulfillment of the requirements

For the Degree of Master of Science

Colorado State University

Fort Collins, Colorado

Spring 2012

Master's Committee:

Advisor: Sue James

Prasad Dasi

Chis Orton

ABSTRACT

DEVELOPMENT OF BIOPOLY[®] MATERIALS FOR USE IN PROSTHETIC HEART VALVE REPLACEMENTS

Since their conception in the 1950s, prosthetic heart valves (HV) have suffered clinical complications. Mechanical HVs, made from synthetic materials and with unnatural hemodynamics, are prone to thrombus formation without anti-coagulation therapy. Bioprosthetic HVs, made from fixed natural tissues, do not generally elicit thrombogenicity, but require long-term antiplatelet therapy and have a shorter lifespan due to calcification and tearing. Polymeric and fabric leaflet HVs potentially have the durability of a mechanical HV with the natural hemodynamics of a bioprosthetic valve; however, previous polymeric leaflet HVs did have problems with thrombus formation and calcification and very little research has been done on fabric leaflet HVs. This research aimed to explore the possibility to improve the hemocompatibility and long term *in vivo* performance of polymeric and fabric HV leaflets by improving polymer surface chemistry. The overall goal of the current project was to develop BioPoly materials for cardiovascular applications.

The percent crystallinity, mechanical properties (i.e. tensile and bending), surface contact angle and hemocompatibility with whole blood of hyaluronan (HA) treated linear low density polyethylene (LLDPE) film and polyethylene terephthalate (PET) fabric were compared to untreated LLDPE film and PET fabric.

Both processes were successful in incorporating HA into the base polymer structures. The swelling method used with the LLDPE allowed for HA concentrations ranging from 0.5% to 1.5%. The open weave of the PET fabric resulted in more controllable HA integration with a range from 0.25% to 3.5% HA. The process used to integrate HA maintained original tensile and bending properties and reduced surface water contact angle compared to LLDPE controls ($86.7\pm 2.3^\circ$ to $39.0\pm 1.1^\circ$). Increasing HA content did not further reduce contact angle when the additional surface dip was utilized. Whole blood clotting was significantly less on the HA-treated materials than the control LLDPE and PET, with clotting becoming negligible at the higher HA concentrations, as confirmed by free hemoglobin and scanning electron microscopy (SEM). The reduction of contact angle in the HA-treated LLDPE indicates the hydrophilic nature of the composite which resulted in better anti-thrombogenic properties.

ACKNOWLEDGEMENTS

I would like to first thank my advisor, mentor and friend, Dr. Susan James, for her guidance support and friendship since my first experience with her as an undergraduate looking for some direction. Without her encouragement, insight and belief in my abilities, I would not have been able to overcome the technical obstacles encountered during my graduate program. Special thanks are owed to the other members of my committee: Dr. Prasad Dasi and Dr. Chris Orton. Their assistance and expertise in both the mechanical and biological aspects of the heart have been invaluable in helping me shape the research. The research presented in this thesis would not have been completed without the help and knowledge from various professional mentors: Mr. John Heaton (Flex-Pak Engineering); Dr. Herb Schwartz and Dr. Janine Campbell (Schwartz Biomedical); Dr. Ketul Papat, Dr. Pat McCurdy, and Dr. Don Heyse (CSU); and the financial support of the Colorado Bioscience Discovery Evaluation Grant Program.

The following individuals motivated my research and without them I would not have accomplished as much as I did; I am very thankful for all of their effort, support and friendship: Dr. David Prawel, Dr. Susan Yonemura, Jason Marini, Trey Rodgers, Hannah Hudson, Tom Triffo, and everyone else from the James Lab and OBRL. Happy hours after (and sometimes during) lab meetings, team building activities at New Belgium, playing with liquid nitrogen, countless energy drinks, my bike, the music of Anchor Point, and home brewing also are owed a special thanks in keeping me going through this adventure.

Immense thanks to my family and friends for their tireless support despite the late nights and long hours. None of this would have been possible without their help and understanding. Last, but certainly not least, I want to thank my wife, best friend, and inspiration, Jessica Dean, who has been patiently waiting for me as I pursued my academic goals. Thank you for holding me together during the most stressful times and for keeping me grounded. Without you I would not have made it as far as I did.

TABLE OF CONTENTS

CHAPTER 1: INTRODUCTION AND OVERVIEW

1.1	Motivation for Research.....	1
1.2	Literature Review.....	2
1.2.1	The Heart & Valve Disorders.....	2
1.2.1.1	Clotting Kinetics.....	4
1.2.2	Commercially Available Valve Prosthetics.....	5
1.2.2.1	Mechanical Valves.....	6
1.2.2.2	Bioprosthetic Valves.....	8
1.2.2.3	Polymeric Valves.....	10
1.2.2.4	Fabric Valves.....	12
1.2.3	Hyaluronan and Its Biomedical Applications.....	12
1.2.3.1	Hyaluronan and Its Derivatives.....	12
1.2.3.2	Biocompatible and Lubricious Coatings.....	14
1.2.3.3	Chemical Modifications of Hyaluronan.....	15
1.2.3.4	Crosslinking.....	15
1.2.4	BioPoly®	16
1.3	Thesis Objectives and Overview.....	18
1.4	References.....	20

**CHAPTER 2: SWELLING OF BASE POLYMERS: LINEAR LOW DENSITY
POLYETHYLENE BLOWN FILM AND POLYETHYLENE TEREPHTALATE
MEDICAL FABRIC**

2.1	Introduction.....	25
2.2	Materials and Methods.....	25
2.2.1	Materials.....	25
2.2.1.1	Linear Low Density Polyethylene.....	25
2.2.1.2	Polyethylene Terephtalate Fabric.....	26
2.2.1.3	Solvent.....	27
2.2.2	Measurement of Degree of Swelling.....	27
2.2.2.1	Swelling Apparatus.....	27
2.2.2.2	Measurement Method.....	28
2.2.2.3	Temperature Variation.....	29
2.2.2.4	Calculations.....	29
2.2.3	Effect of Solvent Swelling on Mechanical Properties.....	30
2.2.4	Statistics.....	31
2.3	Results and Discussion.....	31
2.3.1	Degree of Swelling.....	31
2.3.2	Swelling Kinetics.....	37
2.3.3	Effect of Solvent Swelling on Mechanical Properties.....	37
2.4	Conclusions.....	42
2.5	References.....	44

**CHAPTER 3: SYNTHESIS AND CHARACTERIZATION OF THE
HYALURONAN TREATED MATERIALS**

3.1	Introduction.....	45
3.2	Materials and Methods.	45
3.2.1	Materials.....	45
3.2.1.1	Synthesis of HA-CTA and silyl-HA-CTA.....	46
3.2.2	Synthesis of the HA-treated materials.....	47
3.2.2.1	Swelling silyl-HA-CTA into base polymers.....	47
3.2.2.2	Crosslinking of the silyl-HA-CTA <i>in situ</i>	49
3.2.2.3	Conditioning/Hydrolysis.....	49
3.2.3	Characterization of the HA-treated materials.....	50
3.2.3.1	Thermal Analysis.....	50
3.2.3.2	Mechanical Evaluation.....	51
3.2.4	Statistics.....	53
3.3	Results and Discussion.....	53
3.3.1	Sample Synthesis.....	53
3.3.2	Characterization of the HA-treated materials.....	54
3.3.2.1	Thermal Analysis.....	54
3.3.2.2	Mechanical Evaluation.....	59
3.4	Conclusions.....	64
3.5	References.....	66

**CHAPTER 4: EVALUATION OF THE HA-TREATED MATERIAL
BIOCOMPATIBILITIES**

4.1	Introduction.....	67
4.2	Materials and Methods.....	68
4.2.1	Materials.....	68
4.2.2	Surface Contact Angle.....	69
4.2.3	Toluidine Blue O (TBO).....	70
4.2.4	<i>In Vitro</i> Study.....	70
	4.2.4.1 Biocompatibility of LLDPE-HA and PET-HA Materials.....	70
	4.2.4.2 Scanning Electron Microscopy (SEM).....	71
4.3	Results and Discussion.....	72
4.3.1	Surface Contact Angle.....	72
4.3.2	Toluidine Blue O (TBO).....	76
4.3.3	<i>In Vitro</i> Study.....	77
	4.3.3.1 Biocompatibility of LLDPE-HA and PET-HA Materials.....	77
	4.3.3.2 Scanning Electron Microscopy (SEM).....	83
4.4	Conclusions.....	90
4.5	References.....	92

CHAPTER 5: RESEARCH SUMMARY AND FUTURE WORK

5.1	Research Summary.....	93
5.2	Future Work.....	94
5.2.1	Synthesis of HA-Treated Materials.....	94
5.2.2	HA-Treated Material Characterization.....	95
5.2.3	Valve Design and Manufacture.....	96
5.2.4	<i>In Vitro</i> Testing.....	96
	5.2.4.1 Dynamic Hemocompatibility.....	96
	5.2.4.2 Valve Characterization.....	97
5.2.5	<i>In Vivo</i> Study.....	98
5.3	References.....	99
	APPENDIXES.....	100

CHAPTER 1: INTRODUCTION AND OVERVIEW

1.1 Motivation for Research

Heart valve replacements (HVRs) of diseased cardiac valves by prostheses is common and often life saving [1] for patients with significant valvular lesions, stenosis or regurgitation [2]. Depending on the severity of the condition, HVRs are an expensive yet critical procedure used to restore proper valve function with an increasing number of replacements each year. Worldwide, the number of prosthetic heart valves implanted was approximately 300,000 in 2010 [3] and is increasing at the rate of 5-7% per year [2]. With changing demographics and lifestyle choices, the demand for a more durable and biocompatible prosthesis is on the rise. Factors supporting the need to increase research efforts on HVRs include but are not limited to: an increasing United States (U.S.) population over the age of 65 years old, an increasing life expectancy and an increasing occurrence of valvular heart disease, development of transcatheter procedures that require flexible valves as well as developing world needs for younger patients and cheaper valves.

Ever since their conception in the 1950s, prosthetic heart valves have had many complications, whether design- or materials- related [2]. Mechanical heart valves

(MHVs) which have no biologic component have always been thrombogenic causing thrombus formation and thromboemboli if not corrected using anti-coagulation therapy. Bioprosthesis heart valves (BHVs), made from porcine pericardium do not have long-term thrombogenicity problems with patients without other risk factors but have a shorter lifespan induced by the glutaraldehyde fixing process of the pericardium [4]. Revisions of the HVR are performed frequently due to this tendency for MHVs to form thrombus and BHVs reduced durability.

Thus, this research is aimed at increasing the longevity and reducing thrombogenicity of HVRs and to reduce the number of revision surgeries performed each year. In particular, the research is focused on improving the hemocompatibility of flexible polymeric heart valve leaflets, which may be accomplished by improving the surface chemistry of the polymer for long term use *in vivo*. The following literature review is a concise assessment of current problems and solutions associated with HVR failures and the material science relevant to the research presented in later chapters.

1.2 Literature Review

1.2.1 The Heart & Valve Disorders

The heart is a muscular organ whose function is to deliver blood to the rest of the body (Figure 1.1). It is separated into a left and right side, both composed of atrial and ventricular regions. During the diastolic phase, both the tricuspid and mitral valves open, allowing the ventricles to fill with blood. During systolic phase, the ventricles contract simultaneously, pumping blood into the pulmonary and systemic circulations. Blood enters the right side of the heart through the vena cava, and is passed through the atrium and ventricle before being pumped into the pulmonary circulation and lungs. Oxygenated

blood returns to the left atrium and then the left ventricle, where it is pumped into the systemic circuit.

Valves are located at the exit point of each compartment to regulate the unidirectional flow of blood through the cardiovascular system. They open and close corresponding to pressure differentials during contraction and relaxation of the heart [5]. The mitral and aortic valves, located in the left heart, are the most common sites for heart valve disease. This is a result of the left heart's significantly higher workload [6]. Valvular heart disease can be the result of either congenital or developed defects, including rheumatic fever, endocarditis, calcific degeneration, or congenital anomalies [6]. The two largest problems associated with valvular disease are regurgitation and stenosis. In the former case, the valve does not close completely, and some of the pumped blood flows backwards back into the left ventricle. In the latter case, the opening through which blood can pass becomes narrowed due to the leaflets either becoming rigid or fused together. Both of these valvular diseases result in blood accumulation in the chamber, and the heart is required to work harder in order to supply the body. This increased workload leads to the thickening of the heart muscle and dilating which can result in congestive heart failure. Once the heart valve no longer maintains its normal functionality, drugs can be used to relieve the symptoms but not reverse the disease. Valve replacement surgery is recommended when damage to the valve is considered to be significant enough to pose a life threatening risk.

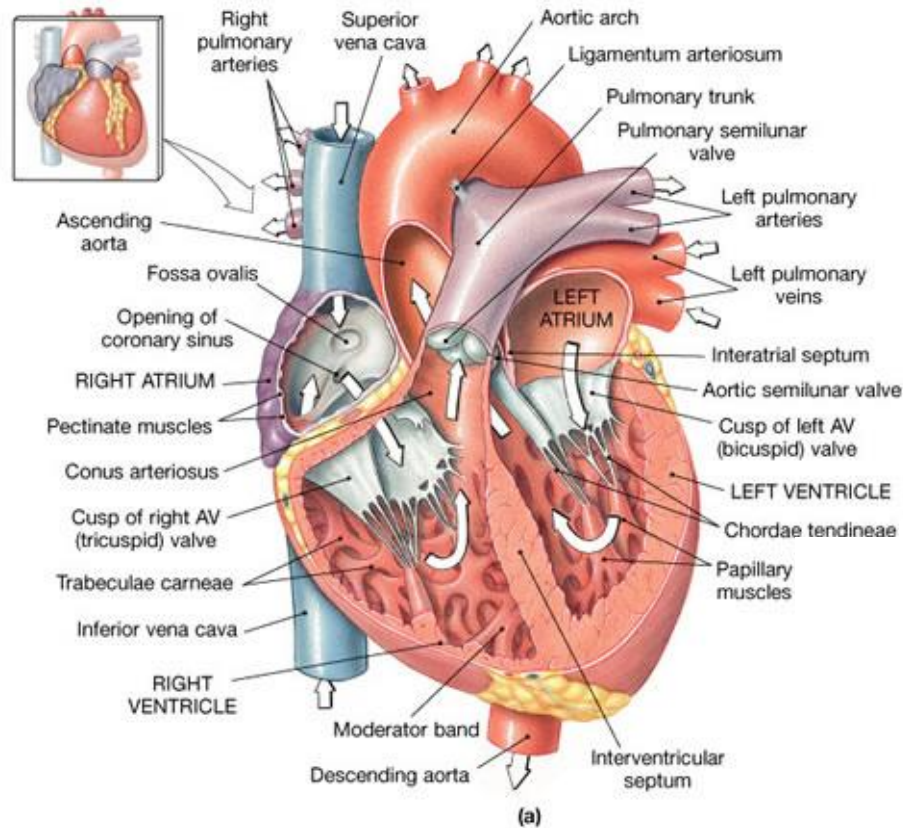


Figure 1.1 A illustrative frontal section through the heart, showing major landmarks and the blood flow pathway [5].

1.2.1.1 Thrombus Formation

The clotting cascade consists of two separate initial pathways (“intrinsic” and “extrinsic”) that ultimately converge on the “common” pathway [7]. The intrinsic and extrinsic pathways essentially serve to activate the protein prothrombin to thrombin. The intrinsic pathway includes the “contact” activation system. The extrinsic system, the principal initiating pathway of blood coagulation in physiological conditions, involves both blood and vascular elements. The critical component is thromboplastin, a glycoprotein embedded with phospholipid in the surface membrane of fibroblasts within and around blood vessels and in various other tissue cells. Under *in vivo* conditions, tissue factor is not exposed to blood, but with damage to vascular or endothelial tissue,

this substance acts in concert with activated tissue factors. The intrinsic pathway can be viewed as coagulation initiated by components entirely contained within the vascular system. This pathway results in the activation of tissue factors, providing a pathway for blood coagulation.

Included in the intrinsic pathway is the contact system where skin, muscle, connective tissue, and a variety of other surfaces may act as activators. However, many other surfaces, especially vascular endothelium, are ineffective as activators which is why bioprosthetics only require anti-platelet therapy. The role of contact system proteins in initiation of the intrinsic pathway of coagulation in hemostasis is questionable, but these proteins do contribute to a number of other events (eg, complement activation, inflammatory response, and fibrinolysis) and are also critical when blood interacts with a foreign surface as in cardiopulmonary bypass [7].

The fibrin molecules accumulate together, trapping platelets, erythrocytes, and leukocytes to form the thrombus. The clot then contracts, drawing together the edges of the injured surface. A clot that remains in the area in which it developed is called a thrombus, and the general condition is called thrombosis. In areas where a small thrombus has formed, there is a propensity for the clot to increase in size for the following reason: as blood flow slows around the thrombus, clot-forming elements (e.g., platelets, red blood cells, and clotting factors) are deposited, producing an enlarging, or propagating thrombus.

1.2.2 Commercially Available Prosthetic Valves

The complete replacement of damaged and diseased heart valves by prostheses has become routine practice, but the type of valve prostheses that is superior is still up for

debate. Current commercially available valves are divided into two primary classes, mechanical and bioprosthetic, each with associated advantages and disadvantages. Factors used to determine which valve is most suited to a patient include the patient's age, comorbidities, need for associated procedures, availability of a given replacement, patient agreement, and surgeon expertise [8]. Today's regulations for heart valves prostheses are very strict, making it difficult for novel valve designs and concepts to enter the market. Consequently, the valves available today represent variations of prostheses with a long-proven history [9, 10].

1.2.2.1 Mechanical Valves

Mechanical valves are the preferred valve for individuals under the age of 65 due to their high durability and longevity [9]. There have been many different developments for mechanical heart valves since their inception in the 1950's. Today the primary designs implanted include the tilting disc design that was introduced in 1969 (Figure 2b), the bileaflet design that was available from 1977 (Figure 2c), and to a lesser extent, the ball and cage design that was introduced in the 1952 (Figure 2a) [10-12]; the two disc valves utilized pyrolytic carbon for the disc portion of the valve.

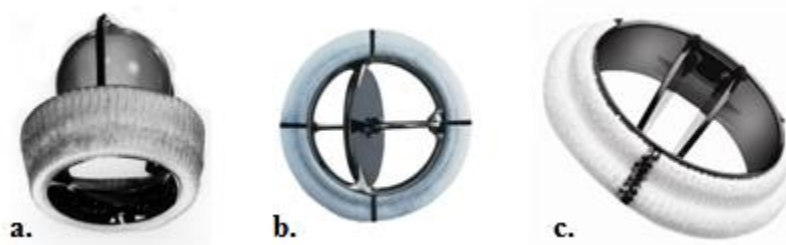


Figure 1.2 Three basic types of mechanical heart valves: (a) Ball and cage valve, (b) Tilting disc valve, and (c) Bileaflet valve [13].

According to a report by Butany *et al.* [2], the St. Jude and Carbomedics bileaflet mechanical valves were the most widely implanted valves in the United States in 2002, accounting for 85% of the mechanical valves implanted. The low profile of the bileaflet mechanical valves allows them to be implanted into smaller hearts without obstruction of other structures such as the mitral valve or coronaries. Bileaflet valves have good hemodynamics with low transvalvular pressure gradient and minimal regurgitation and they are durable, showing a low rate of mechanical failure [9-11]. The tilting disc valves, including the Medtronic Hall and the monostrut Bjork- Shiley, were the second most commonly implanted mechanical valves, accounting for 7% of the valves implanted [2]. Like the bileaflet valves, the tilting disc valves have shown to be durable. However, the hemodynamics of the tilting disc valves is not ideal with lower effective orifice areas and turbulent flow around the disc. The third and least commonly implanted valve is also the oldest valve: the Starr-Edwards Caged Ball valve. The caged ball valve does not have as favorable hemodynamics as the bileaflet and tilting disc valves, but it is still sometimes used when surgeons require a valve that is easy to handle under difficult surgical circumstances [10, 12]. In the 2002 study by the Health Research International [14], it was observed that the further development of bioprosthetic valves had helped them gain increase in the market due to their improved durability. In the 2002 report, mechanical valves only accounted for 40% of all valves implanted, with the St. Jude bileaflet valves still being the gold standard.

One common problem for all the mechanical valve designs is the resulting partial obstruction of blood flow, leading to non-physiological hemodynamic characteristics [9-11]. It is this characteristic that contributes to thrombosis, embolism, and bleeding

complications, often resulting to morbidity and mortality. Consequently, patients receiving mechanical valves are subjected to life-long anticoagulation therapy. Life time anticoagulation therapy has many problems associated with it often resulting in either under or over anticoagulation, and complication associated with hemorrhaging.

1.2.2.2 Bioprosthetic Valves

Bioprosthetic valves first appeared on the market in the 1970's but continue to have been plagued with many problems which result is a reduction in durability in comparison to the mechanical valve options [9-11, 14]. The trileaflet design of the bioprosthetic valve reproduces the central flow characteristics of the natural valve and is less thrombogenic than mechanical valves, so long-term anticoagulation treatment is not required for most recipients. For this reason, bioprosthetic valves have become the first choice for patients with a life expectancy less than 10-15 years. Bioprosthetic valves have also become a popular choice for younger patients to prevent the need for lifetime anticoagulation therapy at such a young age.

Similarly to mechanical valves, there are three main bioprosthetics used as valvular replacements; human, glutaraldehyde-fixed porcine aortic valves (Figure 3a and Figure 3c), and glutaraldehyde-fixed bovine pericardium (Figure 3b). The homografts, which are human valves taken from cadavers, are the least frequently used due to a shortage in both numbers and sizes and because they are difficult to insert [9, 10]. The stented porcine (Figure 3a) and bovine pericardium (Figure 3b) valves are the most commonly implanted, with Edwards Lifesciences and Medtronic valves being the most utilized on the market [9]. According to the 2002 Health Research International report [14], Edwards Lifesciences accounted for 74% of stented valves used in 2001, with the

Carpentier-Edwards Perimount pericardial prosthesis being the most popular. Medtronic accounted for almost 26% of sales, due to their experience with the Hancock porcine bioprosthesis. Both valves have issues with durability with an approximate lifespan of 10-15 years [9].

Metallic or polymer structures are used to support the porcine and bovine pericardium valves. This stent allows the valve to be implanted easily, however, this results in a stenotic region caused by partial orifice obstruction [9]. Stentless porcine valves (Figure 1.3c) were developed to help combat this obstruction. The stentless valves consist of aortic roots modified with a sewing ring [9, 10] which is either implanted within the native root or replaces the root with an increase in effective orifice area. Stentless valves are significantly more complicated to implant than the stented version, and conclusive long-term data of durability of these valves is still unknown but assumed to be similar to stented bioprosthetic valves.

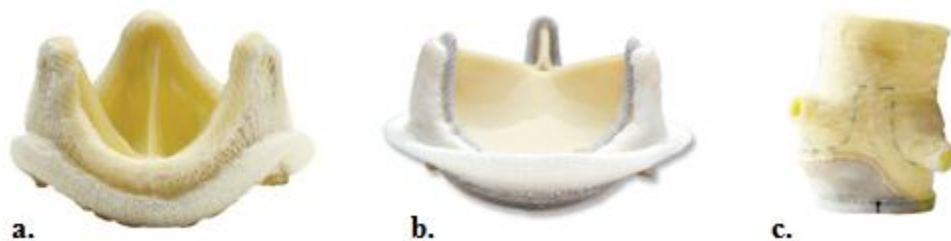


Figure 1.3 Three types of bioprosthetic heart valves: (a) Stented porcine valve, (b) Stented bovine pericardial valve, (c) Stentless porcine valve [13].

Porcine valves are much more restrictive on design due to the valve anatomy but stented pericardial valves can be fabricated in to much more complex designs. Pericardial valves are fabricated from glutaraldehyde fixed sheets of bovine pericardium that can be

oriented to mimic the natural valve in both form and function [10]. The pericardial valves tend to have more desirable hemodynamics than the porcine valves as a result of their improved effective orifice area and leaflet dynamics during forward flow; however, the traditional designs have been made to exhibit significantly higher stresses during diastole when they are under tension.

The main problem that plagues the xenogenic prostheses is tissue failure, which usually is onset within 10 years of implantation [9-11, 14]. This degradation of the valve is as a result of mechanical damage, calcification, or a combination of both, and has been linked to the glutaraldehyde fixation and the stent-valve interaction. Glutaraldehyde treatment effectively cross-links the tissue and reduces its antigenicity while preventing proteolytic degradation. As a result, the tissue loses its mechanical compliance causing an increase in leaflet stress concentrations, accelerating fatigue of the tissue. The presence of calcium deposits on the leaflets can result in stenosis and leaflet tearing.

The world market for bioprosthetic heart valves continues to increase by approximately 5% per year [14]. This is due in part to the increasing percentage of individuals over 65 but also as a result of developments that have increased valve durability and compatibility.

1.2.2.3 Polymeric Valves

Since the 1960s, attempts have been made to develop a polymeric heart valve which was intended to exhibit the durability of mechanical valves combined with the hemocompatibility of tissue valves. Polyurethane (PU) polymeric flexible-leaflet heart valves were first implanted in the 1960s, unfortunately, without much success. Currently there is still no clinically acceptable polymeric leaflet valves beyond those used short-

term in artificial hearts [15]. Polyurethanes have been used in these devices since they exhibit acceptable mechanical properties and performance in the short-term, however, they tend to be very vulnerable to many types of biodegradation and have a tendency to calcify and eventually tear and fail which has limited their successful use. There is still much research in flexible polymeric valves which has focused on polyurethane chemistry. Polycarbonateurethane valves were developed to optimize hemodynamics with the goal to increase durability [16]. While this will increase durability, the material was not specifically designed to prevent calcification, and the literature suggests that material properties (particularly hydrophilicity), in addition to natural hemodynamics is vital to avoid calcification problems. After two *in vivo* juvenile calf studies using these polycarbonateurethane valves (one aortic and one mitral), the explanted valves did show some calcification [16, 17].

Another attempt at flexible polymeric heart valve leaflets were made from a 2% polyhedral oligomeric silsesquioxane-poly(carbonate-urea) urethane (POSS-PCU) [18], a material originally developed for vascular graft use. The material shows good mechanical properties due to the addition of the POSS. However, both the PCU and the POSS-PCU are hydrophobic, with water contact angles (over 100 degrees) [18], calcification was still exhibited by these valves during *in vitro* with no reported *in vivo* performance [19].

Several researchers have looked at the value of surface coatings on hydrophobic synthetic polymers to enhance performance such as grafting sulfonated polyethylene oxide to the surface of PU reduces calcification and thromboembolism [20]. Other research groups have shown that increasing hydrophilicity of glutaraldehyde fixed

bioprosthetic tissue valves can decrease calcification and thromboembolism [21].

1.2.2.4 Fabric Valves

Textile has already been largely used today to manufacture PET grafts (Dacron). Its durability and biocompatibility as graft material have been largely assessed over the last two decades. Even if no *in vivo* results about using textile as heart valve material have been reported, the material properties should match the valve requirements. Because of discontinuous structure, textiles are characterized with low bending stiffness, and its advantageous bending properties have been largely studied. For textile heart valve development [22-24], friction becomes a central issue. Even if global stiffness of fabrics appears to be low, repeated flexure cycling of textile heart valve prosthesis at a physiological rate may lead to fabric structure modifications and filament ruptures through frictional effects [25, 26]. Textiles have shown a dramatic decreases in stiffness that occurred within the first few minutes of cycling, which was attributed to filament and yarn rearrangement (leading to fabric relaxation) within the fabric [27]. Stiffness values then continued decreasing only slightly over the first million cycles up to a final threshold value. Above that value, fabric reaches a completely stabilized state. This relaxation process leads to an improved dynamic *in vitro* behavior for the heart valve prosthesis, which closes more rapidly after cycling due to a decrease in the material's bending stiffness.

1.2.3 Hyaluronan and Its Biomedical Applications

1.2.3.1 Hyaluronan and Its Derivatives

Hyaluronan is a naturally occurring polysaccharide found in all tissues and body fluids of vertebrates as well as in some bacteria and plants. It is a linear polymer with

high molecular weight linear polysaccharide containing alternating N-acetyl-D-glucosamine and D-glucuronic acid residues, with relatively high concentrations in the vitreous humor of eye, the umbilical cord, synovial joint fluid, rooster combs [28] and in native HV leaflets, particularly those regions of the valve subject to compression [29, 30]. HA can be harvested from these sites or through bio-synthesis through certain strains of cultured bacteria, such as streptococci [31].

Hyaluronan was initially discovered and named hyaluronic acid by Karl Meyer and John Palmer in 1934. It was isolated from the vitreous humor of eye as a polysaccharide containing N-acetyl-D-glucosamine and D-glucuronic acid. The term “hyaluronan” was introduced by Endre Balazs in 1986 to cover the different forms of the molecule can take – for example, hyaluronic acid and sodium hyaluronate, which form at physiological pH [32]. From the time of its original isolation, the properties of HA have been the central feature distinguishing it from other aspects of the extracellular matrix. Many individuals including Sandy Ogston, Torvand Laurent, Endre Balazs and Bob Cleveland worked to establish a fundamental understanding of the biophysical properties of HA.

Balazs was the one to originally determine the medical applications for hyaluronan and hyaluronan derivatives. He developed the main concepts for many applications and prepared the first non-inflammatory fraction of sodium hyaluronate [33]. Because of the various properties of hyaluronan solutions, a range of physiological functions have been associated with it, including lubrication, water homeostasis, and regulation of plasma protein distribution [34].

A carboxyl group (-COOH) is attached to each disaccharide unit of HA. When in solution at physiological pH, HA is ionized, resulting in negatively charged -COO⁻. The negatively charged flexible chains take on an expanded conformation and entangle with each other at very low concentrations, acting as a stiff random coil. In solutions with higher concentration of HA stiff random coils will begin to entangle, forming viscoelastic solutions retaining flow without becoming a gel. However, if linked segments were introduced, a network would be introduced that could lead to gel formation. Solutions made of hyaluronan are primarily viscous at low shear rates, but primarily elastic at high shear rate [35]. HA's special molecular structure leads to its viscoelasticity, hydrophilicity and lubricity.

1.2.3.2 Biocompatible and Lubricious Coatings

Glycosylated surfaces may mimic the biochemical activity of the glycocalyx of the blood vessel lumen, which presents heparin-like glycosaminoglycans (GAGs) [36, 37]. Extensive use of GAGs, particularly heparin, has been used to improve hemocompatibility of surfaces. Numerous synthetic plastics and metals that have been modified with heparin show improved hemocompatibility [38-47]. Hyaluronan and chondroitin sulfate are GAGs that have also been used as coatings to reduce platelet adhesion in small diameter vascular grafts [48]. Hyaluronan has been regarded as an ideal lubricant due to its shear-dependent viscosity [34]. Hydrophilic and lubricating coatings have been used for medical devices, such as catheters and guide wires, to improve biocompatibility and lubricity, and to reduce fouling and tissue abrasion [32]. HA has also been used on the plastic implants, such as plastic lenses and orthopedic joints, to improve hydrophilicity and lubrication and has been used for transparent

plastics and glass, such as contact lens and windshields to prevent fogging and optical distortion [49]. It should be noticed that biological lubrication by hyaluronan is not confined to joints. As a natural lubricant present in all tissues of animals, hyaluronan can impart both biocompatibility and lubrication to the surface of these materials.

A crosslinked HA was developed by Balazas to coat onto various prosthetic devices, such as artificial valves, intraocular lenses, and vascular grafts, for improving device biocompatibility [50]. DeFife et al. [51] utilized photochemical immobilization technology to covalently couple HA onto the surface of silicon rubber indwelling catheter to prevent occlusion. The results showed that HA coatings effectively inhibited cell attachment and fibrosis/fibrin deposition, which is part of the host response to an implanted device and reason for catheter occlusion.

1.2.3.3 Chemical Modifications of Hyaluronan

Hyaluronan has many unique advantages as a starting point for biomedical products, but its high water solubility and quick turnover in the body limit the application of native hyaluronan. Crosslinking and coupling reactions are two important ways of HA modification to alter the molecular structure to obtain a more stable solid material improving rheological properties and functionalization of HA.

1.2.3.4 Crosslinking

The swelling properties of HA (i.e. lubricity) can be altered by introducing crosslinks. Segura *et al.* studied the chemical crosslinking of HA at the carboxylic acid groups and/or hydroxyl groups using poly(ethylene glycol) diglycidyl ether [52]. Desmodur N3200™ is a biuret isocyanate derived from hexamethylene diisocyanate[53, 54]. It was chosen by Zhang as a chemical crosslinker for HA in BioPoly (*vide infra*)

because of its crosslinking location on the HA molecule; it crosslinks HA at the hydroxyl groups, not the carboxylic acid groups. This is important because the latter functional groups contribute to the lubricious properties of HA.

1.2.4 BioPoly[®]

Silylated HA, a novel derivative of HA created by Zhang and James ultimately led to the initial development of the HA and UHMWPE composites, known as BioPoly[™] [54-56]. The sodium HA provided by the manufacturer was complexed with quaternary ammonium cations, hexadecetyltrimethylammonium bromide, followed by silylation with hexamethyldisilazane to produce silyl HA-CTA [54]. Silylating the HA increased the hydrophobicity of the GAG, by replacing the active hydrogen of the functional hydroxyl groups with trimethylsilyl groups. A schematic of the fabrication and treatment processes for BioPoly are shown in Figure 1.4.

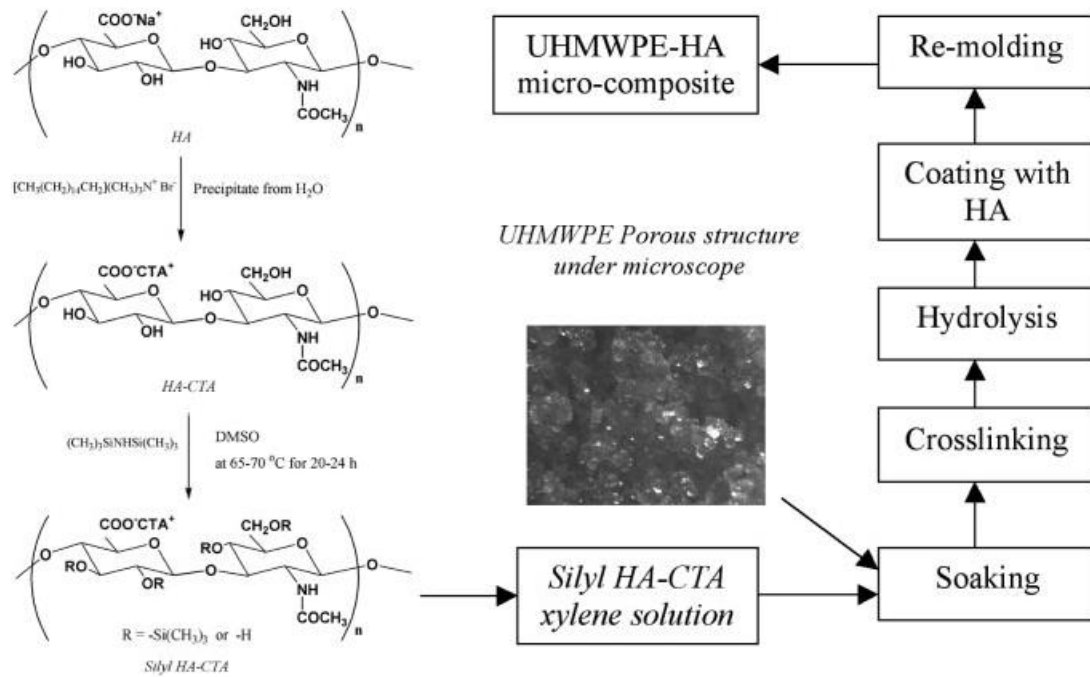


Figure 1.4 Zhang's representation of the formation of BioPoly^[55].

The silyl HA-CTA was placed in solution with xylenes and entered the pores of the UHMWPE porous preform; the silyl HA-CTA was crosslinked *in situ* with a hexamethylene diisocyanate solution (*vide supra*), and then put through a hydrolysis procedure to return the crosslinked silyl HA-CTA to its native state. The surface of the UHMWPE porous preform was dipped in an HA solution and crosslinked *in situ*; lastly, everything was compression molded to full density. The MW of the HA used by Zhang for mechanical and tribological testing was 1.36×10^6 Da. The treatment conditions and sample parameters of Zhang's samples are shown in Tables 1.1.

Table 1.1 Summary of Zhang's different BioPoly sample group treatments [53].

Sample	Conc. of silyl HA	Conc. Of Crosslinker	Soaking & Crosslinking	Hydrolysis	Soaking with HA	Conc. Of HA
1 st batch	Silyl HA-CP	15 µl/ml	I→II→	After molding	No	N/A
	I - 15 mg/ml	OMDI +	OMDI			
	II - 30 mg/ml	4% dilaurate				
2 nd batch	Silyl HA-CTA	Desmodur	I→II→III			
	I - 25 mg/ml	1%	→Desm.			
	II - 50 mg/ml		Two Cycles			
	III - 75 mg/ml					
A				Pre-radiation & After Molding	No	N/A
B				After Molding	No	N/A
C				Before Molding	No	N/A
D				Before Molding	Yes	0.5%
3 rd batch	Silyl HA-CTA	Desmodur	I→Desm.→	Before Molding	Yes	1%
	I - 25 mg/ml	5%	II→Desm.→			
	II - 50 mg/ml		III→Desm.			
	III - 75 mg/ml					
4 th batch	Silyl HA-CTA	Desmodur	I→Desm.→	Before Molding	Yes	1%
	I - 50 mg/ml	2%				

To utilize this composite for heart valve applications, the mechanical and tribological properties of polyethylene components must be optimized to reduce thrombogenesis, enhance biocompatibility, and increase longevity, which may be achieved, in part, by changing the process techniques.

Commercial production of HA containing materials is feasible and affordable and the high molecular weight enables production of interpenetrating network (IPN) between HA and synthetic polymers, maintaining the strength and durability of the synthetic plastic with the added biocompatibility and hydrophilicity of HA in a form much more durable than surface grafting or coating.

1.3 Thesis Objectives and Overview

The overall goal of this research project was to develop the BioPoly[®] technology, to be a commercially viable option for leaflets in tricuspid heart valve prostheses. The effects of varying process conditions, base polymer and resulting composition of the HA-treated material, on the mechanical and hemocompatible properties of BioPoly were investigated. The objective was to achieve hemocompatibility comparable to that of porcine pericardial bioprosthetic valves, the industry product produced by Carpentier-Edwards known as PERIMOUNT[®] while maintaining the structural integrity similar to that of bileaflet mechanical valve, industry product produced by St. Jude Medical[®] known as Regent[™].

The specific aims of the research were: 1) Develop manufacturing methods for cardiovascular BioPoly HA-treated materials by examining how appropriate base polymers (molecular weight, grade and thickness selected for mechanical strength and flexibility) swell and develop a successful procedure to swell HA into the base polymer; 2) Optimize the HA-treated material compositions to meet mechanical performance

requirements for heart valve leaflets in accordance with FDA guidance documents and standards; 3) Optimize the HA-treated material compositions for blood-contact to avoid thrombus formation. Specific aim 1 is covered in Chapters 2 and 3, Specific aim 2 is covered in Chapter 3, Specific aim 3 is covered in Chapters 3 and 4.

1.4 References

1. Schoen, F.J., *Cardiac valves and valvular pathology: Update on function, disease, repair, and replacement*. Cardiovascular Pathology. **14**(4): p. 189-194.
2. Butany, J., et al., *Mechanical heart valve prostheses:: identification and evaluation (erratum)*. Cardiovascular Pathology, 2003. **12**(6): p. 322-344.
3. Mohammadi, H. and K. Mequanint, *Prosthetic aortic heart valves: Modeling and design*. Medical Engineering & Physics, 2011. **33**(2): p. 131-147.
4. Butany, J., et al., *Biological replacement heart valves: Identification and evaluation*. Cardiovascular Pathology. **12**(3): p. 119-139.
5. Zaret, B.L., et al., *Yale University School of Medicine heart book*. 1992: William Morrow and Co.
6. Tortora, G.J. and B.H. Derrickson, *Principles of Anatomy and Physiology, Twelfth Edition with Atlas and Registration Card Binder Ready Version*. 2008: John Wiley & Sons.
7. Colman, R.W., et al., *Factor XI deficiency and hemostasis*. American Journal of Hematology, 1994. **45**(1): p. 73-78.
8. Tillquist MN, M.T., *Cardiac crossroads: deciding between mechanical or bioprosthetic heart valve replacement*. Patient Prefer Adherence, 2011. **5**: p. 91-99.
9. Sako, E., *Newer concepts in the surgical treatment of valvular heart disease*. Current Cardiology Reports, 2004. **6**(2): p. 100-105.
10. Martini, F.H., *Fundamentals of Anatomy and Physiology*. 2011: Pearson Education, Limited.
11. Birchall, I.E., Y.S. Morsi, and F.L. Rosenfeldt, *Artificial aortic valves: an overview*.
12. Senthilnathan, V., et al., *Heart valves: which is the best choice?* Cardiovascular Surgery, 1999. **7**(4): p. 393-397.
13. Edward, L.
<http://www.edwards.com/PatientsandFamilies/MyHeart/ClinicalProcedures/ValveReplacementEU.aspx>. 2012.
14. *U.S. opportunities in heart valve disease management*. . 2002, Health Research International.

15. Zilla, P., et al., *Prosthetic heart valves: Catering for the few*. *Biomaterials*, 2008. **29**(4): p. 385-406.
16. Daebritz, S.H., et al., *Introduction of a flexible polymeric heart valve prosthesis with special design for aortic position*. *European Journal of Cardio-Thoracic Surgery*, 2004. **25**(6): p. 946-952.
17. Daebritz, S.H., et al., *Introduction of a flexible polymeric heart valve prosthesis with special design for mitral position*. *Circulation*, 2003. **108**(10): p. 134-139.
18. Kidane, A.G., et al., *A novel nanocomposite polymer for development of synthetic heart valve leaflets*. *Acta Biomaterialia*, 2009. **5**(7): p. 2409-2417.
19. Ghanbari, H., et al., *The anti-calcification potential of a silsesquioxane nanocomposite polymer under in vitro conditions: Potential material for synthetic leaflet heart valve*. *Acta Biomaterialia*, 2010. **6**(11): p. 4249-4260.
20. Han, D.K., et al., *In vivo biocompatibility of sulfonated PEO-grafted polyurethanes for polymer heart valve and vascular graft*. *Artificial Organs*, 2006. **30**(12): p. 955-959.
21. Oosthuysen, A., et al., *Bioprosthetic tissue preservation by filling with a poly(acrylamide) hydrogel*. *Biomaterials*, 2006. **27**(9): p. 2123-2130.
22. Frédéric Heim, B.D., Jean-Georges Kretz, Nabil Chakfe, *Method for producing an aortic or mitral heart valve prosthesis and resulting aortic or mitral heart valve*, U.s.P. 8043551, Editor. 2011: U.S.
23. Heim, F., B. Durand, and N. Chakfe, *Textile Heartvalve Prosthesis: Manufacturing Process and Prototype Performances*. *Textile Research Journal*, 2008. **78**(12): p. 1124-1131.
24. Heim, F., B. Durand, and N. Chakfe, *Textile heart valve prosthesis: Influence of the fabric parameters on its hydrodynamic performance in vitro*. *Computer Methods in Biomechanics and Biomedical Engineering*, 2005. **8**(sup1): p. 137-138.
25. Skelton, J., *Frictional Effects in Fibrous Assemblies*. *Textile Research Journal*, 1974. **44**(10): p. 746-752.
26. Livesey, R.G. and J.D. Owen, *47—CLOTH STIFFNESS AND HYSTERESIS IN BENDING*. *Journal of the Textile Institute Transactions*, 1964. **55**(10): p. T516-T530.
27. Heim, F., B. Durand, and N. Chakfe, *Textile for heart valve prostheses: Fabric long-term durability testing*. *Journal of Biomedical Materials Research Part B: Applied Biomaterials*, 2010. **92B**(1): p. 68-77.

28. Laurent, T.C., U.B.G. Laurent, and J.R.E. Fraser, *The structure and function of hyaluronan: An overview*. Immunol Cell Biol, 1996. **74**(2): p. A1-A7.
29. Grande-Allen, K.J., et al., *Glycosaminoglycans and proteoglycans in normal mitral valve leaflets and chordae: association with regions of tensile and compressive loading*. Glycobiology, 2004. **14**(7): p. 621-633.
30. James, S.P., et al., *Chapter 18: UHMWPE/Hyaluronan Microcomposite Biomaterials*, in *UHMWPE Handbook*, S. Kurtz, Editor. 2009, Elsevier.
31. P Giusti, L., *Biomaterial comprising hyaluronic acid and derivatives thereof in interpenetrating polymer networks (IPN)*. 1997, M.U.R.S.T. Italian Ministry for Universities and Scientific and Technology Research: US.
32. Balazs E. A., B.P., *Hyaluronic acid: its structure and use*. Cosmetics and toiletries, 1984. **99**(6): p. 65-72.
33. Laurent, T.C., *The Tree - Hyaluronan research in the 20th Century*. www.glycoforum.gr.jp/science/hyaluronan/HA23.html, 2002. **Uppsala University, Department of Medical Biochemistry and Microbiology**.
34. Ogston, A.G. and J.E. Stanier, *The physiological function of hyaluronic acid in synovial fluid; viscous, elastic and lubricant properties*. The Journal of Physiology, 1953. **119**(2-3): p. 244-252.
35. Laurent, T.C., U.B. Laurent, and J.R. Fraser, *Functions of hyaluronan*. Annals of the Rheumatic Diseases, 1995. **54**(5): p. 429-432.
36. Wu, K.K. and P. Thiagarajan, *Role of endothelium in thrombosis and hemostasis*. Annual Review of Medicine, 1996. **47**: p. 315-331.
37. Boddohi, S. and M.J. Kipper, *Engineering Nanoassemblies of Polysaccharides*. Advanced Materials, 2010. **22**(28): p. 2998-3016.
38. Bjorck, C.G., et al., *INVITRO EVALUATION OF A BIOLOGIC GRAFT SURFACE - EFFECT OF TREATMENT WITH CONVENTIONAL AND LOW-MOLECULAR WEIGHT (LMW) HEPARIN*. Thrombosis Research, 1984. **35**(6): p. 653-663.
39. Chen, J.L., et al., *Improving blood-compatibility of titanium by coating collagen-heparin multilayers*. Applied Surface Science, 2009. **255**(15): p. 6894-6900.
40. Ito, Y., Y. Imanishi, and M. Sisido, *INVITRO PLATELET-ADHESION AND INVIVO ANTITHROMBOGENICITY OF HEPARINIZED POLYETHERURETHANEUREAS*. Biomaterials, 1988. **9**(3): p. 235-240.

41. Kim, Y.J., et al., *Surface characterization and in vitro blood compatibility of poly(ethylene terephthalate) immobilized with insulin and/or heparin using plasma glow discharge*. *Biomaterials*, 2000. **21**(2): p. 121-130.
42. Lin, W.C., T.Y. Liu, and M.C. Yang, *Hemocompatibility of polyacrylonitrile dialysis membrane immobilized with chitosan and heparin conjugate*. *Biomaterials*, 2004. **25**(10): p. 1947-1957.
43. Magnani, A., et al., *In vitro study of blood-contacting properties and effect on bacterial adhesion of a polymeric surface with immobilized heparin and sulphated hyaluronic acid*. *Journal of Biomaterials Science-Polymer Edition*, 2000. **11**(8): p. 801-815.
44. Park, K.D., et al., *BLOOD COMPATIBILITY OF SPUU-PEO-HEPARIN GRAFT-COPOLYMERS*. *Journal of Biomedical Materials Research*, 1992. **26**(6): p. 739-756.
45. Tan, Q.G., et al., *Constructing thromboresistant surface on biomedical stainless steel via layer-by-layer deposition anticoagulant*. *Biomaterials*, 2003. **24**(25): p. 4699-4705.
46. Thorslund, S., et al., *Bioactive heparin immobilized onto microfluidic channels in poly(dimethylsiloxane) results in hydrophilic surface properties*. *Colloids and Surfaces B-Biointerfaces*, 2005. **46**(4): p. 240-247.
47. Yang, M.C. and W.C. Lin, *Protein adsorption and platelet adhesion of polysulfone membrane immobilized with chitosan and heparin conjugate*. *Polymers for Advanced Technologies*, 2003. **14**(2): p. 103-113.
48. Kito, H. and T. Matsuda, *Biocompatible coatings for luminal and outer surfaces of small-caliber artificial grafts*. *Journal of Biomedical Materials Research*, 1996. **30**(3): p. 321-330.
49. Beavers, E., *Lens with hydrophilic coating*. 1987: US.
50. E Balazs, A.L., *Hyaluronate modified polymeric articles*. 1985, Biomatrix, Inc.: US.
51. DeFife, K.M., et al., *Effects of photochemically immobilized polymer coatings on protein adsorption, cell adhesion, and the foreign body reaction to silicone rubber*. *Journal of Biomedical Materials Research*, 1999. **44**(3): p. 298-307.
52. Segura, T., et al., *Crosslinked hyaluronic acid hydrogels: a strategy to functionalize and pattern*. *Biomaterials*, 2005. **26**(4): p. 359-371.
53. Zhang, M., *Surface Modification of Ultra High Molecular Weight Polyethylene With Hyaluronan For Total Joint Replacement Application*, in *Mechanical Engineering*. 2005, Colorado State University: Fort Collins.

54. Zhang, M. and S.P. James, *Silylation of hyaluronan to improve hydrophobicity and reactivity for improved processing and derivatization*. *Polymer*, 2005. **46**(11): p. 3639-3648.
55. Zhang, M., et al., *A novel ultra high molecular weight polyethylene–hyaluronan microcomposite for use in total joint replacements. I. Synthesis and physical/chemical characterization*. *Journal of Biomedical Materials Research Part A*, 2006. **78A**(1): p. 86-96.
56. Zhang, M., et al., *A novel ultra high molecular weight polyethylene–hyaluronan microcomposite for use in total joint replacements. II. Mechanical and tribological property evaluation*. *Journal of Biomedical Materials Research Part A*, 2007. **82A**(1): p. 18-26.

CHAPTER 2: SWELLING OF BASE POLYMERS: LINEAR LOW DENSITY POLYETHYLENE BLOWN FILM AND POLYETHYLENE TEREPHTHALATE MEDICAL FABRIC

2.1 Introduction

In order to form an HA and linear low density polyethylene (LLDPE) or polyethylene terephthalate (PET) HA-treated material, the degree of swelling and swelling kinetics in a solvent of interest must be analyzed and understood. A study was performed to understand the above parameters for the swelling of the LLDPE and PET in a range of solvent temperatures in order to identify the swelling parameters to be used in the HA-treated material synthesis.

2.2 Materials and Methods

2.2.1 Materials

2.2.1.1 Linear Low Density Polyethylene

Linear low density polyethylene was selected as the base polymer for the film based on comparable mechanical properties and bending stiffnesses as native and fixed tissues. Three different resins of LLDPE were used in this study. All of the samples were blow molded from known resins by Flex-Pack Engineering, Inc. (Uniontown, OH) with

known melt indexes, densities and crystallinities. The form of all of the samples was blow molded films with a specified thickness of .002” (.0508 mm) each with average actual thickness of .0032” (.0801mm). All of the films were blown without the addition of any filler and no additional processes for surface treatment.

The first type of LLDPE used in the study was film molded from Dowlex 2344 resin with a melt index of 0.7 g/10 min, density of 0.933 g/cm³ and a crystallinity of 42.26 ± 1.35%. The second type of LLDPE used in the study was film molded from Dowlex 2056 resin with a melt index of 1.0 g/10 min, density of 0.920 g/cm³ and a crystallinity of 28.71 ± 2.14%. The third type of LLDPE used in the study was film molded from Dowlex 2036G resin with a melt index of 2.5 g/10 min, density of 0.935 g/cm³ and a crystallinity of 45.21 ± 1.66%. Crystallinity of the films was calculated using differential scanning calorimetry (DSC).

The samples were cut into multiple square samples approximately 3cm x 3cm for the study. This size allowed for a large sample size while reducing the necessary amount of solvent for swelling.

2.2.1.2 Polyethylene Terephthalate Fabric

Polyethylene terephthalate fabric was selected as the textile base material based on its high success in other cardiovascular applications, ability to be woven into a tubular structure and mechanical characteristics. One type of medical grade PET fabric was used in this study. All of the samples were woven by BARD Peripheral Vascular OEM Products (Tempe, AZ). The PET samples were made from Style 6010 thin polyester tubular woven (uncrimped) specimens with a nominal diameter of 22 mm and wall

thickness of $.010'' \pm .001''$. All of the fabrics were woven with no additional processes for surface treatment. The PET used in the study was fabric woven from a Polyethylene Terephthalate resin with the resulting fabric having a density of 1.78 g/cm^3 and a crystallinity of $38.28 \pm 0.54\%$. Crystallinity of the fabric was calculated using differential scanning calorimetry (DSC).

The samples were cut into multiple square samples approximately $3\text{cm} \times 3\text{cm}$ for the study. This size allowed for a large sample size while reducing the necessary amount of solvent for swelling.

2.2.1.3 Solvent

The solvent used for the study was picked based on the successes with the swelling of Ultra High Molecular Weight Polyethylene (UHMWPE) by Beauregard [1]. Xylenes showed the greatest degree of swelling due to the closeness in the Hildebrandt swelling parameters between xylene and UHMWPE, while the Hildebrandt swelling parameters are quite different for xylenes and PET, therefore any resulting solvent absorption is due to wicking into the voids, possibly maintaining mechanical integrity therefore, xylenes was selected as the swelling solvent.. Xylenes (certified A.C.S.) were obtained from Fisher Chemical Company (Pittsburg, PA) and were used as received.

2.2.2 Measurement of Degree of Swelling

2.2.2.1 Swelling Apparatus

To swell the LLDPE or PET in the chosen solvent, two swelling apparatus were utilized. The first, the open-cup method consisted of the LLDPE or PET and the solvent in 50 ml beakers covered with a watch glass in a controlled temperature oil bath. A thermometer placed in the heated oil bath indirectly monitored swelling temperatures.

In the second system, a round bottom flask apparatus was utilized. This method consisted of a 250 ml two-neck round bottom flask, fitted with a 24/40 standard taper ground glass joint and a serum stopper. The ground joint was fitted with a 100 mm West condenser which was capped with a rubber septum. The West condenser was used to prevent evaporation of the solvent by reflux. The sealed round bottom flask was lowered into a heated bath of mineral oil which was used to conduct heat to the solvent. A temperature probe was placed in the mineral oil to regulate the temperature.

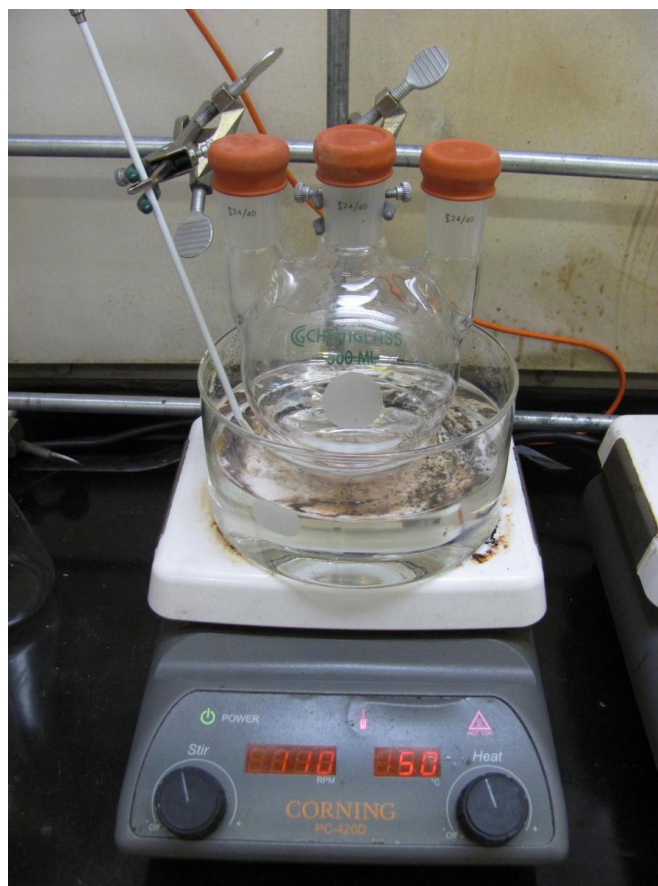


Figure 2.1 Round Bottom Flask swelling apparatus for solvent swelling

2.2.2.2 Measurement Method

Samples were weighed prior to submersion in the solvent. The temperature of the mineral oil was brought to the desired swelling temperature and held, giving time for the

solvent to equilibrate then submerging the LLDPE or PET samples. The samples were allowed to swell for a desired amount of time, dried of surface solvent and weighed.

All measurements were made with a minimum of three samples. Reported data are the average of the three samples \pm the standard deviation.

2.2.2.3 Temperature Variation

When the averaged masses of the samples reached equilibrium, the temperature of the solvent was increase and the weighing procedure repeated until equilibrium was again reached. The temperature of the solvent was increased until the LLDPE film or PET fabric had begun degrading or no changes could be seen.

2.2.2.4 Calculations

Volumetric expansion of the LLDPE and PET was the desired parameter. Therefore, the following equation was used to calculate the percent change in volume of the sample ($dV/V_0\%$):

$$\frac{dV}{V_0} = \frac{(W_t - W_0) / \rho_{solvent}}{W_0 / \rho_{polymer}}$$

where

- $W_t =$ Weight of the sample at time t
- $W_0 =$ Weight of the sample at time t = 0
- $\rho_{solvent} =$ Density of the solvent
- $\rho_{polymer} =$ Density of the polymer

2.2.3 Effect of Solvent Swelling on Mechanical Properties

The effects of the swelling on crystallinity and tensile properties were examined in addition to the degree of swelling. Changes in these parameters helped guide selection of the base polymer and swelling parameters in order to achieve ideal volumetric expansion without compromising the material's mechanical properties. The % χ_c was measured by means of a TA Instruments Differential Scanning Calorimeter (DSC) 2920 in a dry N₂ atmosphere per ASTM D3418-03. LLDPE samples were heated from 24°C to 180°C at a rate of 10°C/minute, and held at equilibrium for one minute (all with N₂ atmosphere). PET samples were heated from 24°C to 275°C at a rate of 10°C/minute, and held at equilibrium for one minute (all with N₂ atmosphere). The H_f was determined to be 288 J/g for 100 % crystalline PE and 113 J/g for 100% crystalline PET [2, 3]. The % χ_c of the sample was calculated by dividing the H_f of the sample by 288 J/g or 113 J/g based on base polymer (because the 100 % crystalline H_f of BioPoly is unknown) and multiplying by 100. Sample control and treatment groups that were characterized: LLDPE virgin film, PET virgin fabric and LLDPE and PET samples for all swelling parameters. All reported average values for % χ_c were calculated from a sample size of three per group.

ASTM D882-10 standard tensile specimens of film thickness were stamped out of swelled LLDPE samples and an electromechanical Tinius Olsen UTM axial test system (Horsham, PA) was used in conjunction with Test Navigator software from Tinius Olsen to perform all tensile tests; a uniaxial (tension/ compression) 1000 N load cell (Model H1K-S) was used. Five tensile bars were stamped out of each sample. Three tensile bars were used for the modulus test for each treatment group. Samples were pulled at a crosshead speed of 500 mm/minute (these strain rates follow the ASTM standard which

states that the time to failure of a polymeric sample must fall within a certain time limit; this can be adjusted for different materials by changing the strain rate). Elongation data was calculated from crosshead data (the change in gage length was divided by the original gage length of the sample, which is specified in the standard).

2.2.4 Statistics

Statistics were analyzed using SigmaStat software (Systat Software Inc.; Richmond, CA). A single-factor ANOVA test with a 95% confidence interval was performed; multiple comparisons were performed via the Holm-Sidak method when sample population standard deviations and population sample sizes were similar. Population means which had unequal variances were analyzed using non-paired t-tests ($\alpha=0.5$). Average values and standard deviation for all treatment group populations were calculated.

2.3 Results and Discussion

2.3.1 Degree of Swelling

Representative data of the percent volume change ($dV/V_0\%$) of the three commercial LLDPE films in xylenes versus time at different temperatures are shown in Figure 2.2, 2.3 and 2.4 for the Dowlex 2344, 2056 and 2036G respectively. Data in these figures result from the open-cup swelling method except for the 70 °C data, which resulted from the round bottom flask method. The two methods gave similar results for xylenes. The equilibrium swelling values at the various temperatures were used to create Figure 2.5.

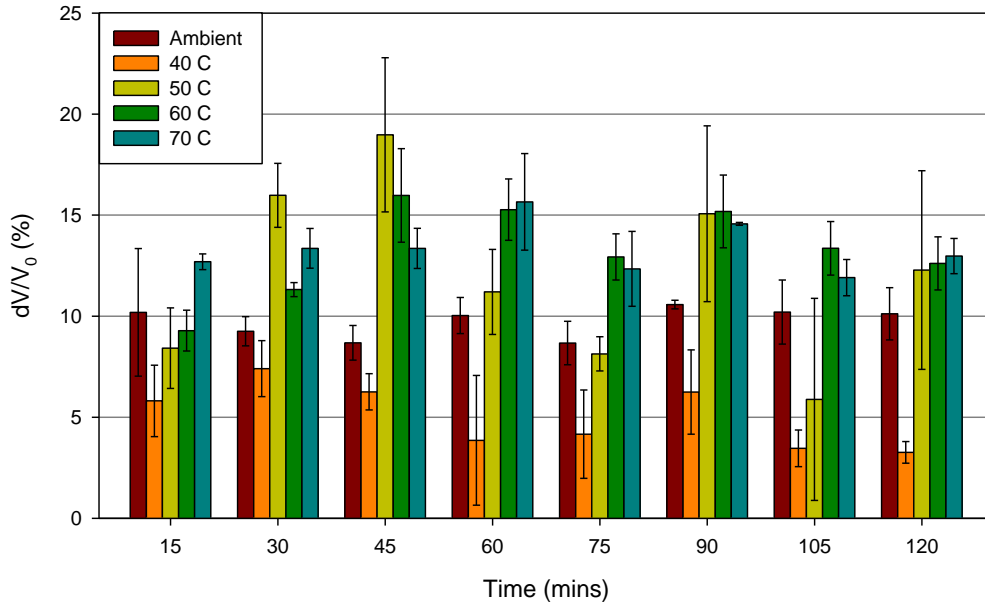


Figure 2.2 Percentage volume change of commercial Dowlex 2344 LLDPE film in xylenes at various temperatures.

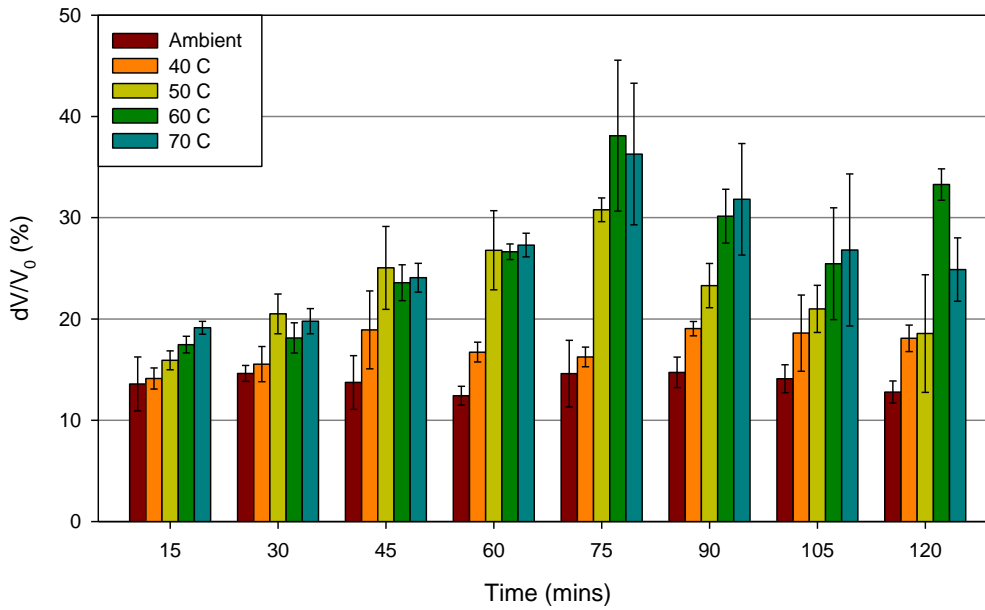


Figure 2.3 Percentage volume change of commercial Dowlex 2056 LLDPE film in xylenes at various temperatures.

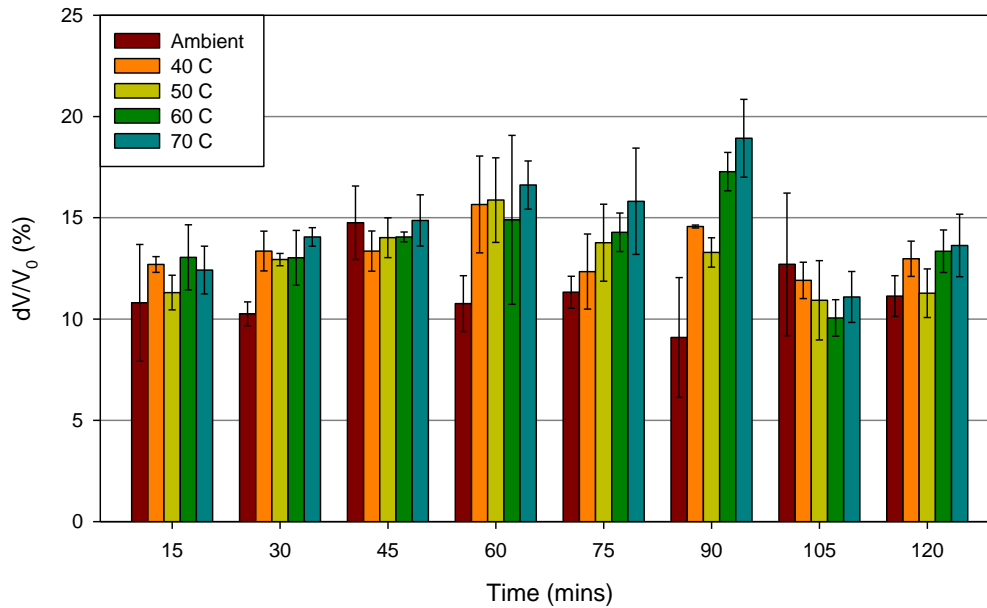


Figure 2.4 Percentage volume change of commercial Dowlex 2036G LLDPE film in xylenes at various temperatures.

Figure 2.5 represents the percentage volume change ($dV/V_0\%$) of the Dowlex LLDPE films in xylenes versus temperature. No differentiation is made between the swelling methods, open cup or closed round bottom flask. Both methods were used and yielded similar results.

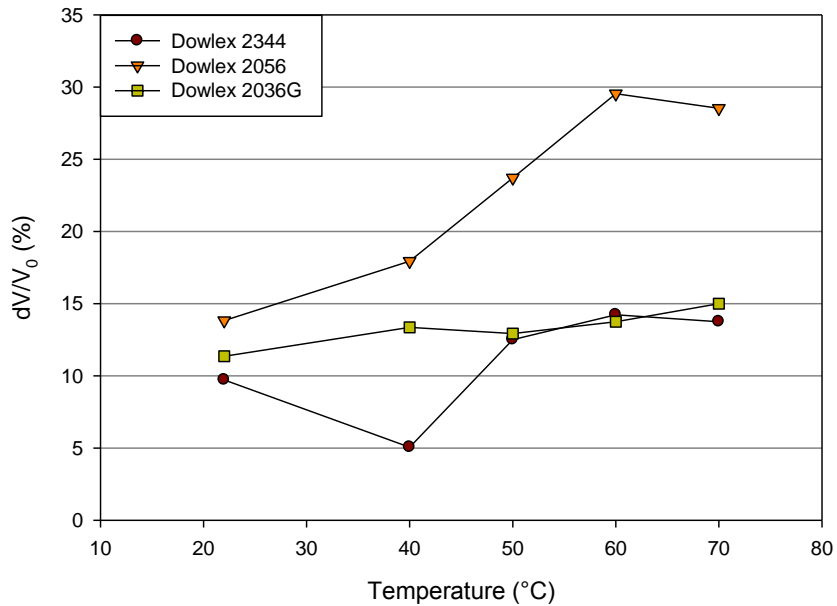


Figure 2.5 Percentage volume change of Dowlex LLDPE film in xylenes at various temperatures.

Focusing on the degree of swelling of the LLDPE films in xylenes vs. temperature, there appears to be a non-linearity for Dowlex 2056 starting around 60°C. It is believed that the swelling to this point has taken place mainly in the amorphous regions of the film [4]. Beyond this point, the crystalline regions prevent the film from swelling further prior to melting of the crystalline regions. The increased crystallinity of the Dowlex 2344 and Dowlex 2036G resins explain the lower degree of swelling. If only the amorphous regions of the LLDPE are swelled it would be expected that the lower crystallinity Dowlex 2056 material would swell to a greater extent [5].

Representative data of the percent volume change ($dV/V_0\%$) of the PET fabric in xylenes versus time at different temperatures are shown in Figure 2.6. Data in this figure result from the open-cup swelling method. Temperature increases were halted at 60°C

due to satisfactory swelling at lower temperatures and no significant differences in swelling with previous temperature increases. The equilibrium swelling values at the various temperatures were used to create Figure 2.7.

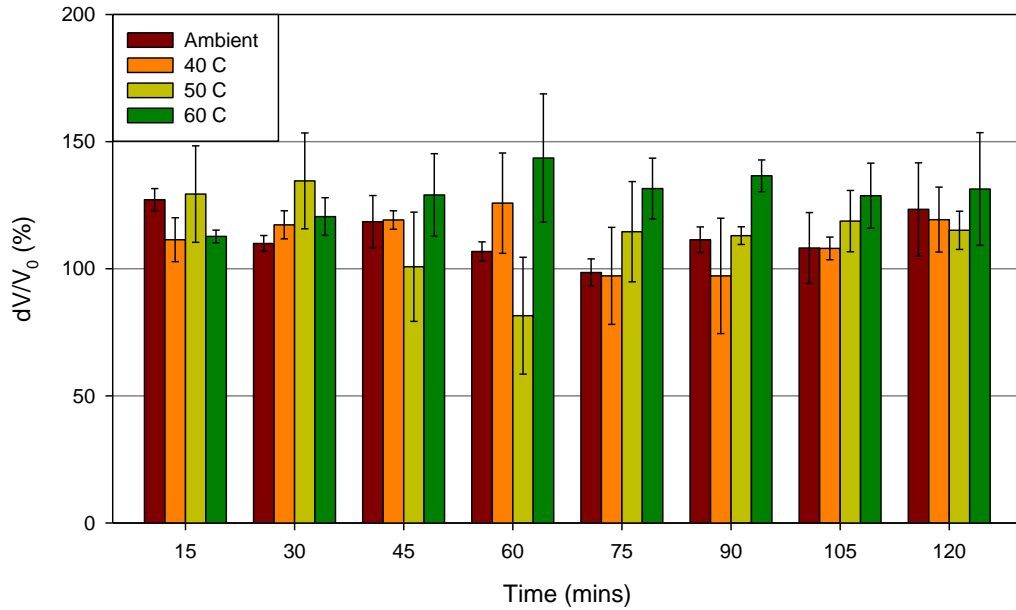


Figure 2.6 Percentage volume change of commercial PET fabric in xylenes at various temperatures.

Figure 2.7 represents the percentage volume change (dV/V_0 %) of the PET fabric in xylenes versus temperature.

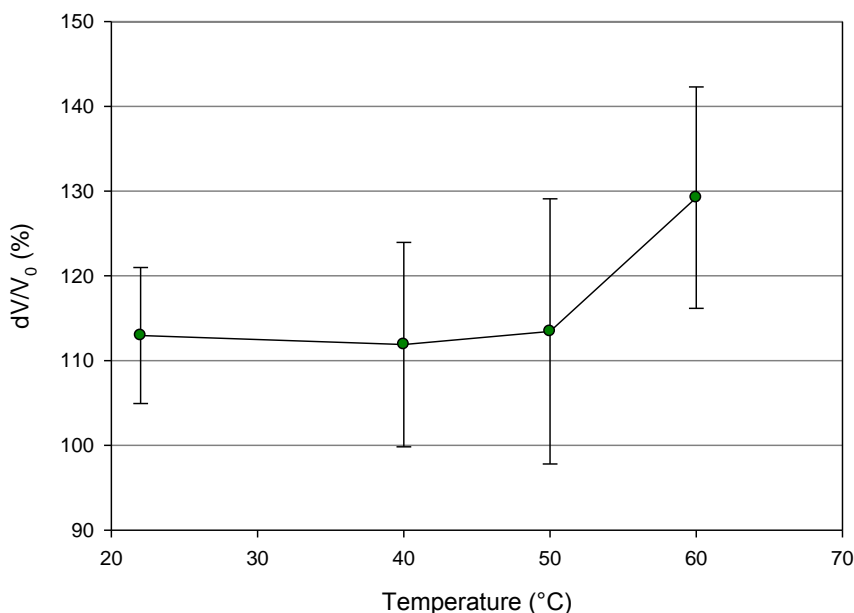


Figure 2.7 Percentage volume change of PET fabric in xylenes at various temperatures.

Focusing on the degree of swelling of the PET fabric in xylenes vs. temperature, at first look there appears to be a non-linearity for the fabric starting around 60°C. Statistically there is no significant difference for the volumetric expansion of the PET at different temperatures. Even though the solubility parameters for xylenes and PET do not lend themselves to provide for significant swelling [4, 6], it is possible that the fabric fibers begin to swell in xylenes at an increased temperature.

For lower temperatures it is seen that temperature does not influence the amount of swelling. It is believed that the solvent is wicked by the weave of the fabric, occupying the voids between fibers and yarns. At elevated temperatures, much higher than necessary for our purposes, the fibers would begin to swell with the solvents increasing the amount of solvent absorption. This was expected since the Hildebrand solubility parameters for xylenes and PET suggest that swelling of the polymer would not occur. The wicking of

the fabric allows for absorption of the solvent solution into the structure without compromising the physical integrity of the polymer. Slight swelling of the fibers could be beneficial in incorporating a semi-interpenetrating polymer network which could hold HA better.

2.3.2 Swelling Kinetics

The Dowlex 2344 and 2056 LLDPE samples reached 90% of the equilibrium swelling value at 50°C in approximately 1 hour while the Dowlex 2036G reach 100% of its equilibrium value within 1 hour. These values are important in the formation of the HA-treated materials because it indicates the end of active solvent transport. The PET fabric reached 100% of its equilibrium swelling value at each temperature within 15 minutes of placement into solvent bath. Extended exposure to solvents did not increase the volumetric expansion of the fabric leading to the belief that the solvent was only penetrating voids between fibers and yarns instead of swelling the PET fibers.

2.3.3 Effect of Solvent Swelling on Mechanical Properties

With the high degree of swelling achieved using xylenes and elevated temperatures, crystallinity of the Dowlex 2056 was increased while the Dowlex 2344 and 2036G were much more thermally stable and did not increase crystallinity. This increase in crystallinity subsequently caused an increase in the modulus and yield strength of the Dowlex 2056 as well. The resulting crystallinity increases can be seen in Figures 2.6, 2.8, and 2.10 and the tensile increases can be seen in Figures 2.7, 2.9, and 2.11 for Dowlex 2344, 2056 and 2036G respectively.

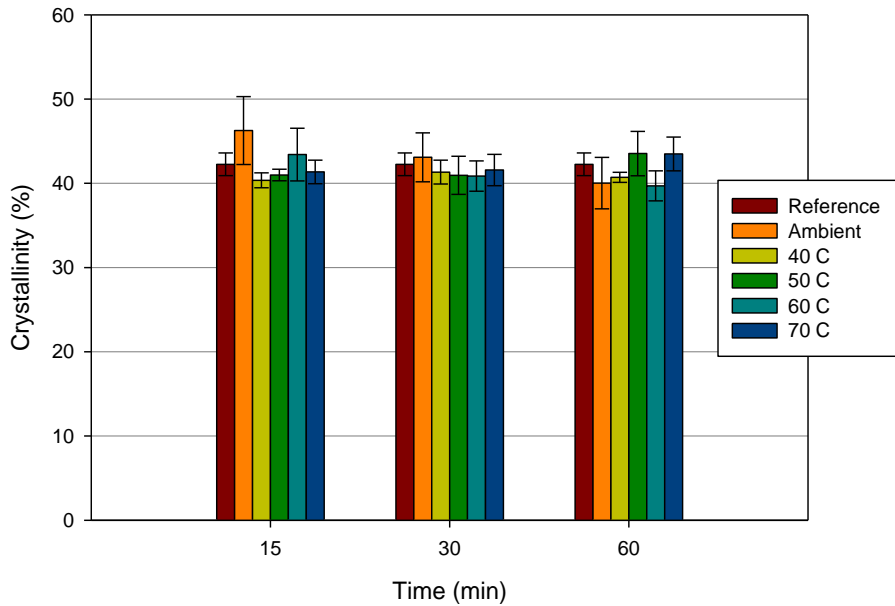


Figure 2.6 Crystallinity of commercial Dowlex 2344 LLDPE following swelling at different temperatures.

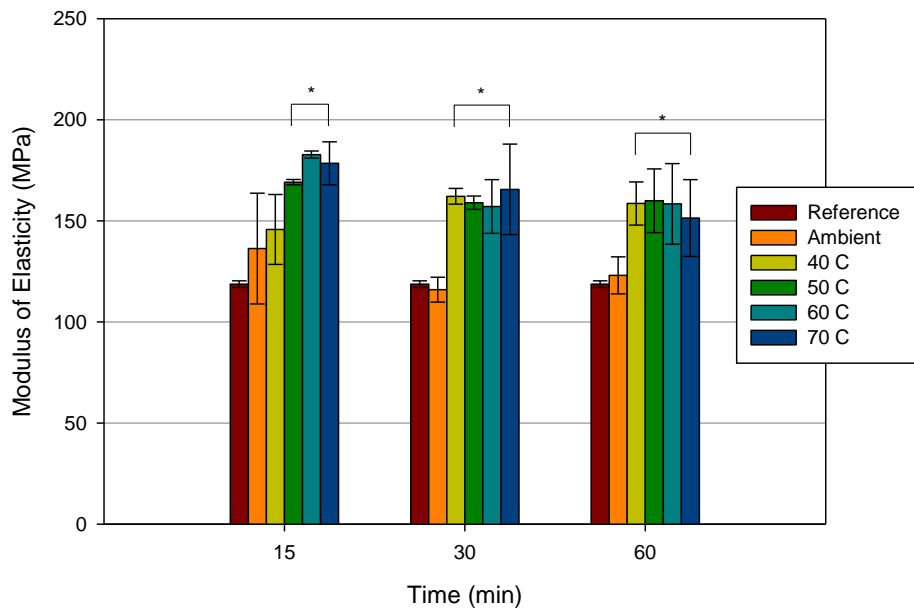


Figure 2.7 Modulus of Elasticity of commercial Dowlex 2344 LLDPE following swelling at different temperatures. An * indicates significant differences ($p < 0.05$) from LLDPE Reference.

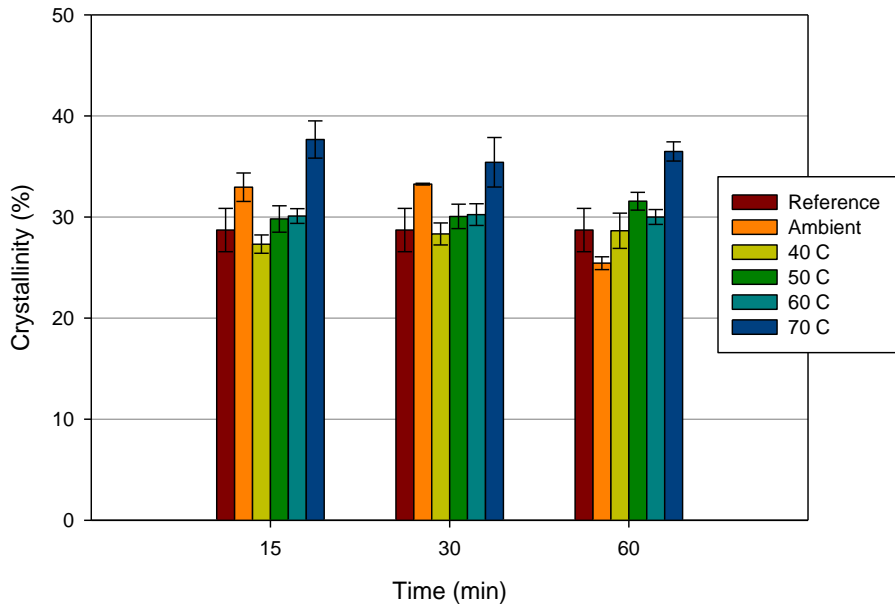


Figure 2.8 Crystallinity of commercial Dowlex 2056 LLDPE following swelling at different temperatures.

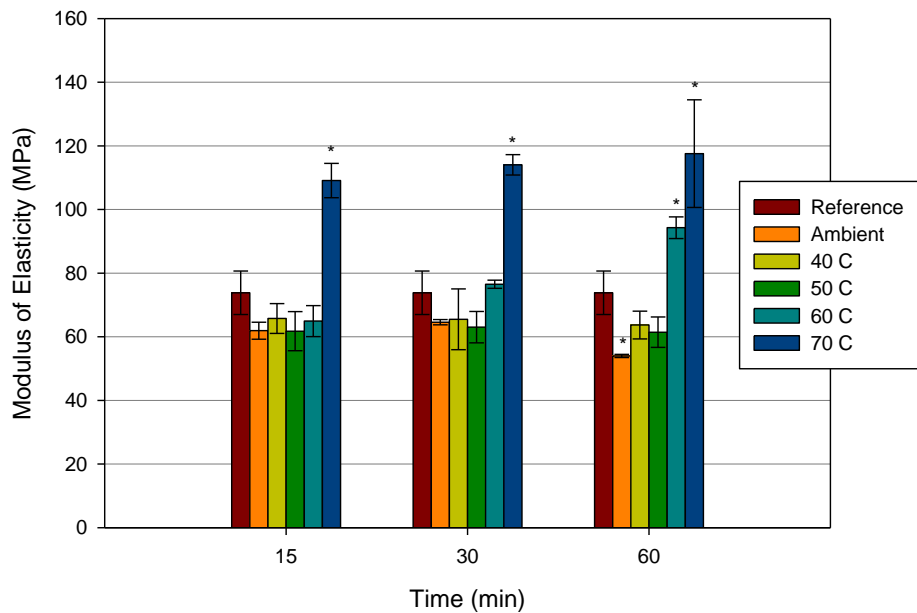


Figure 2.9 Modulus of Elasticity of commercial Dowlex 2056 LLDPE following swelling at different temperatures. An * indicates significant differences ($p < 0.05$) from LLDPE Reference.

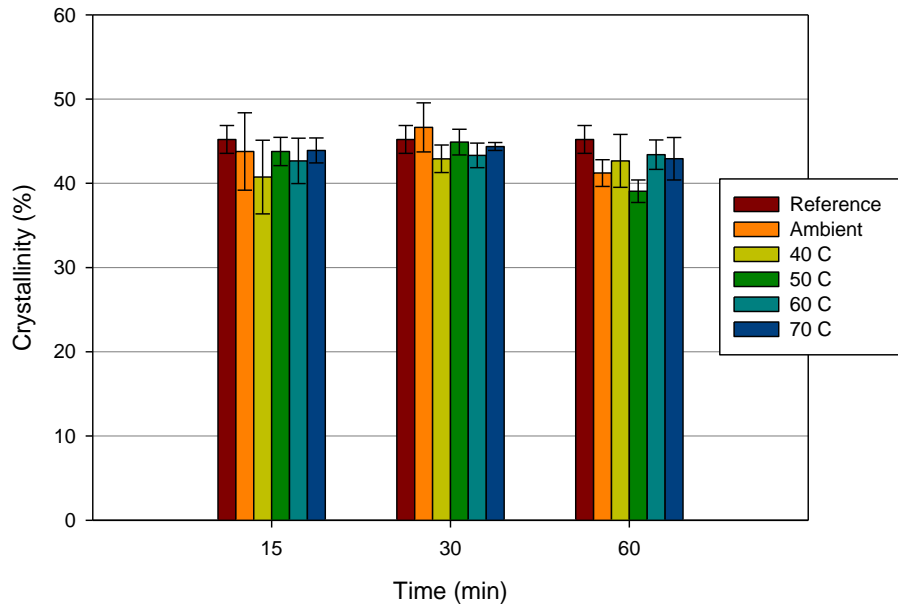


Figure 2.10 Crystallinity of commercial Dowlex 2036G LLDPE following swelling at different temperatures.

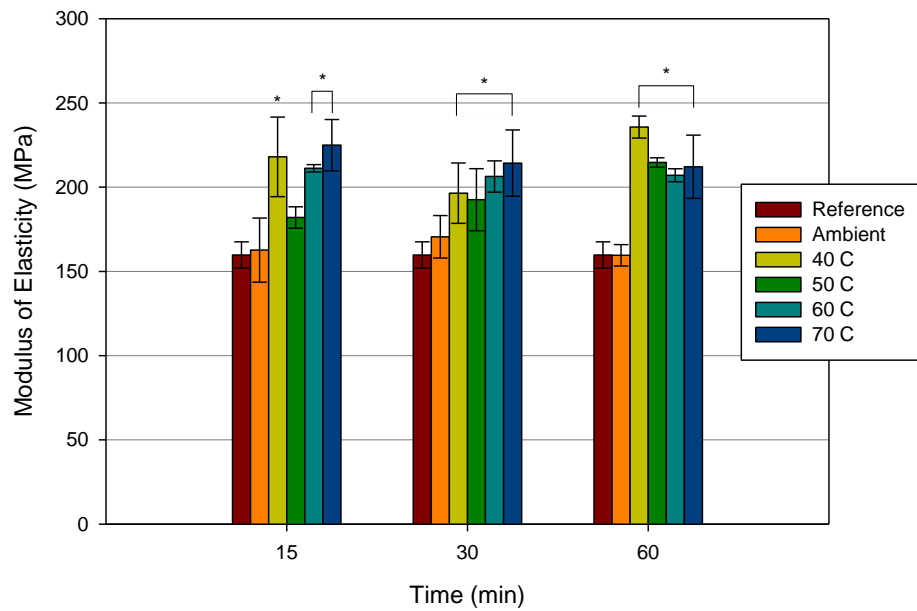


Figure 2.11 Modulus of Elasticity of commercial Dowlex 2036G LLDPE following swelling at different temperatures. An * indicates significant differences ($p < 0.05$) from LLDPE Reference.

The difference in the starting crystallinities of the Dowlex LLDPE films helps illustrate why there are different resulting effects of solvent swelling. With a higher initial crystallinity, the solvent would be able to penetrate less volume of the LLDPE film, providing for a lower degree of swelling and less opportunity of recrystallization at higher temperatures. The Dowlex 2056 which had the lowest initial crystallinity would allow for a higher degree of swelling. The heated solvents would swell the amorphous regions of the film, and allow it to recrystallize during cooling and solvent evaporation. The increase crystallinity would provide for higher modulus of elasticity and yield strength. Both of these phenomena were observed for this resin. An increase in yield strength is not concerning for our potential application in a heart valve, however, the increased modulus of elasticity would provide for a higher bending stiffness, rendering some of these films unusable. The observed increase in modulus of elasticity and yield strength of the Dowlex 2344 and 2036G with no increases in crystallinity can be explained by an increase in tie molecule (figure 2.12) density within the films. This density increase was not characterized but could be investigated more via shear rheometry.

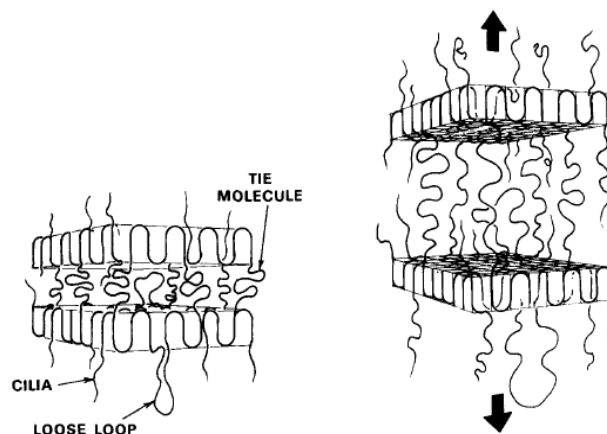


Figure 2.12 Initial steps in deformation of polyethylene. Increases in tie molecule density would increase modulus and yield without increased crystallinity[7]

The lack of swelling of the individual fibers of PET within the fabric prevented any change in mechanical properties for the fabric. Since the solvents only penetrated voids within the structure, drying the PET samples following the swelling removed any trace of solvents, returning the composition to its original state. Thus the crystalline structure remained unchanged during the swelling process as seen in Figure 2.13.

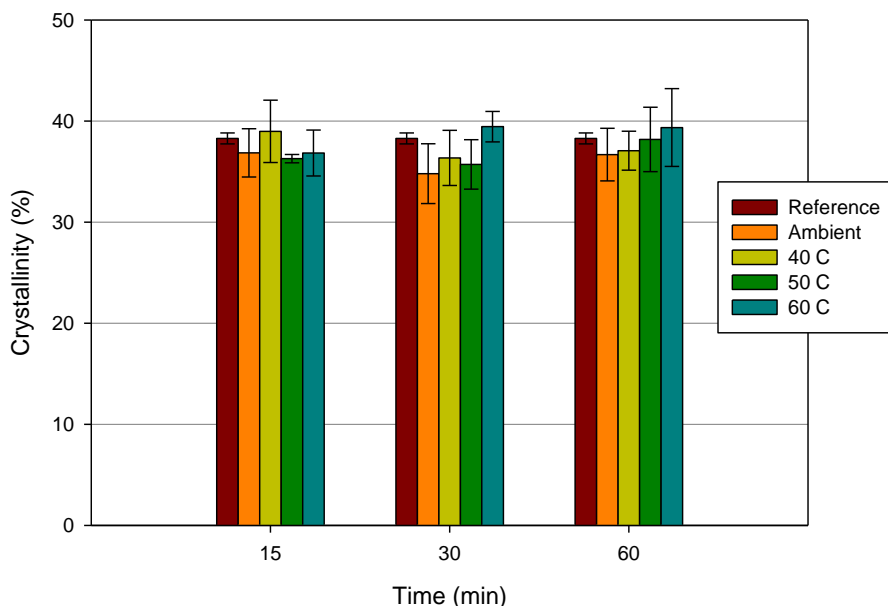


Figure 2.13 Crystallinity of commercial Dowlex 2036G LLDPE following swelling at different temperatures.

2.4 Conclusions

Xylenes provided the greatest degree of swelling in the Dowlex 2056 film. The 50°C temperature of swelling had the largest increase in degree of swelling for the Dowlex 2056 film and provided inconsistent swelling in the other films. For this reason, the Dowlex 2056 film was chosen as the LLDPE base polymer. The crystallinity changes

were largest at the higher temperatures, increasing modulus of elasticity. The percent volume change ($dV/V_0\%$) at 50 °C was equivalent to that at 60 °C at 45 and 60 minutes without the associated increase in crystallinity and modulus of elasticity. For this reason, 50°C was chosen for the swelling temperature for the LLDPE-HA material synthesis. These swelling parameters should enable the absorption of a silyl-HA-CTA and xylene solution without adversely affecting the mechanical characteristics of the base film, maintaining properties acceptable for a heart valve application.

With the dramatic increase in the degree of solvent absorption for the PET fabric over the LLDPE film, incorporation of HA into the structure via wicking transport should not be a concern. In addition to the much higher degree of solvent gain due to wicking, the PET was not affected by the time or temperature for the swelling parameters leading to what could be a quicker and lower temperature treatment process. Therefore, a treatment time of 15 minutes has been selected with the solvent solution at ambient temperature.

2.5 References

1. Beaugregard, G.P., *Synthesis and characterization of a biomimetic UHMWPE-based interpenetrating polymer network for use as an orthopedic biomaterial*, in *Mechanical Engineering*. 1999, Colorado State University: Fort Collins. p. 139.
2. Jin Ho, L. and L. Hai Bang, *A wettability gradient as a tool to study protein adsorption and cell adhesion on polymer surfaces*. *Journal of Biomaterials Science, Polymer Edition*, 1993. **4**(5): p. 467-481.
3. Wang, Y.-X., et al., *Effects of the Chemical Structure and the Surface Properties of Polymeric Biomaterials on Their Biocompatibility*. *Pharmaceutical Research*, 2004. **21**(8): p. 1362-1373.
4. Lee, J.H. and H.B. Lee, *Platelet adhesion onto wettability gradient surfaces in the absence and presence of plasma proteins*. *Journal of Biomedical Materials Research*, 1998. **41**(2): p. 304-311.
5. Akaike, T., *Advances in polymeric biomaterials science*. 1997: CMC Co., Ltd.
6. Elbert, D.L. and J.A. Hubbell, *Surface Treatments of Polymers for Biocompatibility*. *Annual Review of Materials Science*, 1996. **26**(1): p. 365-294.
7. Lustiger, A. and R.L. Markham, *Importance of tie molecules in preventing polyethylene fracture under long-term loading conditions*. *Polymer*, 1983. **24**(12): p. 1647-1654.

CHAPTER 3: SYNTHESIS AND CHARACTERIZATION OF THE HYALURONAN MICROCOMPOSITES

3.1 Introduction

In this chapter, specific aims 1 and 2 (see section 1.3) are addressed, to establish BioPoly manufacturing and to develop methods for manufacturing composite samples for cardiovascular applications. In the development of BioPoly HA-treated materials, the effects on the physical properties, chemical characteristics, and macroscopic appearance, which may affect BioPoly *in vitro* blood clotting, must be considered.

3.2 Materials and Methods

3.2.1 Materials

LLDPE Film (DOW Dowlex 2056, Melt Index: 1.0 g/10 min, Density: 0.920 g/cm³) was purchased from Flex-Pack Engineering Inc. (Uniontown, Ohio). Polyester Fabric (Style 6010 thin polyester tubular woven (uncrimped), nominal diameter of 22 mm and wall thickness of .010" ± .001") was purchased from BARD Peripheral Vascular OEM Products (Tempe, Arizona). Hexadecyltrimethylammonium bromide (CTAB), anhydrous dimethylsulfoxide (DMSO), poly(hexamethylene diisocyanate) (HMDI), hexamethyldisilazane (HMDS, 99.9%), toluidine blue O (TBO), and urea were purchased

from Sigma-Aldrich (Milwaukee, WI). Sodium hyaluronan (HA) (medical grade, EP grade, non-sterile, MW: 700 kDa) was purchased from Lifecore Biomedical (Chaska, MN) and stored at -15°C. Ethyl alcohol (ACS/USP grade) was purchased from AAPER (Shelbyville, KY). Xylenes, acetone, and sodium chloride (certified A.C.S.) were purchased from Fisher (Pittsburgh, PA). All H₂O was deionized. All chemicals were used as received unless otherwise specified.

3.2.1.1 Synthesis of HA-CTA and Silyl-HA-CTA

The methods of producing HA-CTA and silyl HA-CTA have previously been published^{18; 20}. The synthesis of silyl HA-CTA is briefly described here: DMSO was added to HA-CTA under dry N₂ flow; the solution was stirred at 50°C until the HA-CTA was completely dissolved. The HA-CTA and DMSO solution temperature was increased to 75°C and HMDS was added under dry N₂ flow; the reaction was carried out for 36 hours.

Once stirring ceased, the resultant two phase solution was separated and the top layer was saved and vacuum dried at 50°C (until no change in weight was observed); the bottom layer was discarded. The dry powder, silyl HA-CTA, was washed five times with xylenes. The silyl HA-CTA was dried in a 50°C vacuum oven (until no change in weight was observed).

3.2.2 Synthesis of the HA-treated materials

3.2.2.1 Swelling of silyl-HA-CTA into base polymers

All treated LLDPE BioPoly (LLDPE-T) samples were fabricated from blown LLDPE film. All treated PET BioPoly (PET-T) samples were fabricated from stretch knit PET. The synthesis parameters of LLDPE-T and PET-T samples are shown in Table 3.1.

Table 3.1 Table of synthesis parameters (n.a. – not applicable).

Sample	Conc. of silyl HA	Conc. Of Crosslinker	Hydrolysis	Dip with HA	Conc. Of HA
LLDPE-T	Silyl HA-CTA	HMDI	After Treatment	No	N/A
	0.5% w/v - 5 mg/ml	2%			
	1.5% w/v - 15 mg/ml				
	2.5% w/v - 25 mg/ml				
LLDPE-T-D	Silyl HA-CP	HMDI	Before HA Dip	Yes	1%
	0.5% w/v - 5 mg/ml	2%			
	1.5% w/v - 15 mg/ml				
	2.5% w/v - 25 mg/ml				
PET-T	Silyl HA-CTA	HMDI	After Treatment	No	N/A
	0.5% w/v - 5 mg/ml	2%			
	1.5% w/v - 15 mg/ml				
	2.5% w/v - 25 mg/ml				
PET-T-D	Silyl HA-CP	HMDI	Before HA Dip	Yes	1%
	0.5% w/v - 5 mg/ml	2%			
	1.5% w/v - 15 mg/ml				
	2.5% w/v - 25 mg/ml				

The HA treatment processes for LLDPE-T and PET-T differed due to the swelling kinetics (see section 1.2.3 and Figure 1.11). LLDPE film and PET fabric were soaked in xylenes for 12 hours and vacuum dried another 12 hours (or until no change in weight was observed) (*original weight was recorded*). The LLDPE films were then swelled at

50°C in a silyl-HA-CTA xylenes solution with a varying silyl-HA concentration, ranging from 0.5 to 2.5% (w/v) (*vide supra*) (to achieve a range of XL HA final bulk weight in the film) for 60 minutes, saturating the entire film sample. The treated LLDPE films were vacuum dried at 50°C for 3 hours (or until no change in weight was observed) (*weight gain was recorded*). The PET treatments differed due to the rapid swelling of the bulk fabric. Following the 12 hour xylenes wash and dry, the PET samples were then soaked in a silyl-HA-CTA xylenes solution with a varying silyl-HA concentration, ranging from 0.5 to 2.5% (w/v) (*vide supra*) (to achieve a range of XL HA final bulk weight in the fabric) at ambient temperature for 15 minutes, saturating the entire fabric sample. The treated PET fabric samples were vacuum dried at 50°C for 3 hours (or until no change in weight was observed) (*weight gain was recorded*).

The treated LLDPE films and PET fabric received the same hydrolysis process to revert the XL HA-CTA to XL HA (*vide infra*) (*weight loss was recorded*). (At this time the LLDPE and PET samples which did not have the final HA dip, were stored for testing.) Following hydrolysis, the LLDPE and PET samples requiring a final HA dip were dipped in a 1% (w/v) aqueous HA solution; the samples were submerged for several minutes to create an HA film on the surface. The dip coated sample was then vacuum dried at 50°C (until no change in weight was observed) (*weight gain was recorded*). The LLDPE and PET hydrolyzed, treated samples were then dipped in a 2% (v/v) poly(hexamethylene diisocyanate) xylenes solution and vacuum dried for 3 hours at 50°C, washed in acetone for 15 minutes, and vacuum dried at room temperature (until no change in weight was observed) (*weight gain was recorded*).

3.2.2.2 Crosslinking of the silyl-HA-CTA *in situ*

The treated LLDPE films were then swelled at 50 °C in a 2% (v/v) poly (hexamethylene diisocyanate) xylenes solution (i.e. HA crosslinking solution) for 60 minutes, and the crosslinker was cured in a vacuum oven at 50°C for 3 hours. The treated PET fabric samples were then soaked in a 2% (v/v) poly (hexamethylene diisocyanate) xylenes solution for 15 minutes at ambient temperature, and the crosslinker was cured in a vacuum oven at 50°C for 3 hours.

The treated samples were then washed with acetone to remove excess poly (hexamethylene diisocyanate) and vacuum dried at room temperature (until no change in weight was observed) (*weight gain was recorded*).

3.2.2.4 Conditioning/Hydrolysis

Before the final HA treatment, the treated samples were put through the following hydrolysis process (*vide infra*) to return silyl-HA-CTA to HA. The treated film and fabric samples were placed in a pre-heated 45°C 0.2M NaCl solution (H₂O:ethyl alcohol, 1:1) in an ultrasonic bath for 60 minutes. One hour later the hydrolyzing solution was changed, and the treated film and fabric samples were placed again in a fresh 0.2M NaCl solution and placed in an ultrasonic bath for 60 minutes. This solution change was repeated and the treated samples were again placed in the ultrasonic bath for 60 minutes. One hour later the hydrolyzing solution was changed, to a 0.2M NaCl aqueous solution (without ethyl alcohol), and the treated film and fabric samples were placed in an ultrasonic bath for 60 minutes. The treated film and fabric samples were immediately placed in an H₂O and ethyl alcohol ((v/v) 3:2) solution. Two hours later the treated film and fabric samples were placed in H₂O and placed in an ultrasonic bath for 30 minutes. The hydrolyzed

treated film and fabric samples were removed from the solution, washed with H₂O, and then soaked in acetone for 1 hour. The hydrolyzed treated samples were dried in a 50°C vacuum oven (until no change in weight was observed). A summary of the hydrolysis procedure for treated samples (i.e. BioPoly) is shown in Table 3.2.

Table 3.2 Hydrolysis procedure for silyl HA-CTA treated preforms (n.a. – not applicable).

Step	Total Time (hours)	Solution	Sonication Time (min)
1	1	0.2M NaCl (H ₂ O:ethyl alcohol (1:1))	60
2	1	0.2M NaCl (H ₂ O:ethyl alcohol (1:1))	60
3	1	0.2M NaCl (H ₂ O:ethyl alcohol (1:1))	60
4	1	0.2M NaCl aqueous	60
5	2	H ₂ O:ethyl alcohol (3:2)	n.a.
6	0.5	H ₂ O	30
7	1	Acetone	n.a.

3.2.3 Characterization of the HA-treated materials

3.2.3.1 Thermal Analysis

Differential Scanning Calorimetry (DSC): The % χ_c was measured by means of a TA Instruments Differential Scanning Calorimeter (DSC) 2920 in a dry N₂ atmosphere per ASTM D3418-03. Samples were heated from 24°C to 180°C at a rate of 10°C/minute, and held at equilibrium for one minute (all with N₂ atmosphere). The H_f was determined to be 288 J/g for 100 % crystalline PE and 113 J/g for 100% crystalline PET. The % χ_c of the sample was calculated by dividing the H_f of the sample by 288 J/g [1, 2] or 113 J/g [3] based on base polymer (because the 100 % crystalline H_f of BioPoly is unknown) and multiplying by 100. Sample control and treatment groups that were characterized: LLDPE virgin film, PET virgin fabric, LLDPE and PET sham controls,

and all LLDPE-T/PET-T samples. All reported average values and standard deviation for % χ_c were calculated from a sample size of three per group.

Thermo Gravimetric Analysis (TGA): The degradation temperatures (T_d) and composition of the samples were determined using a TA Instruments thermal gravimetric analyzer (TGA) 2950 at a heating rate of 10°C/minute in helium. Masses of individual specimens ranged from 5-15 mg. Sample control and treatment groups that were characterized: LLDPE virgin film, PET virgin fabric, LLDPE and PET sham controls, and all LLDPE-T/PET-T samples. All reported average values and standard deviations for compositions and T_d were calculated from a sample size of three per group.

3.2.3.2 Mechanical Evaluation

Tensile Tests: ASTM D882-10 standard tensile specimens of film thickness were stamped out of treated LLDPE samples and an electromechanical Tinius Olsen UTM axial test system (Horsham, PA) was used in conjunction with Test Navigator software from Tinius Olsen to perform all tensile tests; a uniaxial (tension/ compression) 1000 N load cell (Model H1K-S) was used. Five tensile bars were stamped out of each sample. Two tensile bars were used for the modulus test for each treatment group, while three tensile bars were used for the measurement of yield strength, tensile strength and elongation to failure for each treatment group. Composites were pulled at a crosshead speed of 500 mm/minute (these strain rates follow the ASTM standard which states that the time to failure of a polymeric sample must fall within a certain time limit; this can be adjusted for different materials by changing the strain rate). Elongation data was calculated from crosshead data (the change in gage length was divided by the original

gage length of the sample, which is specified in the standard). All samples were placed in diH₂O for 60 minutes, allowing the HA to hydrate.

Bending Stiffness: The ASTM D1388-08 testing standard was used to determine the bending modulus of the LLDPE and PET samples. Bending specimens were stamped out of treated LLDPE and PET samples and a Shirley Stiffness Tester (Model M003B) was used. One sample of each treatment group was used to measure bending stiffness at both ends, on opposite faces for a total of four measurements per sample group. The samples were exposed to the standard atmosphere for conditioning for at least 24 hours or until the mass of the specimen did not change by more than 0.25% in 2 hour intervals. Samples were then placed in diH₂O for 60 minutes, allowing the HA to hydrate. Specimens were slid at a uniform rate until the bending length is determined. This was used to calculate the flexural rigidity G (mg/cm):

$$G = 0.10MC^3$$

where

M = Mass per unit area (g/m²)

C = Bending length (cm)

The bending modulus K (kg/cm²) is then given by the following formula:

$$K = \frac{12G * 10^{-6}}{t^3}$$

where

G= Flexural rigidity (mg/cm)

t = Sample thickness (cm)

3.2.4 Statistics

Statistics were analyzed using SigmaStat software (Systat Software Inc.; Richmond, CA). A single-factor ANOVA test with a 95% confidence interval was performed; multiple comparisons were performed via the Holm-Sidak method when sample population standard deviations and population sample sizes were similar. Average values and standard deviation for all treatment group populations were calculated.

3.3 Results and Discussion

3.3.1 Sample Synthesis

Crosslinked HA weight percentages (where applicable) for all LLDPE and PET composites are summarized in Tables 3.5 and 3.6.

Table 3.5 Crosslinked HA composition of treated LLDPE samples (n.a. – not applicable).

Treatment Group	Bulk Weight % XL HA	Surface Weight % XL HA
LLDPE-T-0.5	0.507 ± 0.01	n.a.
LLDPE-T-1.5	1.32 ± 0.18	n.a.
LLDPE-T-2.5	1.00 ± 0.07	n.a.
LLDPE-T-0.5-D	0.542 ± 0.05	0.035 ± 0.01
LLDPE-T-1.5-D	1.47 ± 0.37	0.146 ± 0.01
LLDPE-T-2.5-D	1.05 ± 0.22	0.043 ± 0.01

Table 3.6 Crosslinked HA composition of treated PET samples (n.a. – not applicable).

Treatment Group	Bulk Weight % XL HA	Surface Weight % XL HA
PET-T-0.5	0.242 ± 0.02	n.a.
PET-T-1.5	0.973 ± 0.18	n.a.
PET-T-2.5	1.228 ± 0.07	n.a.
PET-T-0.5-D	1.260 ± 0.26	1.018 ± 0.002
PET-T-1.5-D	1.996 ± 0.13	1.023 ± 0.002
PET-T-2.5-D	3.510 ± 1.21	2.283 ± 0.012

The reported values were determined from weight loss/gain calculations measured throughout the treatment processes and confirmed using TGA. PET samples comprised of high weight percentages of crosslinked HA exhibited an increased bending stiffness when dry. This affect, however, was removed once the sample was placed in solution, allowing the HA to swell and become lubricious.

3.3.2 Characterization of the HA-treated materials

3.3.2.1 Thermal Analysis

Differential Scanning Calorimetry (DSC): The percent crystallinity of treatment groups LLDPE-T and PET-T versus controls are listed below in Tables 3.7 and 3.8.

Table 3.7 Crystallinity of LLDPE controls, and HA treated samples (average \pm std. dev.).

Treatment Group	% X _c
LLDPE-Ref	28.14 \pm 2.36
LLDPE-T-0.5	32.97 \pm 1.07
LLDPE-T-0.5-Dip	31.54 \pm 1.12
LLDPE-T-1.5	30.13 \pm 1.88
LLDPE-T-1.5-Dip	31.74 \pm 3.01
LLDPE-T-2.5	32.66 \pm 2.31
LLDPE-T-2.5-Dip	31.86 \pm 1.59

Table 3.8 Crystallinity of PET controls, and HA treated samples (average \pm std. dev.).

Treatment Group	% X _c
PET-Ref	38.28 \pm 0.54
PET-T-0.5	38.98 \pm 3.09
PET-T-0.5-Dip	36.28 \pm 0.42
PET-T-1.5	34.30 \pm 0.13
PET-T-1.5-Dip	33.51 \pm 3.91
PET-T-2.5	39.44 \pm 1.51
PET-T-2.5-Dip	39.36 \pm 3.85

The crystallinity of the LLDPE film was not significantly altered during the treatment process in comparison to the reference film. The thermal processing (i.e. swelling) of LLDPE film was maintained by the selected swelling parameters. The lack of swelling of the individual fibers of PET within the fabric prevented any change in crystallinity for the fabric. Since the silyl-HA-CTA solution only penetrated voids within the structure, drying the PET samples following the swelling removed any trace of solvents, returning the composition to its original state with the exception of the additional silyl-HA-CTA. Thus, the crystalline structure remained unchanged during the swelling process.

Thermo Gravimetric Analysis (TGA): Synthesis of multiple HA-Treated Materials with differing quantities of HA was successful with a range from 0.5 to 1.5% HA for LLDPE samples (Figure 3.1) and from 0.25 to 3.5% HA for PET (Figure 3.3).

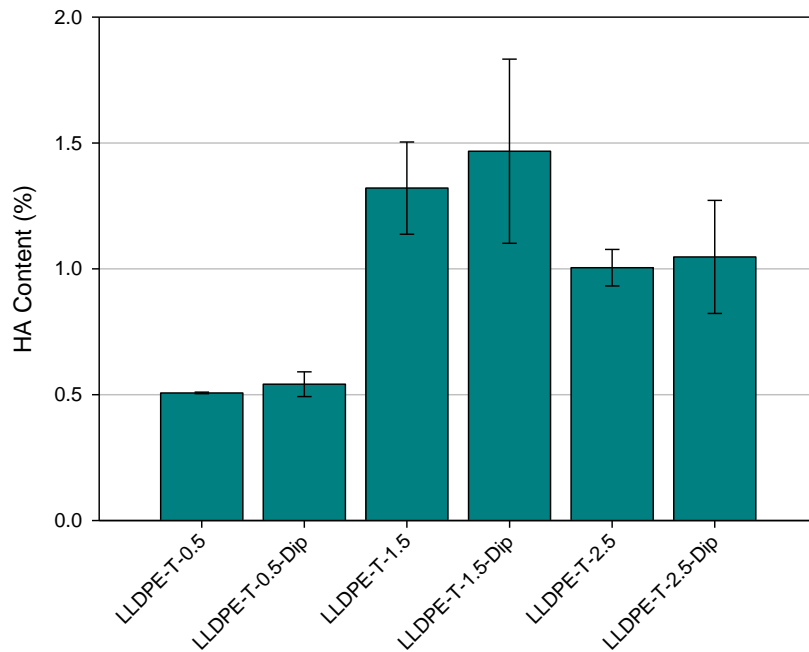


Figure 3.1 HA Content (by weight %) for treated LLDPE samples.

An expected increase in HA concentration was seen when going from LLDPE-T-0.5 samples to LLDPE-T-1.5 samples due to the increased swelling solution concentration. However, this increase was not observed when increasing from LLDPE-T-1.5 samples to LLDPE-T-2.5 samples. The concentration of HA in the composite decreased by ~33%. This observation can be described by the high viscosity of the swelling solution. With the higher concentration of silyl-HA-CTA in xylenes during swelling, the viscosity continues to increase linearly as seen in Figure 3.2 [4].

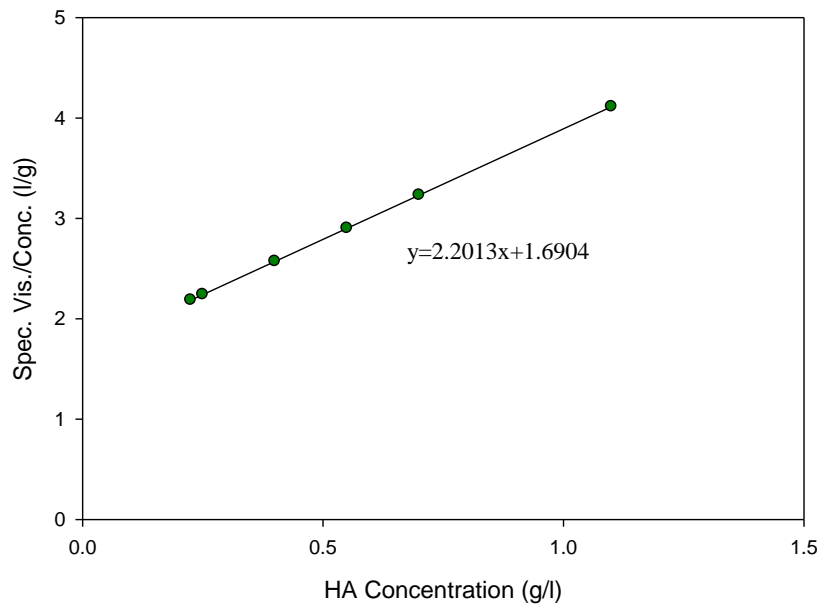


Figure 3.2 Viscosity of HA solution

With this increase in swelling solution viscosity, it is concluded that the swelling of the LLDPE sample was only able to diffuse into the outer polymer structure. While not obtaining the highest concentration of HA, it is thought that the HA that was incorporated into the structure is concentrated at the surface region, potentially providing superior hydrophilicity and hemocompatibility.

The addition of post treatment dip coating of HA did not significantly increase the %HA concentration of the samples. The process used for dip coating was very difficult to control uniformity of coating application, increasing the overall variance. It is expected that the samples that had the highest HA content based on the non-dipped samples, would gain the highest amount of HA through a successful surface dip of HA. With a higher bulk concentration of HA, the additional dip applied via the dipping process would have more attached HA to link to. Further development is needed in order to provide a successful, uniform HA surface application through the dipping process. The samples examined above were removed from the aqueous HA solution and hung horizontally in a vacuum oven in an attempt to prevent the HA attaching to any surface the samples were placed on. Due to this apparatus, droplets of the HA solution collected at any low point of the film, consolidating and dripped off. This consequently prevented a uniform application of HA to the surface. To counter act this, the film samples could be left in a petri dish of the aqueous HA solution placed in a vacuum oven at 50°C until the water had evaporated, leaving a uniform coating of HA.

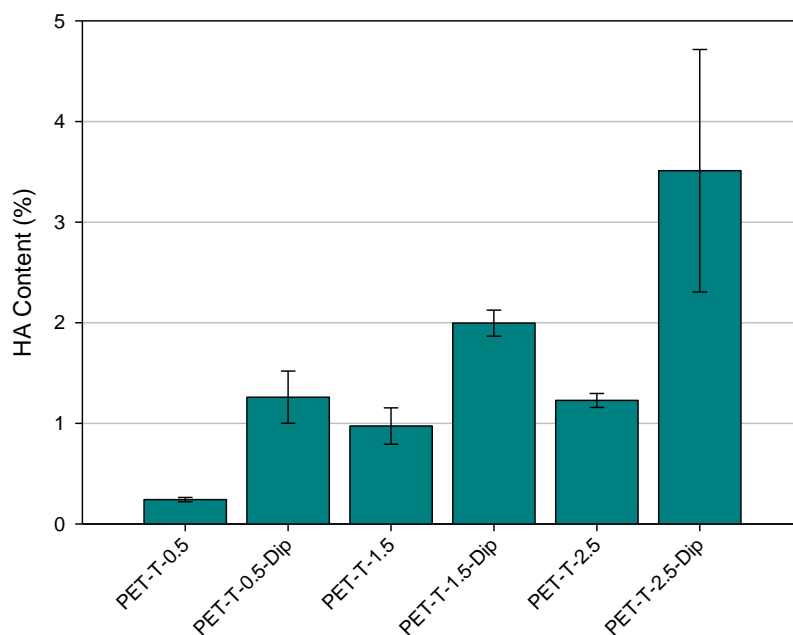


Figure 3.3 HA Content (by weight %) for treated PET samples.

Expected increases in HA concentration were seen with increasing concentration of the swelling solution. The increased viscosity of the solution, which affected the LLDPE samples, was not seen due to the much higher degree of swelling seen in the PET samples. The high degree of swelling seen in Chapter 2 and the high porosity of the fabric allows for easy absorption of the swelling solution. Since the solution was penetrating the voids between fibers and yarns, it is known that the infiltration of the silyl-HA-CTA swelling solution was full thickness, and assumed to be uniform distribution.

Post treatment dip coating did prove to significantly increase the HA concentration in the PET samples. Again, because of the high degree of swelling associated with the PET, the dip coating fully penetrated the fabric structure and easy to control uniformity. The surface dip treatments of the samples are more of a secondary,

full thickness dip due to the swelling kinetics of the fabric. Therefore, the additional HA applied is not concentrated only at the surface as in the LLDPE samples.

3.3.2.2 Mechanical Evaluation

Tensile Tests: The tensile properties of treatment groups LLDPE-T versus controls are shown in Figures 3.4 and 3.5 and Table 3.9. All samples were pulled at a strain rate of 500 mm/minute. Percent elongation values were calculated from crosshead displacement.

Small increases in yield strength were observed among all treatment groups but were not enough of an increase to warrant concern for cardiovascular applications. The modulus is the property of most concern with the LLDPE film. Only the T-1.5 treatment group had a significantly ($p \leq 0.05$) higher modulus (99.71 MPa) compared to Reference film (73.82 MPa). All other sample groups were not significantly different from each other. These small increases are associated with the small, but not significant increases in crystallinity (Table 3.7). Samples were tested both dry and with full HA hydration to determine the impact of HA hydration on the tensile properties. The relatively small amount of HA present within the material kept the mechanical properties from being altered when fully hydrated. The following results are for the dry samples.

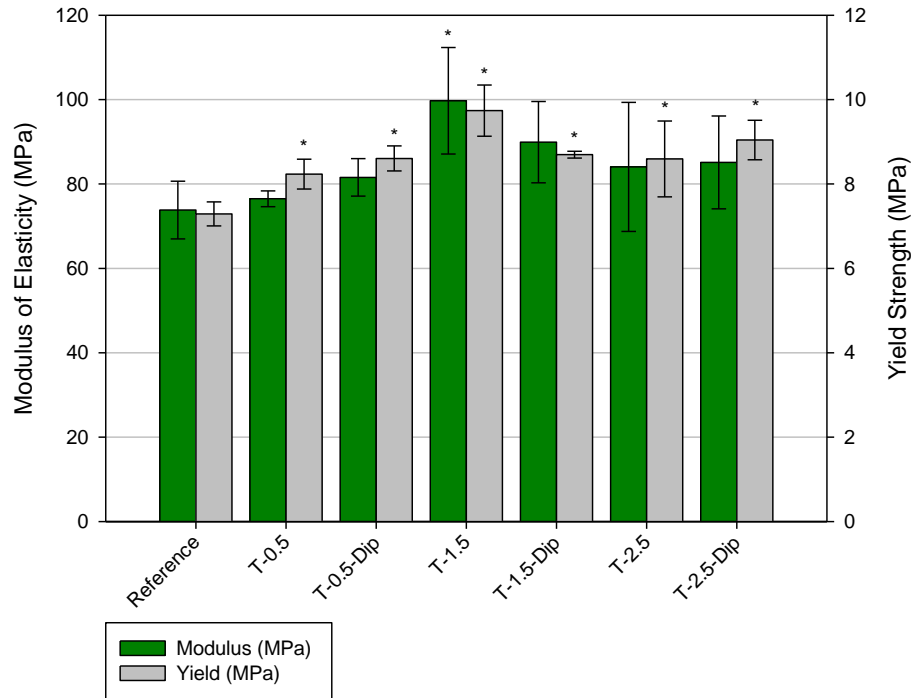


Figure 3.4 Modulus of Elasticity and Yield Strength of Reference LLDPE film and treated LLDPE samples using treatment parameters listed in Table 3.1. An * indicates significant differences ($p < 0.05$) from LLDPE Reference.

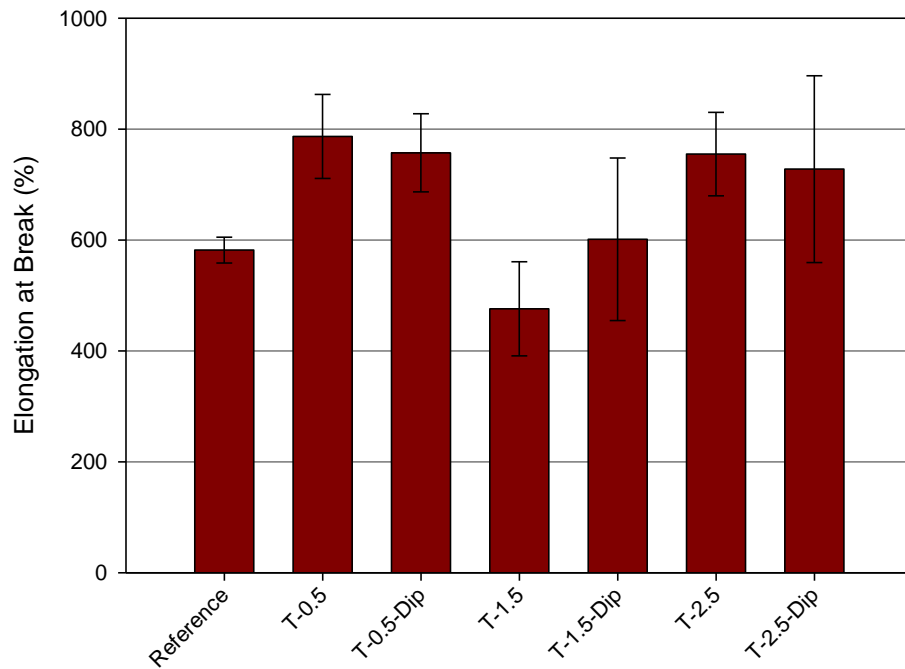


Figure 3.5 Elongation to Failure of Reference LLDPE film and treated LLDPE samples using treatment parameters listed in Table 3.1.

No significant changes in the elongation to failure were observed in the treated LLDPE films. The variation in the elongation was increased with the treatment process, which is not concerning since all films still exceeded any elongation that would be seen in a physiological environment [5]. Statistical significance is shown in Table 3.9, which summarizes tensile data and % χ_c for LLDPE reference film and treated LLDPE samples; starred values (*) represent a significant difference ($p \leq 0.05$) compared to the reference film.

Table 3.9 Mechanical properties and % χ_c of control and treated LLDPE samples (see table 3.1 for treatment parameters); (average \pm std. dev.)

	Modulus (MPa)	Yield (MPa)	% Elongation	% χ_c
Reference	73.82 \pm 6.83	7.29 \pm 0.29	582 \pm 23	28.14 \pm 2.36
T-0.5	76.49 \pm 1.86	8.23 \pm 0.35*	787 \pm 76	32.97 \pm 1.07
T-0.5-Dip	81.56 \pm 4.44	8.61 \pm 0.30*	757 \pm 70	31.54 \pm 1.12
T-1.5	99.71 \pm 12.62*	9.74 \pm 0.61*	476 \pm 85	30.13 \pm 1.88
T-1.5-Dip	89.92 \pm 9.64	8.70 \pm 0.08*	601 \pm 147	31.74 \pm 3.01
T-2.5	84.05 \pm 15.30	8.59 \pm 0.90*	755 \pm 75	32.66 \pm 2.31
T-2.5-Dip	85.12 \pm 11.01	9.04 \pm 0.47*	728 \pm 168	31.86 \pm 1.59

Bending Stiffness: Mechanical characterization of the PET fabric required bending stiffness analysis rather than tensile testing due to the weave structure of the fabric [6]. LLDPE was also characterized using the same bending stiffness protocol since bending stiffness is the principal property of concern for heart valve applications. The resulting bending stiffness of LLDPE and PET treatment groups versus controls are shown in Figures 3.6 and 3.7. The comparison is also made to stiffness values for native valve leaflets and glutaraldehyde fixed xenograft leaflets reported by Vesely et al. to confirm that the treated specimen were within physiological ranges [7]. Bending stiffness values were calculated from the bending length and known densities.

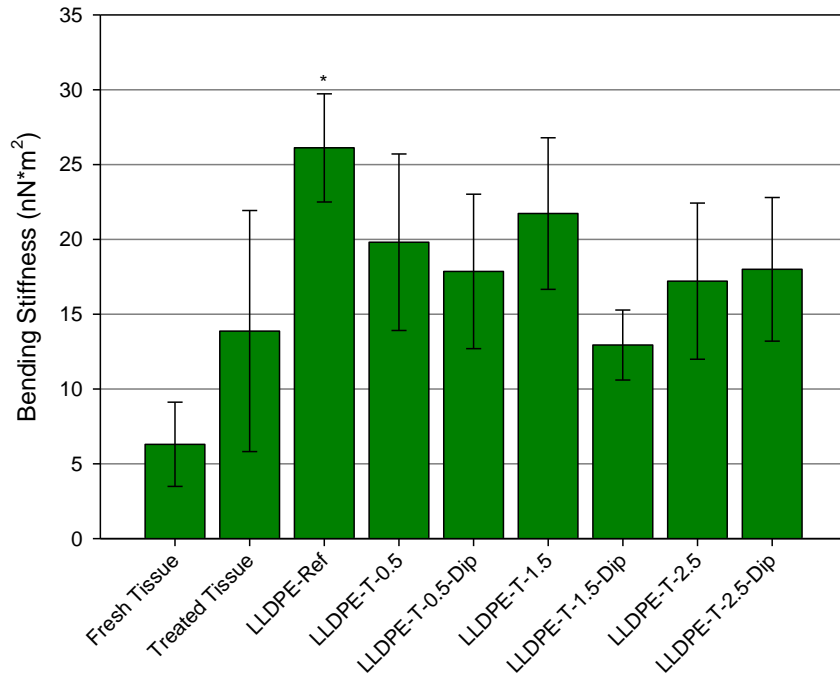


Figure 3.6 Bending stiffness values for reference tissue and all treated and untreated LLDPE samples using treatment parameters listed in Table 3.1. An * indicates significant differences ($p < 0.05$) from LLDPE Reference.

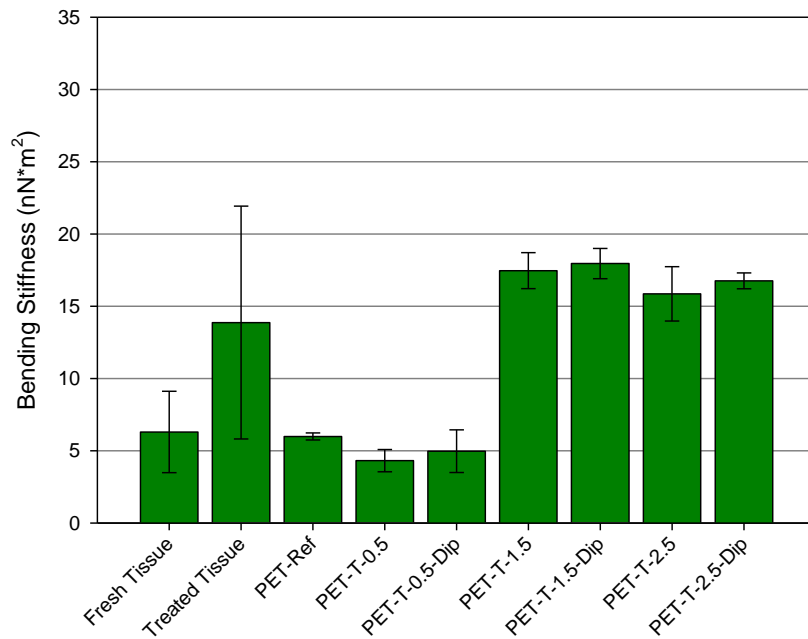


Figure 3.7 Bending stiffness values for reference tissue and all treated and untreated PET samples using treatment parameters listed in Table 3.1.

The bending stiffness' of the LLDPE samples were within the physiological range of the native tissue and glutaraldehyde fixed xenograft tissue with the exception of the untreated reference film. No significant differences were seen between the treatment groups, indicating that the incorporation of HA into the polymer matrix would have acceptable bending properties with any of the tested HA concentrations for a heart valve application. The hydration of the HA via solution swelling did not affect the bending stiffness. The bending stiffness of glutaraldehyde treated tissue can be up to four times greater than fresh tissue. This increased bending stiffness of the treated tissue may ultimately lead to the observed leaflet tearing, calcification and eventual failure of the xenograft due to the anisotropy of the tissue [7]. With the isotropic LLDPE, this fatigue failure is not a concern. Calcification of the material could be avoided with the HA treatment of the LLDPE but should be examined.

The increased bending stiffness of the treated PET fabric containing $\geq 1.0\%$ HA is likely correlated to the linking of fibers by the HA and not a simple stiffening of the fibers as seen in the glutaraldehyde fixed xenografts. The glutaraldehyde alters the complex mechanical interactions existing between the tissue constituents that are responsible for the unique flexibility of the normal valve [7]. The lubrication and expansion of the HA with exposure to a solution reduced the observed bending stiffness and could assist in prevention of fiber fatigue and frictional stress between fibers.

3.4 Conclusions

Integration of HA into the base matrix was successful for both LLDPE film and PET fabric. The LLDPE film had a smaller range of HA concentrations due to the low porosity of the material and the increased viscosity of the swelling solution. This accounts for the reduced dV/V_0 compared to that seen in Chapter 2. The addition of an HA surface dip was successful in placing additional HA on the surface of the film. However, the surface dip was not distributed uniformly due to the approach taken for water evaporation. Potential changes to the dipping application discussed above would likely improve the process to avoid this non-uniform distribution.

The PET fabric demonstrated a higher amount of HA concentration controllability. The wicking of the swelling solution into the voids of the structure was unaffected by increases in solution viscosity. The surface dip of the fabric was successful in additional HA integration, however, it was integrated throughout the entire structure and not concentrated at the surface.

For subsequent research, the characterized HA-treated materials will be addressed based on their HA content and if they received the additional surface dip (SD). The sample identifications can be seen in Table 3.10 and 3.11.

Table 3.10 Sample Identification for subsequent testing of LLDPE samples

Treatment Group	Sample Identification	Bulk Weight % XL HA	Surface Weight % XL HA
LLDPE-Ref	LLDPE-Reference	n.a.	n.a.
LLDPE-T-0.5	LLDPE + 0.5%HA	0.507 ± 0.01	n.a.
LLDPE-T-2.5	LLDPE + 1.0%HA	1.00 ± 0.07	n.a.
LLDPE-T-1.5	LLDPE + 1.3%HA	1.32 ± 0.18	n.a.
LLDPE-T-0.5-Dip	LLDPE + 0.5%HA + SD	0.542 ± 0.05	0.035 ± 0.01
LLDPE-T-2.5-Dip	LLDPE + 1.0%HA + SD	1.05 ± 0.22	0.043 ± 0.01
LLDPE-T-1.5-Dip	LLDPE + 1.5%HA + SD	1.47 ± 0.37	0.146 ± 0.01

Table 3.11 Sample Identification for subsequent testing of PET samples

Treatment Group	Sample Identification	Bulk Weight % XL HA	Surface Weight % XL HA
PET-Ref	PET-Reference	n.a.	n.a.
PET-T-0.5	PET + 0.25%HA	0.242 ± 0.02	n.a.
PET-T-1.5	PET + 1.0%HA	0.973 ± 0.18	n.a.
PET-T-2.5	PET + 1.2%HA	1.228 ± 0.07	n.a.
PET-T-0.5-Dip	PET + 1.3%HA + SD	1.260 ± 0.26	1.018 ± 0.002
PET-T-1.5-Dip	PET + 2.0%HA + SD	1.996 ± 0.13	1.023 ± 0.002
PET-T-2.5-Dip	PET + 3.5%HA + SD	3.510 ± 1.21	2.283 ± 0.012

Native valves must function such that the stresses generated within the material are low enough to prevent fatigue failure during the normal lifetime of a healthy valve. One of the factors reducing stresses is its extreme pliability. The pliability of both of these HA-treated materials exhibit behaviors that make them preferable for leaflet replacements, if proven to be hemocompatible.

3.5 References

1. Wang, Y.-X., et al., *Effects of the Chemical Structure and the Surface Properties of Polymeric Biomaterials on Their Biocompatibility*. Pharmaceutical Research, 2004. **21**(8): p. 1362-1373.
2. Lee, J.H. and H.B. Lee, *Platelet adhesion onto wettability gradient surfaces in the absence and presence of plasma proteins*. Journal of Biomedical Materials Research, 1998. **41**(2): p. 304-311.
3. Jin Ho, L. and L. Hai Bang, *A wettability gradient as a tool to study protein adsorption and cell adhesion on polymer surfaces*. Journal of Biomaterials Science, Polymer Edition, 1993. **4**(5): p. 467-481.
4. Zhang, M., *Surface Modification of Ultra High Molecular Weight Polyethylene With Hyaluronan For Total Joint Replacement Application*, in *Mechanical Engineering*. 2005, Colorado State University: Fort Collins.
5. Grashow, J.S., Yoganathan, and Sacks, *Biaxial Stress-Stretch Behavior of the Mitral Valve Anterior Leaflet at Physiologic Strain Rates*. Annals of Biomedical Engineering, 2006. **34**(2): p. 315-325.
6. Standard, A., *Standard Test Method for Stiffness of Fabrics*. 2008, ASTM International: West Conshohocken, PA.
7. Vesely, I. and D. Boughner, *Analysis of the bending behaviour of porcine xenograft leaflets and of natural aortic valve material: Bending stiffness, neutral axis and shear measurements*. Journal of Biomechanics, 1989. **22**(6-7): p. 655-659, 661-671.

CHAPTER 4: EVALUATION OF THE MICROCOMPOSITES' BIOCOMPATIBILITY

4.1 Introduction

Interactions of various blood components with a biomaterial are initiated at implantation. Therefore, it is extremely important to understand the biocompatibility of the HA-treated materials. The materials must not cause certain events such as adhesion, platelet aggregation, blood coagulation or fibrin deposition. Therefore it is useful to study the hemocompatibility of these composites in an *in vitro* environment to understand basic interactions that will take place.

The LLDPE and PET HA-treated materials synthesized in Chapter 3 take advantage of the natural anti-thrombotic properties of HA. It was investigated if the HA-treated materials are inherently non-thrombogenic and actively participate in the inhibition of platelet adhesion.

In this chapter, specific aim 3 (see section 1.3) is addressed, to optimize the HA-treated material compositions for blood-contact to avoid thrombus formation for cardiovascular applications. In the development of BioPoly HA-treated materials, the effects on the physical properties, chemical characteristics, and macroscopic appearance, which may affect the *in vitro* blood clotting, must be considered.

4.2 Materials and Methods

4.2.1 Materials

LLDPE Film (DOW Dowlex 2056, Melt Index: 1.0 g/10 min, Density: 0.920 g/cm³) was purchased from Flex-Pack Engineering Inc. (Uniontown, Ohio). Polyester Fabric (Style 6010 thin polyester tubular woven (uncrimped), nominal diameter of 22 mm and wall thickness of .010" ± .001") was purchased from BARD Peripheral Vascular OEM Products (Tempe, Arizona). Hexadecyltrimethylammonium bromide (CTAB), anhydrous dimethylsulfoxide (DMSO), poly(hexamethylene diisocyanate) (HMADI), hexamethyldisilazane (HMDS, 99.9%), toluidine blue O (TBO), and urea were purchased from Sigma-Aldrich (Milwaukee, WI). Sodium hyaluronan (HA) (medical grade, EP grade, non-sterile, MW: 700 kDa) was purchased from Lifecore Biomedical (Chaska, MN) and stored at -15°C. Ethyl alcohol (ACS/USP grade) was purchased from AAPER (Shelbyville, KY). Xylenes, acetone, and sodium chloride (certified A.C.S.) were purchased from Fisher (Pittsburgh, PA). All H₂O was deionized. All chemicals were used as received unless otherwise specified. The method of producing HA-CTA has previously been published (see section 3.2.1.1 for synthesis methods).

The synthesis of silyl HA-CTA is briefly described here: DMSO was added to HA-CTA under dry N₂ flow; the solution was stirred at 50°C until the HA-CTA was completely dissolved. The HA-CTA and DMSO solution temperature was increased to 75°C and HMDS was added under dry N₂ flow; the reaction was carried out for 36 hours.

Once stirring ceased, the resultant two phase solution was separated and the top layer was saved and vacuum dried at 50°C (until no change in weight was observed); the bottom layer was discarded. The dry powder, silyl HA-CTA, was washed five times with

xylenes. The silyl HA-CTA was dried in a 50°C vacuum oven (until no change in weight was observed).

The same methods previously described (see section 3.2.2) were applied to create the LLDPE-HA and PET-HA materials. Briefly, LLDPE film and PET fabric were soaked in xylenes for 12 hours and vacuum dried another 12 hours. The LLDPE films were swelled at 50 °C in a silyl-HA-CTA xylenes solution with specified concentration for 60 minutes, then treated LLDPE films were vacuum dried at 50°C for 3 hours. The PET samples were soaked in a silyl-HA-CTA xylenes solution with specified concentration at ambient temperature for 15 minutes, and then the treated PET fabric samples were vacuum dried at 50°C for 3 hours. The treated LLDPE films were swelled at 50 °C in a HA crosslinking solution for 60 minutes, the treated PET fabric samples were then in a HA crosslinking solution for 15 minutes at ambient temperature after which the crosslinker was cured in a vacuum oven at 50°C for 3 hours.

All samples were hydrolyzed using the parameters in Table 3.2 to revert the XL HA-CTA to XL HA. Samples that received an additional HA dip coating were placed in an aqueous HA solution for 15 minutes, dried and crosslinked. All samples remained in a 50°C vacuum oven until use. All samples were conditioned in diH₂O for 24 hours before any testing. It is crucial to allow the HA to hydrate in order to observe any changes or benefits associated with the HA incorporation.

4.2.2 Surface Contact Angle

Static water contact angles were measured for the LLDPE samples using the sessile drop method with a Krüss DSA 10 goniometer (KRÜSS GmbH, Hamburg). At room temperature, a diH₂O drop with a known volume (3 µl) was applied to the sample

surface through the automatic dosing feature of DSA 10. The contact angles were determined with circle fitting profile after the video system imaged the H₂O drop (time duration was approximately two seconds). Two different locations on each sample surface were tested; sample size was three per group. The contact angle was recorded immediately after the droplet of fluid had been placed on the sample surface. The following samples were characterized: cast HA film, LLDPE-Ref, and all LLDPE-T samples (with and without final HA dip with several HA concentrations). PET samples were not tested due to the morphology of the weave producing unreliable results. A TBO stain was used to identify the integration of HA (*vide infra*).

4.2.3 Toluidine Blue O (TBO)

A 0.1% TBO solution (in 8M urea) was added drop wise to the surface of samples. After 10 minutes the TBO solution was rinsed away with H₂O, leaving behind only bound TBO. Three samples from each treatment group were photographed. The following samples were characterized: PET-Ref and all PET-T samples (with and without final HA dip with several HA concentrations). The TBO dye binding assay provides a convenient, nondestructive assay for bound hyaluronan [1].

4.2.4 *In Vitro* Study

4.2.4.1 Biocompatibility of LLDPE-HA and PET-HA Materials

Reference LLDPE and PET samples as well as all treated LLDPE and PET samples were sterilized via ethanol and UV methods and placed in sterile 24-well plates containing sterile saline for 24 hours to enable sample hydration. Whole blood was drawn from a healthy adult with no clotting disorders into a 50 ml tube. The first 10 ml was discarded to prevent contamination from the tissue thromboplastin activated by the

needle puncture. Five μl of whole blood was placed onto the surface of each specimen. At identified time points (30 min and 60 min), samples were placed into a designated within a secondary sterile 24-well plate containing 500 μl diH₂O. Special care was required to prevent disturbing the droplet of blood. Once placed in the diH₂O, the well plates were agitated for 30 seconds, then sat for a total of 5 minutes. Samples were then removed from the water filled well plates and placed in a dry, sterile well plate to be processed for scanning electron microscopy (SEM).

Once all samples had completed the testing, 200 μl of the water/blood mixture from each well plate was placed into a 96-well plate for examination with a BMG Labtech FLOUstar Omega plate Reader. A designated absorbance program was run using the plate reader. The red blood cells that were not trapped in a thrombus were lysed with the addition of distilled water, thereby releasing hemoglobin into the water for subsequent measurement. The concentration of hemoglobin in solution was assessed by measuring the absorbance at 540nm with 20 flashes per well. Omega MARS Data Analysis Software was used to determine the free hemoglobin in terms of absorbance. The size of the clot is inversely proportional to the absorbance value. The well plates containing the HA-treated materials and reference samples were placed in a desiccator until dry for SEM imaging. Tests were performed on 5 samples from each sample group, for each time point.

4.2.4.2 Scanning Electron Microscopy (SEM)

Unmodified LLDPE and PET, and treated LLDPE and PET samples were imaged using SEM. The surface was coated with 10 nm of gold. Prepared specimens were stored in a vacuum oven at room temperature prior to imaging; images were taken using a JOEL

JSM-6500F field emission SEM (Tokyo, Japan). Images of the samples and the HA dipped surfaces were taken at 25x, 500x, 1000x and 5000x at 15.0 keV. One sample per group was selected for SEM analysis.

4.3 Results and Discussion

4.3.1 Surface Contact Angle

Aqueous contact angle measurements indicated that carboxylate groups (i.e. the salts and anions of carboxylic acids) were present and did effect the surface properties of the HA treated composites (see Table 4.1).

Table 4.1 Aqueous contact angle measurements of samples verse controls at 10 minutes.

Sample	Aqueous Contact Angle (°)
LLDPE-Reference	86.7 ± 2.3
LLDPE + 0.5%HA	62.3 ± 2.6
LLDPE + 1.0%HA	54.4 ± 1.0
LLDPE + 1.3%HA	42.5 ± 2.7
LLDPE + 0.5%HA + SD	39.0± 1.1
LLDPE + 1.0%HA + SD	39.1 ± 5.9
LLDPE + 1.5%HA + SD	43.5 ± 6.7

The aqueous contact angles of those composites which had a final HA dip were significantly different compared to the contact angle of film that did not receive the additional dip treatment with the exception of the LLDPE + 1.3%HA and LLDPE + 1.5%HA + SD samples, however all samples still exhibited hydrophilic surfaces. The contact angle of the LLDPE control was very high exhibiting hydrophobic surfaces (Figure 4.1). All treated LLDPE sample groups exhibited significantly lower contact angles ($p \leq 0.05$) compared to reference LLDPE samples.

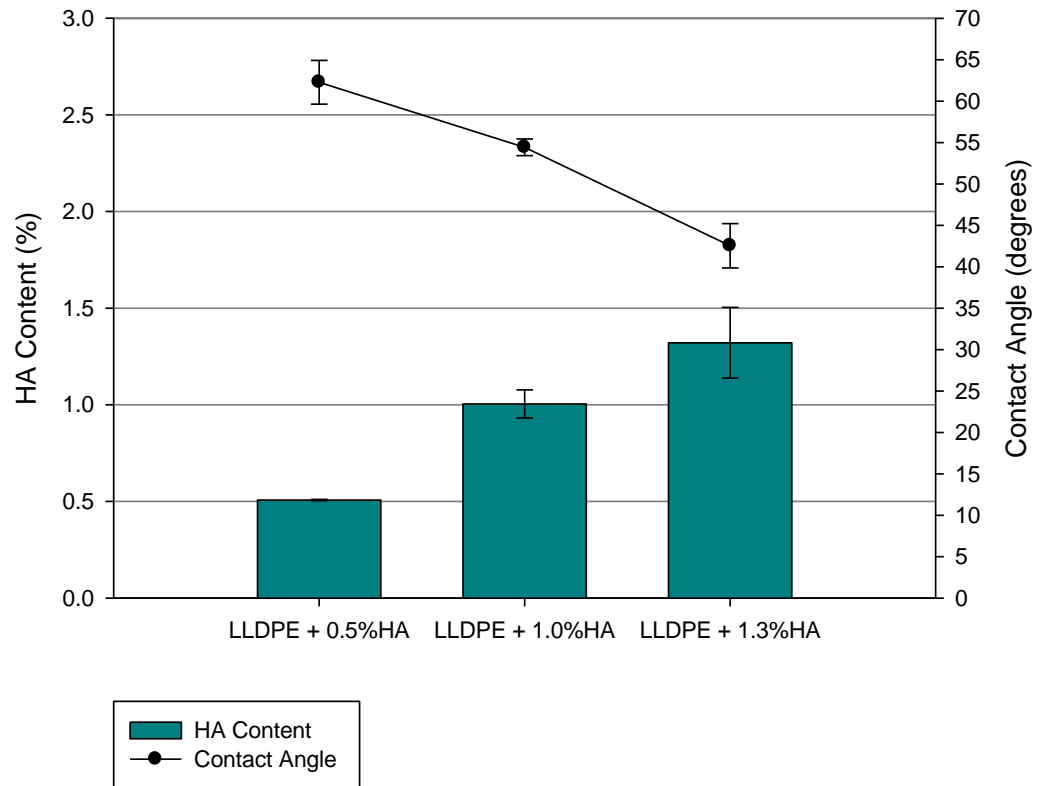


Figure 4.1 A correlation is shown between the HA content and the contact angle for the treated LLDPE samples that did not receive an additional HA dip.



Figure 4.2 Untreated LLDPE (left) and LLDPE+1.3%HA (right) films 10 minutes after drop placement.

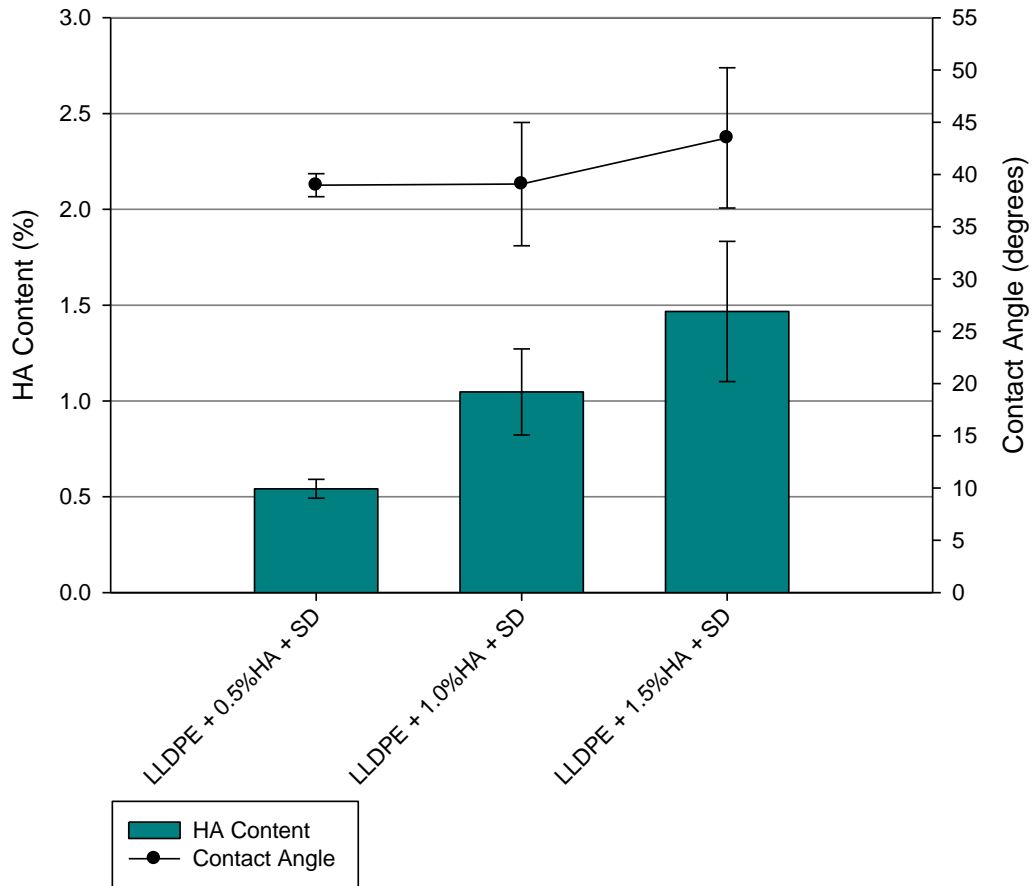


Figure 4.3 No significant correlation is shown between the bulk HA content and the contact angle for the treated LLDPE samples that did receive an additional HA surface dip due to the increased HA content at the surface.

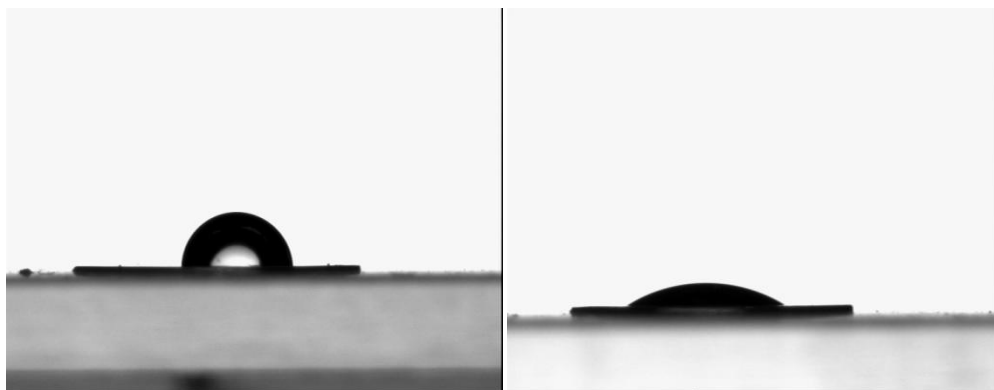


Figure 4.4 Untreated LLDPE (left) and LLDPE+1.0%HA+SD (right) films 10 minutes after drop placement.

The relationship between the contact angle and HA surface density is apparent: with increasing HA surface density, contact angles decrease [2]. Although there was a lower amount of HA in the LLDPE samples that were treated with the highest swelling solution concentration (LLDPE + 1.0%HA (+SD)) in comparison to 1.3%HA and 1.5%HA+SD, it showed to have the lowest contact angles with the additional dip treatment. Due to the viscosity of the initial solution, it is thought that the increased viscosity of the solution was only able to partially diffuse into the LLDPE, providing a higher surface density of HA for the 1.0%HA (+SD) samples.

Samples that received the 1.5% w/v swelling treatment showed no difference with the addition of a post hydrolysis HA dip treatment while the other two treatments benefited from this dip. Since the 1.3%HA and 1.5%HA+SD samples had the highest bulk HA concentration, the HA-treated material may have resulted in a threshold of HA that the LLDPE will retain. A second and more likely explanation is the differences in results arose from inconsistencies with the dip coating application. The additional % (w/w) XL HA on the surface could be the main contributor to the composite's lubricious properties and further reduction contact angle.

The HA treatment of the fabric reduced the water permeability of the fabric, evidenced by slower wicking times during contact angle attempts, which could be beneficial in heart valve applications, preventing regurgitation via passage of blood through the fabric.

4.3.2 Toluidine Blue O (TBO)

The incorporation of HA on the PET treated material surfaces was demonstrated by dye assay. TBO is a cationic dye, which can bind negatively charged groups on the structure, such as sulfate groups on heparin and carboxyl groups on HA, so it is often used to visualize or quantify polysaccharide in coatings and tissue sections [1]. Images of treated and control PET samples, which had been stained via TBO dye, are shown in Figure 4.2.

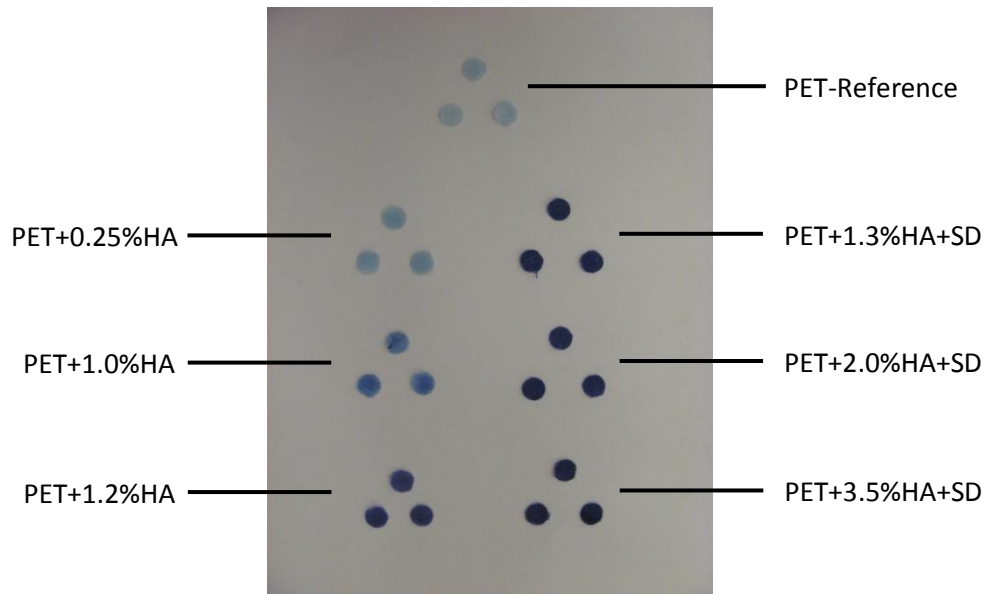


Figure 4.2 TBO stained PET fabric samples

The round samples show the relative comparison of the HA surface concentrations among the samples. The intensity of the dye is linearly proportional to the amount of HA on the surface: brighter blues correspond to higher concentrations of HA. It has been shown throughout the literature that property values obtained from surface analyses (e.g. contact angle measurements) make a significant contribution to the understanding of materials surfaces' morphology and subsequently the *in vivo*

biocompatibility [3-5]. In the case of BioPoly, surface energy has been related to the lubricity of the biomaterial's surface [6].

4.3.3 *In Vitro* Study

4.3.3.1 Biocompatibility of LLDPE-HA and PET-HA Materials

There are many potential reasons why materials fail in cardiovascular applications, but the most prevalent problem is occlusion due to blood coagulation. Whole blood was used to assess clotting times. In this test, higher absorbance values correlate with improved thromboresistance of the material (Figures 4.5-4.8). The resistances to clotting results of LLDPE with and without additional dip coating are shown in Figures 4.5 and 4.6 respectively. The reference lines indicate the average absorbance for whole blood with zero clotting \pm one standard deviation. This was used as a reference to gauge clotting percentages. Starred values (*) represent a significant difference ($p \leq 0.05$) compared to the control, which is the LLDPE-Reference sample.

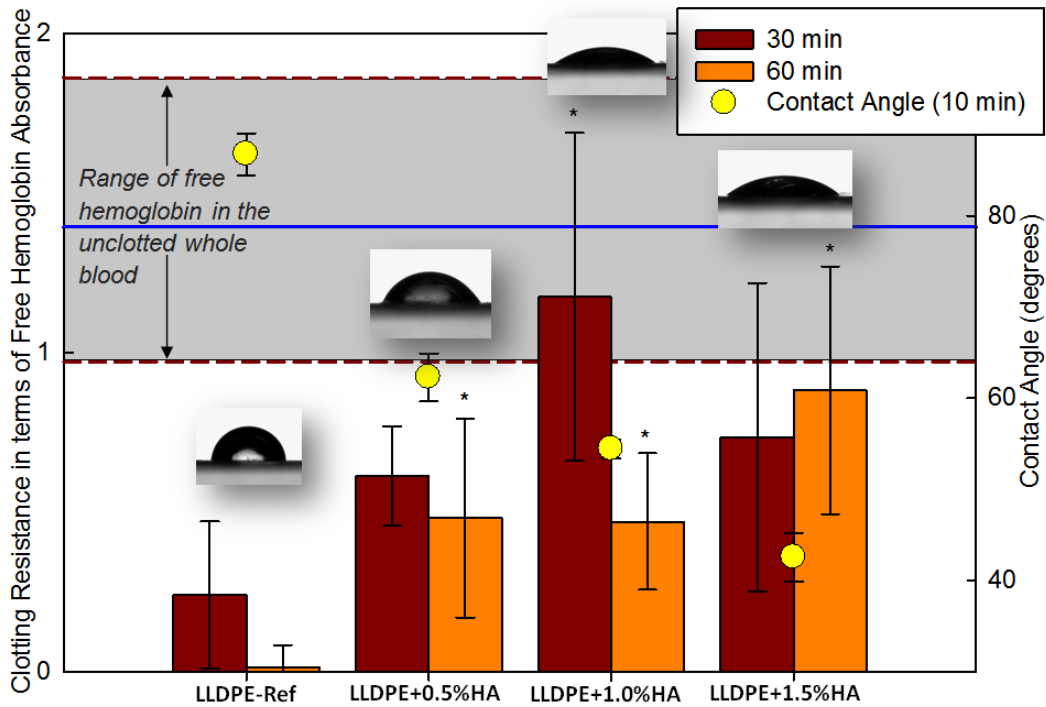


Figure 4.5 Resulting clotting resistance (in terms of free hemoglobin absorbance) for **non-dipped** samples for the 30 minute and 60 min time points ($\text{---} \bar{x}$, $\text{- - -} \pm \sigma$ for unclotted blood). Overlay of contact angle measurements and images 10 minutes after drop application. An * indicates significant differences ($p < 0.05$) from LLDPE Reference.

The reference control was the Dowlex 2056 film, washed in xylenes and dried prior to use. The LLDPE+1.0%HA treatment group had significantly higher ($p \leq 0.05$) resistance to clotting compared to LLDPE-Reference at 30 minutes while the other treatment groups did not have significant reduction in clotting, but did trend toward clotting reduction. However, all treatment groups had significant reduction of clotting after 60 minutes when compared to the untreated LLDPE-Reference samples, on which nearly all blood had clotted. The clotting was not significantly different between the treatment groups, indicating that these samples may have reached an equilibrium point for clotting. The LLDPE+1.0%HA sample at 30 minutes was the only sample that did not show a significant amount of clotting ($p \leq 0.05$). Similar results were also observed using

SEM to image the clotting on various surfaces (*vide infra*). There was no significant difference in the degree of clotting between the treatment groups.

The overlaid plot of contact angle demonstrates a correlation between the reduction of contact angle and the increased clotting resistance. At 30 minutes, there is not as strong of a correlation, however, at 60 minutes the contact angles are well correlated to the hemocompatibility.

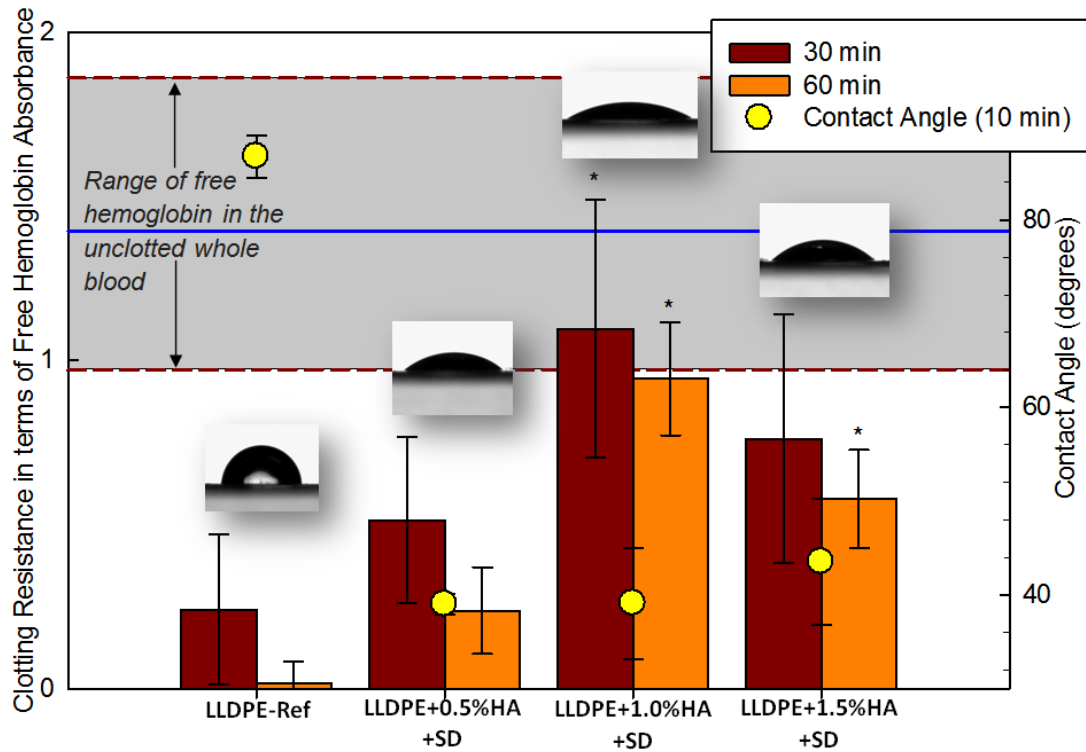


Figure 4.6 Resulting clotting resistance (in terms of free hemoglobin absorbance) for **dipped** samples for the 30 minute and 60 min time points (\bar{x} , $\pm\sigma$ for unclotted blood). Overlay of contact angle averages and images 10 minutes after drop application. An * indicates significant differences ($p < 0.05$) from LLDPE Reference.

Again, the reference control used was the Dowlex 2056 film, washed in xylenes and dried prior to use. The LLDPE+1.0%HA+SD treatment group had significantly higher ($p \leq 0.05$) resistance to clotting compared to LLDPE-Reference at 30 minutes while the other treatment groups did not have significant reduction in clotting, but did trend

toward clotting reduction. However, all treatment groups had significant reduction of clotting after 60 minutes when compared to the untreated LLDPE-Reference samples, on which nearly all blood had clotted. The clotting resistance was significantly different between the treatment groups, with significantly less clotting on the LLDPE+1.0%HA+SD samples. Even though these samples did not have the highest HA content in the bulk polymer, it is thought that due to the viscous swelling solution, diffusion into the film via swelling did not penetrate as deep. If this is true, it would be found that the HA contained in the LLDPE+1.0%HA(+SD) samples was concentrated at the surface providing a higher surface concentration of HA, even with a lower bulk concentration. The LLDPE+1.0%HA+SD sample was the only sample that did not show a significant amount of clotting ($p \leq 0.05$) for all time points. Similar results were also observed using SEM to image the clotting on various surfaces (*vide infra*). There was no significant difference in the degree of clotting between treatment groups until 60 min, at which point blood incubated with the LLDPE+1.0%HA+SD had a lower degree of clotting than both LLDPE+1.5%HA+SD and LLDPE+0.5%HA+SD treatments ($p \leq 0.05$) and the LLDPE+1.5%HA+SD had a lower degree of clotting than LLDPE+0.5%HA+SD treatments ($p \leq 0.05$).

The overlaid plot of contact angle demonstrates a correlation between the reduction of contact angle and the increased clotting resistance. While the decrease in surface angle does not necessarily correlate directly to the clotting kinetics, it is a good indicator over the untreated LLDPE film. This point is indicative of the fact that the contact angle reduction is not the only aspect of hemocompatibility being affected by the incorporation of the HA.

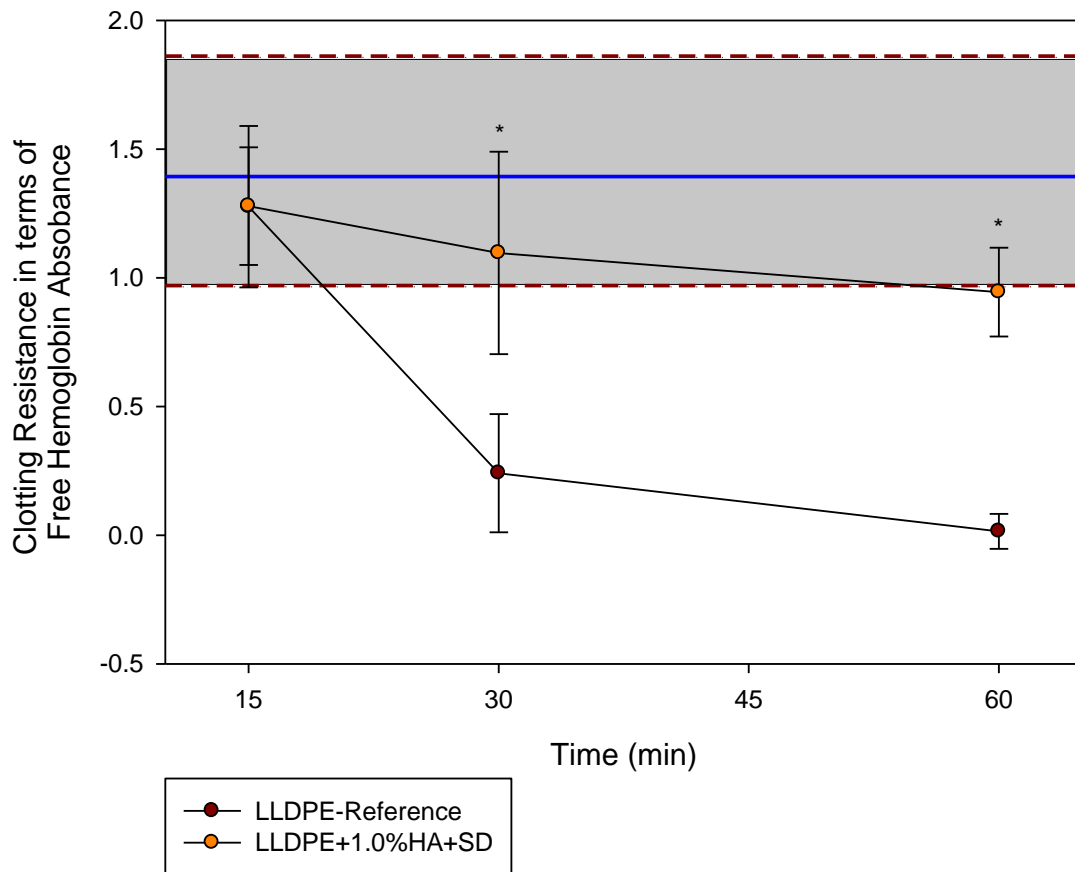


Figure 4.7 Resulting clotting resistance (in terms of free hemoglobin absorbance) versus time for LLDPE+1.0%HA+SD (— \bar{x} , - - $\pm\sigma$ for unclotted blood). An * indicates significant differences ($p < 0.05$) from LLDPE Reference.

Blood incubated with untreated LLDPE completely clotted within 60 minutes and therefore used as a reference thrombogenic material by which all comparisons were made. At each time point measured, blood incubated with LLDPE-T-2.5-Dip had a significantly higher absorbance than LLDPE ($p \leq 0.05$), indicating that its thromboresistance was greater due to the introduction of HA (Figure 4.7).

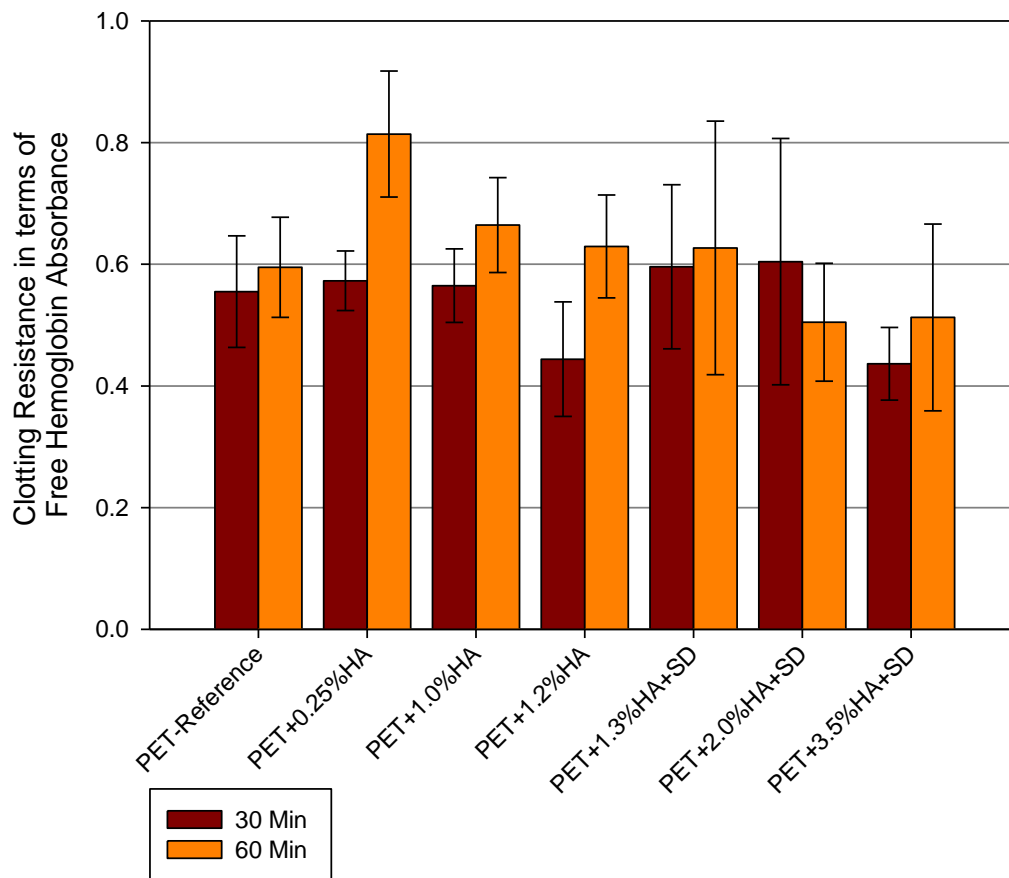


Figure 4.8 Resulting free hemoglobin concentrations (in terms of absorbance) for PET samples for the 30 minute and 60 min time points.

For PET fabric whole blood clotting, the reference control was the BARD Style 6010 thin polyester tubular woven (uncrimped) fabric, washed in xylenes and dried prior to use. Due to the morphology of the material, the whole blood passed through the matrix of PET fibers and remained in the first well plate after passing through the fabric. This resulted in inconclusive results for whole blood clotting time with the PET fabric shown in Figure 4.8. However, qualitative analysis using SEM (*vide infra*) illustrated a thromboresistance quality exhibited by the treated fabrics. This resistance to thrombus formation was increased with the increasing in HA content. Unlike the LLDPE film, the higher viscosity of the T-2.5 swelling solution did not alter the swelling kinetics of the

PET. The high porosity of the fabric due to the voids between fibers and yarns allows for greater, full penetration absorption of the swelling solutions whereas the LLDPE is thought to only have HA penetrating the surface with the higher viscosity solutions.

4.3.3.2 Scanning Electron Microscopy (SEM)

Scanning electron micrographs of the LLDPE and PET after being contacted with whole blood for 30 and 60 minutes are presented in Figures 4.9 – 4.12, which clearly show that whereas the surface of the unmodified LLDPE and PET samples was covered with an accumulation of fibrin and thrombus, while that of treated LLDPE and PET had almost no sign of any cellular matter on it. This *in vitro* experiment clearly confirms that these HA treatments on LLDPE and PET could inhibit platelet adhesion and activation. The possible cause for this inhibition could be the reduction in contact angle at the blood and surface interface, preventing protein absorption by the material. This reduction in protein absorption prevented the progression of the coagulation cascade.

Coagulation is the culmination of a series of reactions, ultimately resulting in the thrombin-catalyzed transformation of fibrinogen into an insoluble fibrin clot. Thrombin is formed upon the convergence of the intrinsic and extrinsic pathways of coagulation. This transformation is clearly exhibited in the untreated PET samples incubated with blood for 30 and 60 minutes. The progression of the coagulation cascade develops an insoluble clot. This clot formation was prevented with the addition of the HA treatments to the samples.

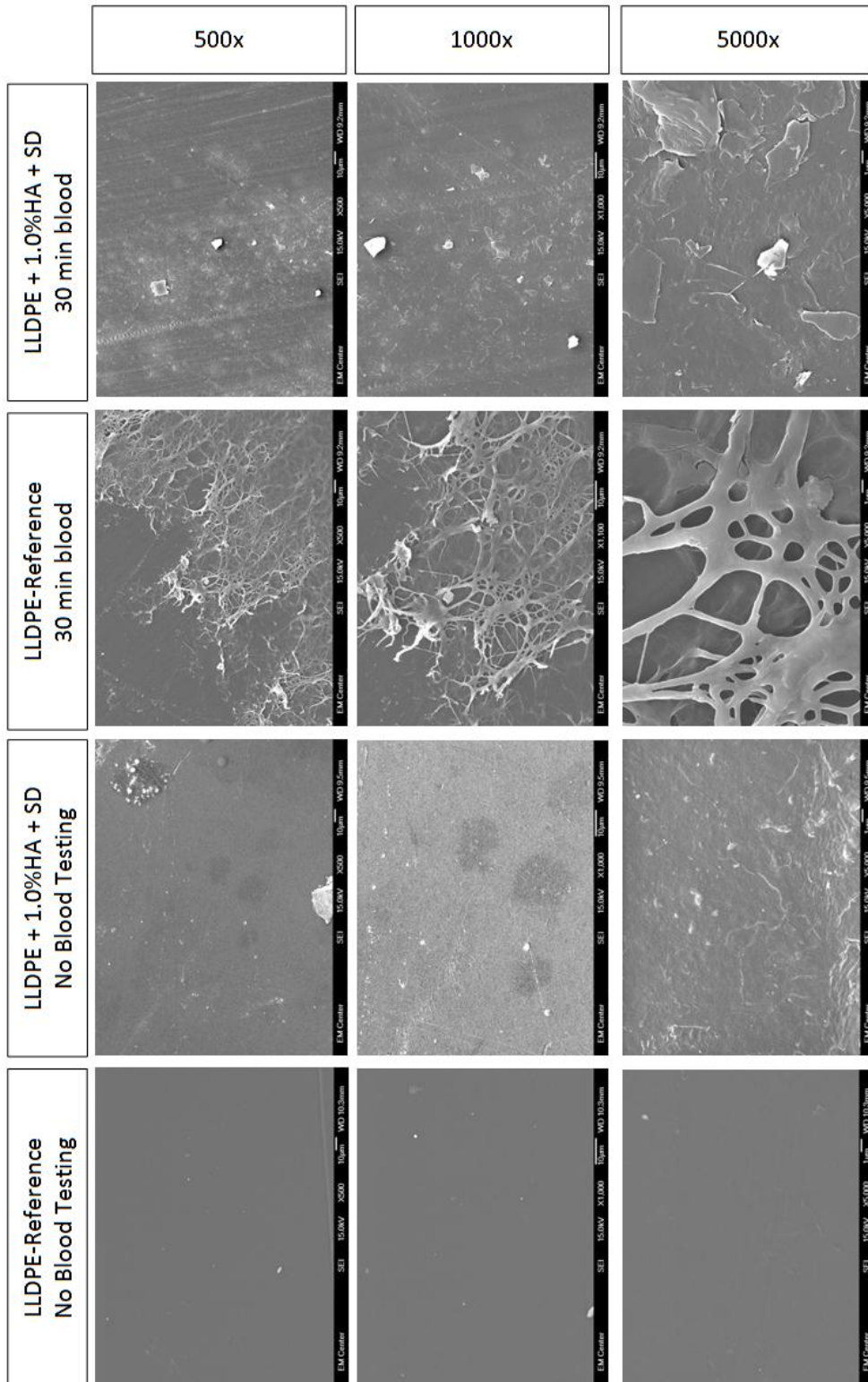


Figure 4.9 Scanning Electron Microscopy (SEM) images of LLDPE samples prior to blood clotting compared to the same micro composite and reference samples following 30 minute whole blood clotting.

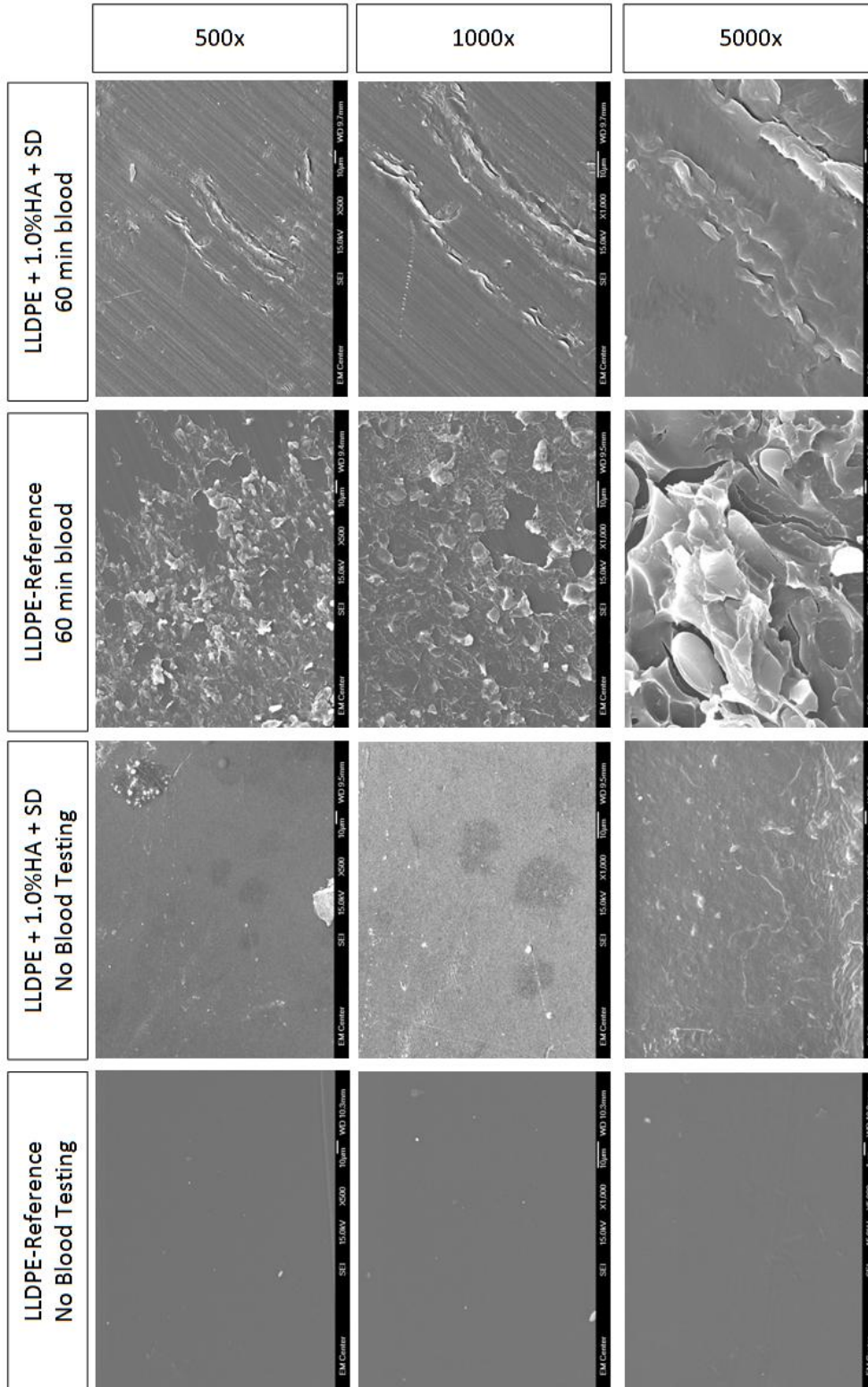


Figure 4.10 Scanning Electron Microscopy (SEM) images of LLDPE samples prior to blood clotting compared to the same micro composite and reference samples following 60 minute whole blood clotting.

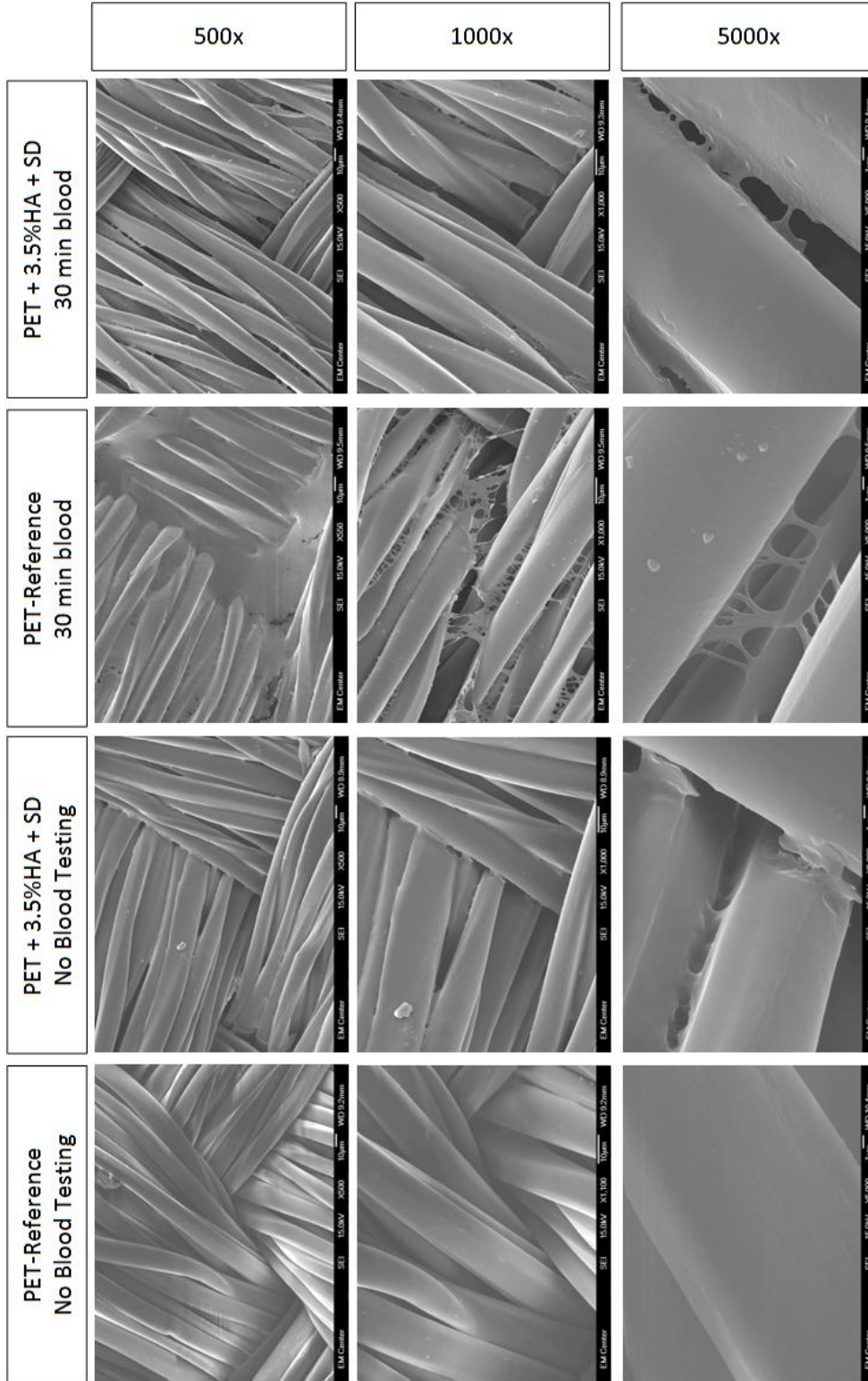


Figure 4.11 Scanning Electron Microscopy (SEM) images of PET samples prior to blood clotting compared to the same micro composite and reference samples following 30 minute whole blood clotting.

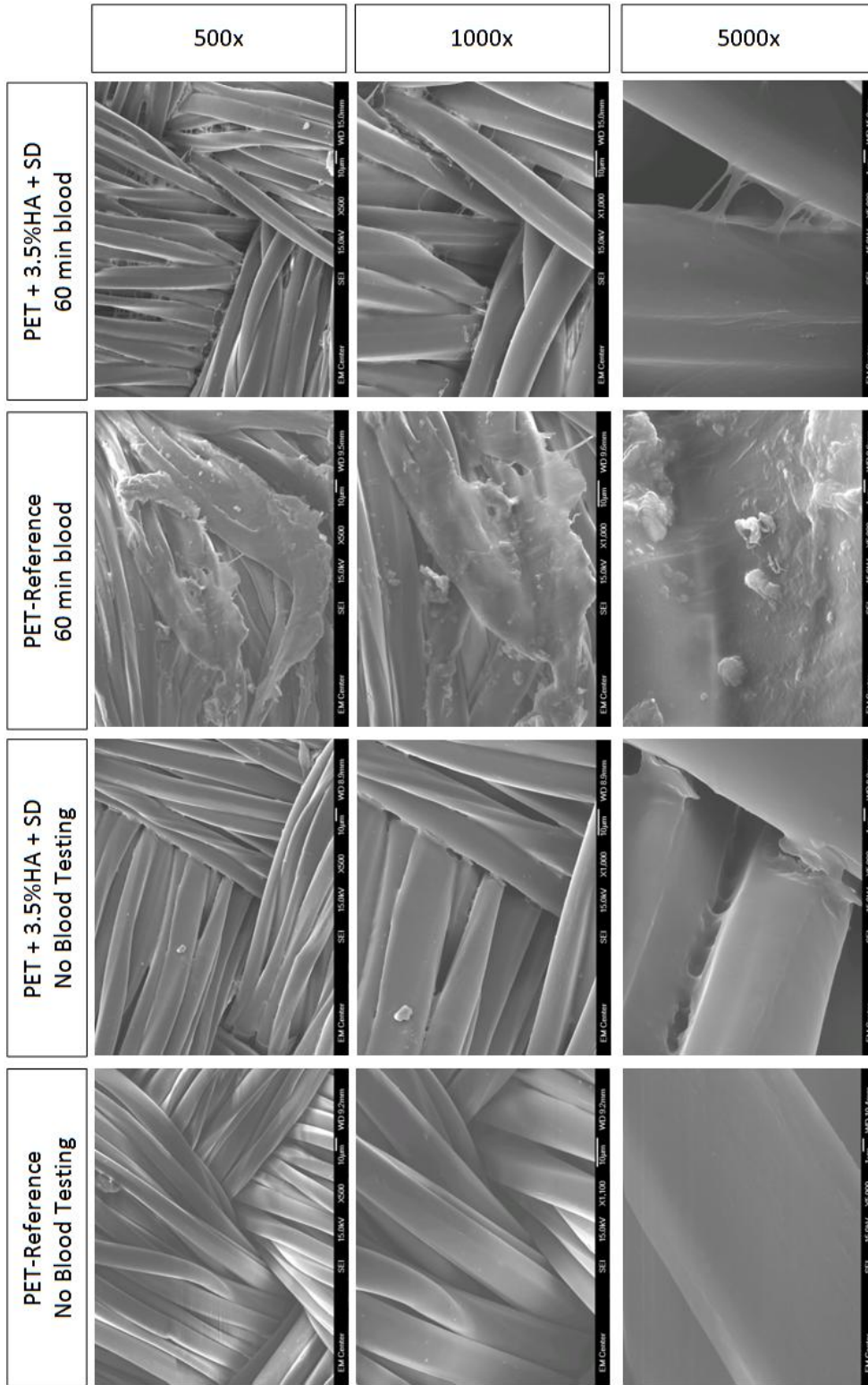


Figure 4.12 Scanning Electron Microscopy (SEM) images of PET samples prior to blood clotting compared to the same micro composite and reference samples following 60 minute whole blood clotting.

Fibrin is clearly seen in Figure 4.9 on the untreated LLDPE samples after 30 minutes of exposure with whole blood. After 60 minutes, it is apparent that the fibrin attachment has progressed to begin forming thrombus on the surface of the untreated samples. This attachment is not seen in the treated LLDPE sample. In the images of the treated sample prior to blood testing, the HA addition is seen on the surface. The surface looks very similar after exposed to whole blood for 30 minutes. Islands of HA are seen which could be correlated to the non-uniform distribution of surface HA from the poor application of the addition HA dip. After 60 minutes, this thromboresistance is still very noticeable as seen in Figure 4.10. Some cellular attachment is seen in clumps of fibrin; however, these spots were very few and far between on the sample. Significant surface attachment is seen in the untreated control LLDPE, indicating the poor hemocompatibility. The thrombus looks slightly crystallized due to the SEM preparation process.

PET fabric had more astounding results from the SEM imaging. The addition of the HA is clearly seen between the fibers in the second column of Figures 4.12 and 4.11. This explains the increased bending stiffness of the higher HA content samples. This HA is effectively linking some fibers together, until bent at which point the HA breaks into separate sections. Both the treated and untreated PET samples were permeable to blood, allowing the majority of the cells to pass between the fibers. The effects of the treatment are still seen however. The attachment of fibrin is clearly seen in the untreated samples after 30 minutes of blood exposure. In some areas, voids between yarns were almost completely occluded. This attachment was not seen for the HA treated samples. HA connections between fibers were still visible with not fibrin attachment. After 60 minutes,

the effects of the HA treatment are astounding. The untreated samples have formed significant clotting, covering many fibers and voids. Some fibrin can be seen in the treated PET sample after 60 minutes of exposure to whole blood but it is still significantly less than the untreated samples after 30 minutes. This reduction in thrombus indicates a good hemocompatibility with the addition of the HA to the structure.

The resulting images from SEM demonstrate the excellent hemocompatibility with whole blood. The reduction in fibrin attachment and lack of whole blood clotting in the treated LLDPE and PET samples indicate that the treatments were successful. Again with the PET, the T-2.5 treatment (PET+1.2%HA and PET+3.5%HA+SD samples) appeared to have the greatest thromboresistance. Since the fabric was able to absorb the high viscosity solution, full penetration of HA is seen for all treatments, therefore enabling higher control with a larger range of HA content capable of being achieved within the HA-treated materials.

The behavior of the absorption and desorption of blood proteins on polymeric materials depend on the surface characteristics such as hydrophilicity/hydrophobicity [5]. When a foreign material comes into contact with blood, initially there is a rapid adsorption of plasma proteins onto its surface followed by platelet adhesion and activation. Platelet activation initiates the coagulation process, resulting in the formation of clots [7-9]. In general, hydrophobic surfaces tend to adsorb larger amounts of proteins than hydrophilic ones [10]. Therefore, some investigators have proposed that to increase blood compatibility, one should attempt to incorporate hydrophilic surfaces [11]. It has been observed that in the presence of plasma proteins the platelet adhesion decreased gradually with the increasing surface wettability [12].

4.4 Conclusions

TBO dye staining and surface contact angle measurements demonstrated the presence of HA on the surface of the HA-treated materials. In comparison with the controls, the contact angles of the appropriately treated LLDPE micro composites significantly decreased, and the degree of decrease was related to the surface density of HA. The higher the surface density of HA, the lower the contact angles of the LLDPE micro composites. The intensity of the dye within the PET samples shows a sharp contrast to the control PET representative of a gradient of HA content.

Unexpectedly, the high silyl-HA-CTA content within the LLDPE+1.3%HA and LLDPE+1.5%HA+SD samples did not achieve the lowest contact angles treatment groups. Furthermore, too high of a concentration of silyl-HA-CTA in swelling solution creates a very viscous solution that does not infiltrate the LLDPE as deep as lower concentrations. However, this lack of depth leads to a higher surface density of HA within the LLDPE+1.0%HA(+SD) samples.

Blood incubated with untreated samples clotted within 60 minutes and therefore used as a reference thrombogenic material by which all comparisons were made. At each time point measured, blood incubated with T-2.5-Dip LLDPE and PET treated samples had a significantly reduced cellular adhesion compared to untreated samples, indicating that the HA treatment was successful in improving hemocompatibility. This study used whole blood clotting as an overall assessment of hemocompatibility, using various assays that assess the contributions of different blood components when evaluating the hemocompatibility of the biomaterial is also important to consider. These data suggest that under the conditions tested, treated PET and LLDPE are less thrombogenic than untreated reference samples.

The reduced contact angles of LLDPE following treatment, compared to those of non-treated LLDPE controls, correlate to a reduction in thrombus formation, which was shown by an increased absorbance and decrease in cellular attachment. Sample groups which exhibited lower contact angles displayed better *in vitro* hemocompatibility; however, this connection is not directly correlated and may be more associated with the surface concentration of HA. In the future, different methods of accessing the lubricity of treated LLDPE samples should be explored to better quantify material surface properties and surface densities of HA. While contact angle information was not collected for the PET fabric due to its morphology, the qualitative analysis using SEM revealed increased hemocompatibility with an increasing HA content providing good biomaterial candidates for cardiovascular applications.

4.5 References

1. Johnston, J.B., *A simple, nondestructive assay for bound hyaluronan*. Journal of Biomedical Materials Research, 2000. **53**(2): p. 188-191.
2. Zhang, M., *Surface Modification of Ultra High Molecular Weight Polyethylene With Hyaluronan For Total Joint Replacement Application*, in *Mechanical Engineering*. 2005, Colorado State University: Fort Collins.
3. Jacobs, H., et al., *Surface Modification for Improved Blood Compatibility*. Artificial Organs, 1988. **12**(6): p. 506-507.
4. Okano, T., et al., *Effect of hydrophilic and hydrophobic microdomains on mode of interaction between block polymer and blood platelets*. Journal of Biomedical Materials Research, 1981. **15**(3): p. 393-402.
5. Jin Ho, L. and L. Hai Bang, *A wettability gradient as a tool to study protein adsorption and cell adhesion on polymer surfaces*. Journal of Biomaterials Science, Polymer Edition, 1993. **4**(5): p. 467-481.
6. Zhang, M. and S.P. James, *Silylation of hyaluronan to improve hydrophobicity and reactivity for improved processing and derivatization*. Polymer, 2005. **46**(11): p. 3639-3648.
7. Ward, C.A., *Blood Protein-Material Interactions That Lead to Cellular Adhesion*, in *Proteins at Interfaces*. 1987, American Chemical Society. p. 551-565.
8. Brash John, L., *Protein Adsorption at the Solid-Solution Interface in Relation to Blood-Material Interactions*, in *Proteins at Interfaces*. 1987, American Chemical Society. p. 490-506.
9. Andrade, J.D., *Surface and Interfacial Aspects of Biomedical Polymers: Protein adsorption*. 1985: Plenum Press.
10. Elbert, D.L. and J.A. Hubbell, *Surface Treatments of Polymers for Biocompatibility*. Annual Review of Materials Science, 1996. **26**(1): p. 365-294.
11. Akaike, T., *Advances in polymeric biomaterials science*. 1997: CMC Co., Ltd.
12. Lee, J.H. and H.B. Lee, *Platelet adhesion onto wettability gradient surfaces in the absence and presence of plasma proteins*. Journal of Biomedical Materials Research, 1998. **41**(2): p. 304-311.

CHAPTER 5: RESEARCH SUMMARY AND FUTURE WORK

5.1 Research Summary

The goal of this research was to modify LLDPE and PET via introduction of hyaluronan to reduce thrombus formation and the enhance biocompatibility for cardiovascular applications, and HV prostheses in particular. Hyaluronan could potentially be introduced into LLDPE and PET through solvent infiltration by exploitation of the swelling kinetics of the materials. A swelling approach was used for both LLDPE film and PET fabric instead of a porous perform, which has been used in previous BioPoly application, due to the high degrees of swelling achieved in a much shorter time span than traditional UHMWPE samples. In xylenes solution, silylated HA quickly diffused into the film of the LLDPE film and the voids between fibers of the PET fabric, so the treatment process was fast and simple. The final micro-composites obtained through appropriate treatments had a uniform distribution of HA, which were water hydrophilic, lubricious and stable. The treatment process of HA treatment did not significantly affect the tensile properties of the LLDPE of PET. The presence of HA did significantly affect the bending stiffness of the PET fabric, but the changes were acceptable. There is a range of safe swelling temperatures, above which would significantly alter the mechanical properties due to recrystallization of the LLDPE film.

The presence of HA within the HA-treated material significantly reduced the static contact angles of water for all LLDPE samples. The additional dip coating of HA following hydrolysis resulted in non uniform distribution of HA on the surface for the LLDPE but still further reduced the contact angles significantly in all but the 1.5% w/v LLDPE samples. By optimizing treatment parameters and improving swelling environment, HA-treated materials with more controlled qualities can be obtained, and is expected to have a much more uniform HA distribution and even better thrombus resistance than the current materials.

5.2 Future Work

5.2.1 Synthesis of HA-Treated Materials

The film and fabric treatment methods and processes influence the properties of the HA-treated materials by changing the micro-structure and morphology of the material. The structure and morphology of the HA-treated material, and their relationship with the treatment processes need to be investigated in future studies. Investigation of additional PET surgical fabrics may be beneficial in control permeability and surface morphology of the samples as well as directional weaves in order to provide anisotropy similar to that of the native valve.

Additional iterations of optimal treatment parameters may be necessary if dynamic hemocompatibility results differ significantly from the static results reported earlier. However, since the procedures of HA treatments have been investigated, composition of the HA-treated materials would be the focal point of these iterations.

5.2.2 HA-Treated Material Characterization

In addition whole blood hemocompatibility, individual coagulation factors should be assessed to better understand which factors of the coagulation cascade remain unaffected by the HA treatment, in order to optimize composition of the HA-treated materials. *In vitro* tests such as the activated platelet adhesion and activation, partial thromboplastin time (aPTT), prothrombin time (PT), and thrombin time (TT), measure the time elapsed from activation of the coagulation cascade (Figure 5.1) at different points to the generation of fibrin giving a worst case scenario.

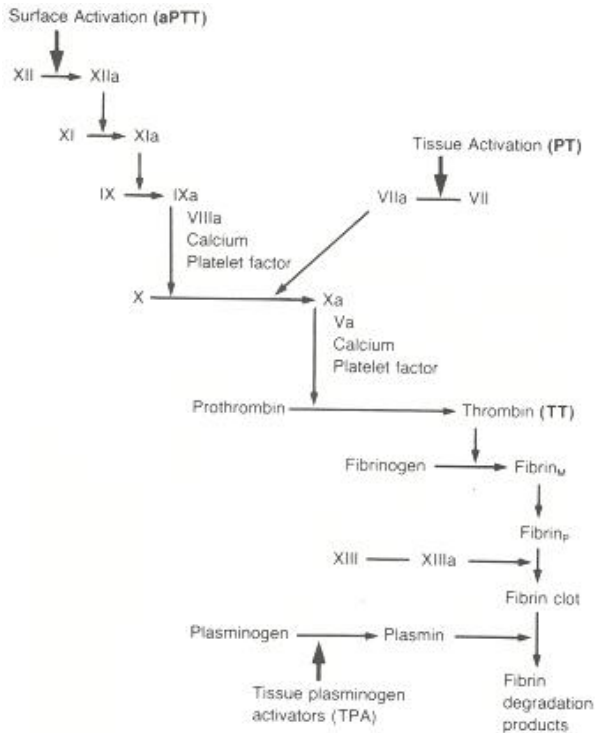


Figure 5.1 The coagulation cascade. Bold type indicates the starting point of the coagulation test noted [1].

5.2.3 Valve Design and Manufacture

The high dynamic stress environment acting on leaflets is a primary cause of mechanical degradation, producing cracks and tears of the leaflet. These failures have been shown to be sites for calcification in polyurethane valves, but eventually, these defects will cause catastrophic failure of the valve. It is thought that this problem can be overcome by improving valve geometry and reinforcement so that it will effectively reduce the high stress concentrations in the leaflet, thereby reducing the initiation of these failure sites. High stress is known to introduce degradation in materials exposed to cyclic fatigue [2].

The three key parameters affecting leaflet stress concentrations include the stent flexibility, leaflet properties, and the geometry of the leaflet. Valve models including varying valve and leaflet geometries should be evaluated to determine their impact on leaflet stress concentrations. By making iterative changes to the design parameters, the optimal valve design can be selected to maintain acceptable stresses.

5.2.4 *In Vitro* Testing

5.2.4.1 Dynamic Hemocompatibility

Tests which do not simulate the conditions of a device during use may not predict accurately the nature of blood/device interactions which may occur during clinical applications [3]. A static whole blood clotting examination of the HA-treated materials assisted in analyzing the starting point for hemocompatibility. These testing methods do not mimic biological conditions they would be under within a valve. Dynamic coagulation tests will be used to investigate any flow dependent hemocompatibility of the surfaces. Standard dynamic models include centrifugations systems, flow chambers,

chandler systems, circulation models or agitators [3]. It is not anticipated that the dynamic environment will alter the hemocompatibility of the treated surfaces, possibly even improving them however it is necessary to confirm these assumptions prior to moving to *in vivo* examinations.

5.2.4.2 Valve Characterization

In vitro hydrodynamic testing is a key element in the evaluation of performance for a prosthetic valve [4]. The ISO 5840:2005 and FDA standards stipulate the specifics for testing equipment and conditions, providing strict parameters to assess acute valve function.

The system must be capable of producing pressure and flow environments that approximate a range of physiological conditions for both rest and exercise conditions, and the arrangement of resistance and compliance elements must simulate the arterial tree in the human body in order for the hydrodynamic evaluation to be significant. Pressure and flow measurements are the principal determinants of valve performance, and hydrodynamic performance will be evaluated with respect to stroke volume, regurgitation, cardiac output, and mean systolic pressure difference. Resulting performance will be compared to minimum performance requirements for prosthetic in ISO 5840:2005.

It becomes necessary to estimate valve longevity in order to evaluate the potential risks and failure modes associated with prostheses. Durability testing of heart valve prostheses will be used to assure that rigid heart valve substitutes remain functional for over 400 million cycles (10 years) and flexible heart valve substitutes remain functional for over 200 million cycles (5 years). Qualitative assessment during testing should be

used to examine for general degradation, cracking or tearing of the valve in addition to hydrodynamic performance.

5.2.5 *In Vivo* Study

It is a given that techniques for *in vitro* hemocompatibility studies act as an important first screening of a biomaterial. *In vivo* studies are incredibly valuable for understanding how the blood and material interface will be affected once placed in the circulatory system.

The swine model is a newly developed *in vivo* model to test thromboembolism and the juvenile sheep model was developed as a model for calcification potential in heart valve prostheses and show remarkable anatomical and physiological similarities [5]. The coagulation system of this model closely approximates that of the human neonate [6]. This model could be used to provide an *in vivo* test of BioPoly HA-treated materials with selected treatment parameters to examine the hemocompatibility in physiological conditions, examining the presence of thrombus, calcification and material failures such as cracking or tearing. The concentration of HA remaining in the leaflets should be evaluated to examine HA resorption and degradation over time to help predict the lifespan of the treatment. An *in vivo* study will establish if the heart valve satisfies minimum industry standards.

5.3 References

1. Jacobs, H., et al., *Surface Modification for Improved Blood Compatibility*. Artificial Organs, 1988. **12**(6): p. 506-507.
2. Okano, T., et al., *Effect of hydrophilic and hydrophobic microdomains on mode of interaction between block polymer and blood platelets*. Journal of Biomedical Materials Research, 1981. **15**(3): p. 393-402.
3. Seyfert, U.T., V. Biehl, and J. Schenk, *In vitro hemocompatibility testing of biomaterials according to the ISO 10993-4*. Biomolecular Engineering, 2002. **19**(2-6): p. 91-96.
4. Johnston, J.B., *A simple, nondestructive assay for bound hyaluronan*. Journal of Biomedical Materials Research, 2000. **53**(2): p. 188-191.
5. Li, D., et al., *A SWINE MODEL FOR LONG-TERM EVALUATION OF PROSTHETIC HEART VALVES*. ANZ Journal of Surgery, 2007. **77**(8): p. 654-658.
6. Daebritz, S.H., et al., *Introduction of a flexible polymeric heart valve prosthesis with special design for mitral position*. Circulation, 2003. **108**(10): p. 134-139.

Appendix 1. Protocols

1.1.1 HA-CTA Complexation

Objective

Hydrophobic modification of hyaluronan for reaction in anhydrous solvents

Materials & Equipment

- Sodium hyaluronate (HA)
- Cetyltrimethylammonium bromide (CTAB)
- Distilled deionized water
- 1000 ml beaker or flask
- 500 ml beaker or flask
- magnetic stir bars
- stir plates
- Freezer mill
- Liquid nitrogen

Procedure

- Prepare a 0.30% w/v solution of sodium hyaluronate in DI H₂O (e.g. 1.5g HA in 500 ml DI H₂O). Make sure to minimize large clumps when adding NaHA. Allow to stir at room temperature until completely dissolved. This can take several hours depending upon the molecular weight of the HA.
- Prepare a 1.00% w/v solution of CTAB in DI H₂O (e.g. 1.6875g CTAB in 168.75 ml DI H₂O); Dissolve until clear using sonication and/or heat (set to 40°C).
- Slowly add the CTAB solution to the HA solution using addition funnel at a dropwise rate of 1-2 drops per second under magnetic stirring. The mixture will become increasingly opaque as CTAB solution is added, until at the reaction end point a white precipitate forms and the supernatant becomes clear.
- Collect the precipitate by centrifugation.
- Wash the precipitate by rinsing with DI H₂O and re-centrifuging several times to remove CTAB residue. The CTAB residue will have a “soapy” character, so rinse until no soapy bubbles form.
- Dry HA-CTA in a vacuum oven (-25 mm Hg, 50°C) 24 hours or until no weight change is observed.
- Grind dried HA-CTA to a powder using the freezer mill.
- HA-CTA should be sealed in vials and stored in a desiccator.

1.9.1 HA-CTA Silylation

Objective

Hydrophobic modification of hyaluronan for reaction in anhydrous solvents

Materials & Equipment

- Hyaluronan-cetyl trimethylammonium complex (HA-CTA)
- Dimethyl sulfoxide (DMSO)
- Hexamethyldisilazane $\geq 99.9\%$ ReagentPlus (HMDS)
- 250 ml Round Bottom Flask (RBF)
- Serum stoppers
- Copper wire
- Keck clip
- Condenser
- N₂ (dry) gas
- Magnetic stir bar
- Stir plates
- Vacuum oven

Procedure

- Place ground HA-CTA into 250 ml 3-neck RBF.
- Add 50 ml of DMSO for every 1.5g of starting Na HA to RBF via cannula and dry N₂.
- Allow the HA-CTA to swell in the DMSO at room temperature until it is gel-like.
- Lower RBF into 60°C oil bath and continue to stir until starting material is fully dissolved (4-24 hrs.).
- Add 25 ml of HMDS for every 1.5g of starting Na HA to RBF via cannula and dry N₂ and increase temperature to 75°C and maintain reaction under N₂ flow for 26-41 hours.
- Once stirring is ceased, cool reaction to room temperature.
- Pour reaction mixture into 250 ml separatory funnel, allowing the two phases to separate.
 - The upper HMDS layer contains the silylated HA-CTA.
 - The bottom layer is DMSO.

- Dispose of DMSO and vacuum dry top layer at 50°C until no change in weight is observed.
- Wash the dry powder, silyl HA-CTA, five times with Xylenes, drying each time.
- Dry the silyl HA-CTA at 50°C until no weight change is observed.

References

- Kurkowski, R. *The chemical crosslinking, compatibilization, and direct molding of ultra high molecular weight polyethylene and hyaluronic acid microcomposites*, M.S. thesis, Colorado State University Department of Mechanical Engineering, Fort Collins, CO (2007).
- Zhang, M. and James, S.P., (2005). *Silylation of hyaluronan to improve hydrophobicity and reactivity for improved processing and derivatization.* , **46**(11):3639-3648.

Sample Synthesis

Materials & Equipment

- Silylated Hyaluronan (Silyl HA)
 - Xylenes
 - Hexamethyldisilazane (HMDS)
 - [Poly\(hexamethylene diisocyanate\)](#) (HMDI)
 - Precut LLDPE samples
 - Qty. 3 two-necked round-bottomed flasks (RBF)
 - Serum stoppers
 - Copper wire
 - Keck clips
 - Condensers
 - N₂ gas
 - Oil bath
 - Weigh boat(s)
 - Analytical scale
 - Magnetic stir bar(s)
 - Stir plate(s)
 - Ultrasonic bath
 - NaCl
 - Deionized water
- Vacuum oven

Procedure

Stock Solutions/Swelling

Note: Allow a minimum of 2 hours prior to swelling for preparation of stock solutions. Precautions for air/water-sensitive chemistry should be observed, i.e. Silyl HA powder should be vacuum dried a minimum of 24 hours prior to use, glassware and cannula should be stored at 100 °C to ensure it is completely dry, stir bars should be rinsed with acetone before use.

Silylate all glassware that will contact the Silyl HA prior to solution preparation.

- Add 10 – 15 mL of HMDS to the two RBFs that will contain Silyl HA. Swish the HMDS around in the RBF making sure to contact the entire flask below the necks. Remove the excess HMDS.

Prepare a concentrated solution of Silyl-HA in Xylenes. A 1.5% w/v concentration is appropriate for Silyl HA prepared from HA in the 450-500 kDa size range.

- Weigh Silyl-HA and place along with stir bar in an appropriately-sized RBF.
- Seal side neck of RBF with a serum stopper secured with copper wire.
- Transfer appropriate volume of Xylenes (100 ml for every 1.5g Silyl HA) into flask.
- Attach RBF to condenser with a Keck clip, lower into oil bath, set temperature to 60°C and begin stirring.
- Flush flask with N₂ by plugging vent, allowing slight positive pressure to build, and releasing plug a total of 3 times; plug vent and remove along with cannula, leaving slight positive pressure of N₂ in the flask.
- When Silyl-HA is fully dissolved, maintain temperature while RBF containing samples is prepared.

Note: Sample weight should be recorded before and after each step of the swelling/crosslinking/hydrolysis procedure to help determine the amount of weight gain through each step of the process. This requires the identification of each sample individually.

Prepare RBF for sample swelling.

- Silylate RBF by adding 10 – 15 mL of HMDS to the RBF. Swish the HMDS around in the RBF making sure to contact the entire flask below the necks. Remove the excess HMDS.
- Place precut samples into RBF and seal side neck of RBF with a serum stopper secured with copper wire.
- Attach RBF to condenser with a Keck clip, lower into oil bath, flush with N₂ 3 times leaving a slight positive pressure of N₂, set temperature to 60°C.

Transfer Silyl-HA/Xylene solution to RBF containing samples.

- Insert vent needle and transfer cannula into rubber serum stopper. Transfer entire volume of Silyl-HA/Xylene solution into flask via cannula under N₂ flow.
- Flush flask with N₂ by plugging vent, allowing slight positive pressure to build, and releasing plug a total of 3 times; plug vent and remove along with cannula, leaving slight positive pressure of N₂ in the flask.
- Allow samples to swell in the Silyl-HA/Xylene solution for 1 hr with stirring before returning the remaining solution back to original RBF via cannula.

Crosslinking

- Base formulation: 200 ml 2% (v/v) Poly(hexamethylene diisocyanate) in

Xylenes (i.e. HA crosslinking solution)

- Prepare solution in clean RBF and stir At 80°C for 1 hr.

Place dried and treated samples into second clean RBF and seal side neck of RBF with a serum stopper secured with copper wire.

Attach RBF to condenser with a Keck clip, lower into oil bath, flush with N₂ 3 times leaving a slight positive pressure of N₂, set temperature to 80°C and begin stirring.

Transfer HA crosslinking solution to RBF containing treated samples.

- Insert vent needle and transfer cannula into rubber serum stopper. Transfer entire volume of HA crosslinking solution into flask via cannula under N₂ flow.
- Flush flask with N₂ by plugging vent, allowing slight positive pressure to build, and releasing plug a total of 3 times; plug vent and remove along with canula, leaving slight positive pressure of N₂ in the flask.
- Allow samples to swell in the HA crosslinking solution for 1 hr before returning the remaining solution back to original RBF via canula.

Remove the RBF from the oil and quickly lower into a liquid N₂ bath. Once at temperature, remove the samples and place in a vacuum oven at 50°C for 2 hours.

Remove samples from vacuum and wash with acetone to remove excess poly(hexamethylene diisocyanate) and vacuum dry at room temperature until no change in weight is observed.

References

- Yonemura, S. *Copolymer Washing*. Standard operating protocol, Colorado State University Orthopaedic Bioengineering Research Laboratory, Fort Collins, CO (2007).
- Kurkowski, R. *The chemical crosslinking, compatibilization, and direct molding of ultra high molecular weight polyethylene and hyaluronic acid microcomposites*, M.S. thesis, Colorado State University Department of Mechanical Engineering, Fort Collins, CO (2007).
- Beauregard, G. *Synthesis and characterization of a biomimetic UHMWPE-based interpenetrating polymer network for use as an orthopedic biomaterial*, Ph.D. Dissertation, Colorado State University Department of Mechanical Engineering, Fort Collins, CO (1999).

Sample Hydrolysis

Materials & Equipment

- Magnetic stir bar(s)
- Stir plate(s)
- 70x50 crystallizing dish
- Ultrasonic bath
- Acetone
- NaCl
- Deionized water
- Ethanol (EtOH)

Procedure

- Prepare a 0.2M NaCl H₂O: Ethyl Alcohol (1:1) hydrolyzing solution in a large beaker or flask. Add the hydrolyzing solution to the crystallizing dish and sonicate for 60 minutes.
- Replace hydrolyzing solution with fresh .2M NaCl H₂O: Ethyl Alcohol (1:1) hydrolyzing solution and sonicate for 60 minutes.
- Replace hydrolyzing solution once more with fresh .2M NaCl H₂O: Ethyl Alcohol (1:1) hydrolyzing solution and sonicate for 60 minutes.
- Prepare a 0.2M NaCl aqueous hydrolyzing solution in a large beaker or flask. Remove the .2M NaCl H₂O: Ethyl Alcohol (1:1) hydrolyzing solution and add the 0.2M NaCl aqueous hydrolyzing solution to the crystallizing dish and sonicate for 60 minutes.
- Prepare a H₂O: Ethyl Alcohol (3:2) solution in a large beaker or flask. Add the hydrolyzing solution to the crystallizing dish and let the samples swell in solution for 2 hours without sonication.
- Replace H₂O: Ethyl Alcohol (3:2) solution with deionized H₂O and sonicate for 30 minutes.
- Record the weight of the samples.
- Dehydrate samples by soaking in acetone a 60 mins; drain acetone and completely dry in a vacuum oven at 50 °C equipped with a solvent trap at -25 inches Hg until there is negligible change in weight.
- Once they samples are dry, record the weight of the samples.

References

Cranson, C. *HA-co-HDPE synthesis methods for DBM carrier*. Standard operating protocol, Colorado State University Orthopaedic Bioengineering Research Laboratory, Fort Collins, CO (2007).

Kurkowski, R. *The chemical crosslinking, compatibilization, and direct molding of ultra high molecular weight polyethylene and hyaluronic acid microcomposites*, M.S. thesis, Colorado State University

Materials & Equipment

- Toluidine Blue O (TBO) (Dye content 84%) (Aldrich; 19804BA)
 - Store at room temperature
- Urea (99+%, A.C.S. reagent) (Sigma-Aldrich; U2709)
 - Store at room temperature
- Distilled H₂O
 - Store at room temperature
- 250 mL glass beaker
- Glass Petri dish

Procedure

- Prepare a 0.1% TBO solution (in 8M urea)
 - Add 96.08864 g urea to 200 mL H₂O and mix at room temperature for 30 minutes.
 - Add 0.2 g of TBO to the aqueous urea solution allowing it to dissolve completely.
- Submerge sample in TBO solution for 10 minutes at room temperature
- Rinse off excess TBO using distilled H₂O, leaving behind bound TBO.
 - Dip stained sample in fresh distilled H₂O and agitate. Rinse the stained sample with distilled H₂O until no more dye is leached out.
- Take a picture of samples from each treatment group.

References

Kurkowski, R. *The chemical crosslinking, compatibilization, and direct molding of ultra high molecular weight polyethylene and hyaluronic acid microcomposites*, M.S. thesis, Colorado State University Department of Mechanical Engineering, Fort Collins, CO (2007).

1.8.1 Thermogravimetric Analysis

Materials

- Sample for analysis
 - 5-10 mg for dry samples
 - Aluminum pans
 - Forceps
 - TGA platinum loading pan (“basket-like” pan with handle)
 - TA Instruments 2950 Thermogravimetric Analyzer

Procedure

- The TGA is programmatically controlled by TA Advantage software. Start the software and set-up control program.
 - Typical program settings for bulk compositional analysis and thermal stability testing: temperature range from ambient to 600°C, 10°C/min ramp rate.
Note: Do not exceed 600 °C when using aluminum pans. Sample should be placed directly on the TGA platinum pan if higher temperatures are required.
 - For hygroscopic samples, temperature may be held isothermally for 15 minutes at 110°C to evaporate unbound water (will need to adjust for lost water weight during analysis).
 - Include external trigger if concurrent mass spectrometry will be used.
 - Set the instrument end-of-test condition to air-cool.
- Using forceps, place an empty aluminum pan on the TGA loading tray. Tare by pressing the “tare” button on the TGA instrument control panel and allowing the robotic stage to load the pan on the balance.
 - If the pan mis-loads, DO NOT attempt to place the loading pan on the balance wire manually (the balance is a precision instrument, and “dropping” a sample on the balance wire can damage the instrument).
 - Wait for the robotic stage to return to its start position, then rotate the TGA loading pan to reposition its “basket” handle.
 - Push the tare button again and observe the position of the handle relative to the balance wire. If it looks like the pan will mis-load again, gently guide the balance wire by pushing and holding it in proximity to the pan handle with forceps. Allow the instrument to load pan on to the balance wire.
 - The pan will be loaded into the furnace, then the instrument will automatically tare the pan. Wait for the instrument to return the pan to the start position.

- Prepare samples for analysis. Generally, for dry samples the most consistent results will be obtained from samples with high surface area, e.g. powders.
 - Pack powder into tared aluminum pan and place on TGA loading pan with forceps. Load the sample by pushing the “load” button on the TGA control panel. Observe the same precautions as described for taring the pan if the sample mis-loads
 - Observe the sample weight measured by the instrument – powdered samples should be in the 5-10 mg range. If sample weight is not in the right range, unload the sample by pushing “unload” on the instrument panel. Adjust sample and repeat load process.

Note: the sample will not be loaded into the TGA furnace until the TGA program is started
- Click “run” in the TA Advantage software to load the sample and run the control program.
- Analyze collected data using TA Universal Analysis software. Plot the weight% and derivative weight% as a function of temperature. Typical analysis parameters to identify include start and end temperatures for degradation steps, peak degradation rate temperatures, % mass loss over a degradation step, and sample residues.

References

ASTM E1131-08, *Standard Test Method for Compositional Analysis by Thermogravimetry*. West Conshohocken, PA: ASTM International.

Contact Angle

Materials & Equipment

- Kruss DSA 10 Drop Tester
- Computer with Drop Shape Analysis software
- Samples
- Double sided tape
- Glass Petri dish

Procedure – Measuring Contact Angle

- Fill out the log sheet with time in.
- Turn on the machine using the green power button located on the DSA 10 control unit.
- Using the knob just below the platform, lower the platform as low as it will go so that the needle does not hit it when the software is started.
- Double click the Drop Shape Analysis (DSA) icon on the desktop.
- Click on the video recorder (camcorder on the toolbar. The FG Window lights up. This is a live screen which enables you to view the drops.
- Flush Channel A (ultrapure H₂O)
 - Leave 50-100 µl and enter amount to dispense
 - ↑ to flush the system
 - Refill tab
 - Refill now
- Repeat Channel A flush
- Reset Dispense liquid volume to 5 µl.
- Place a sample on some double sided tape placed on the platform.
 - Use gloves to no add oils to the surface
- Position the sample and platform under the needle using the three knobs located on the machine.
- Lower the needle into view of the camera
- Zoom and focus the camera on the needle filament
- ↑ to dispense and load the drop
 - The needle may need to be lowered to bring the drop into contact with the sample, then raised to release it.

- Click on the still camera (snapshot) icon to take an image.
- Line up the horizon using the up and down arrow keys and left and right arrows to angle it.
 - The line going through the drop needs to go through each corner of the drop.
- Go to Profile → Contact Angle Using → Circle Fit
- Record the contact angle for that sample.
- Save the image (File → Save as) with the following nomenclature:
 - Batch ID-Sample ID-Time Point
- Repeat each minute for 10 minutes (total of 11 time points including the start)
- Use 3 samples per sample group.
- When finished, close the software and turn of Kruss DSA 10 machine.

Whole Blood Clotting

Materials & Equipment

- 24-well plate (qty. 9)
 - Sterilized
- 96-well plate
- Plate Reader
- Prepared test samples (qty. 15 of each sample)
 - Cut to .5 cm² squares
- Distilled H₂O
 - Store at room temperature
- ~10 mL whole blood
- Pipette
- Tweezers
- Timer

Procedure

- Place samples in 24-well plates and sterilize.
 - All well plate should be sterilized.
 - Organize samples so each well plate is a different time point with organized sample sets.
- Place 5 µL of whole blood onto each specimen.
 - Easiest if the sample is held down at a corner with tweezers.
 - Also place 5 µL of whole blood into positive control wells in secondary well plate.
- At indicated time points, remove sample and place in another sterilized 24-well plate.
 - Each well of secondary well plate should contain 500 µL diH₂O.
 - Do not disrupt the blood droplet with the tweezers.
- Gently shake (agitate) well plate for 30 seconds and let it sit for a total of 5 minutes.
- Remove the sample from water filled well and place in to third sterilized, dry well plate for SEM.
- Repeat previous 3 steps until all samples have been rinsed.

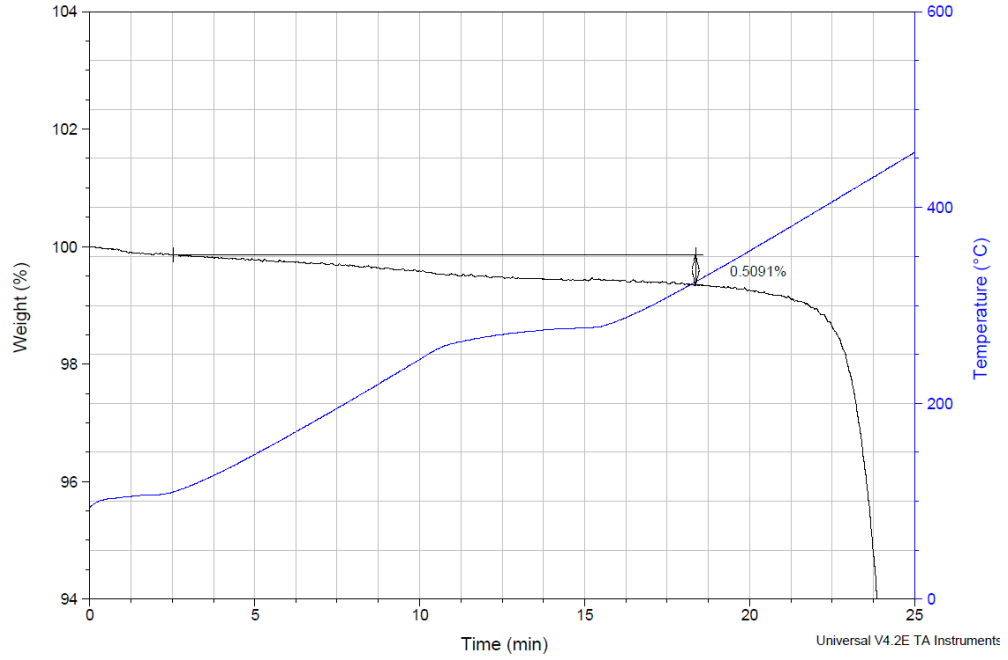
- Obtain 200 μL of water/blood mixture from each well and place into 96 well plate, organized by time and sample set.
- Run plate reader – designated absorbance program and save results.
- Set SEM samples into desiccators until ready to image.

Appendix 2. Thermal Analysis Curves

Sample: LLDPE-T-0.5-2
Size: 4.3450 mg
Method: Casey TGA
Comment: LLDPE-T-0.5-

TGA

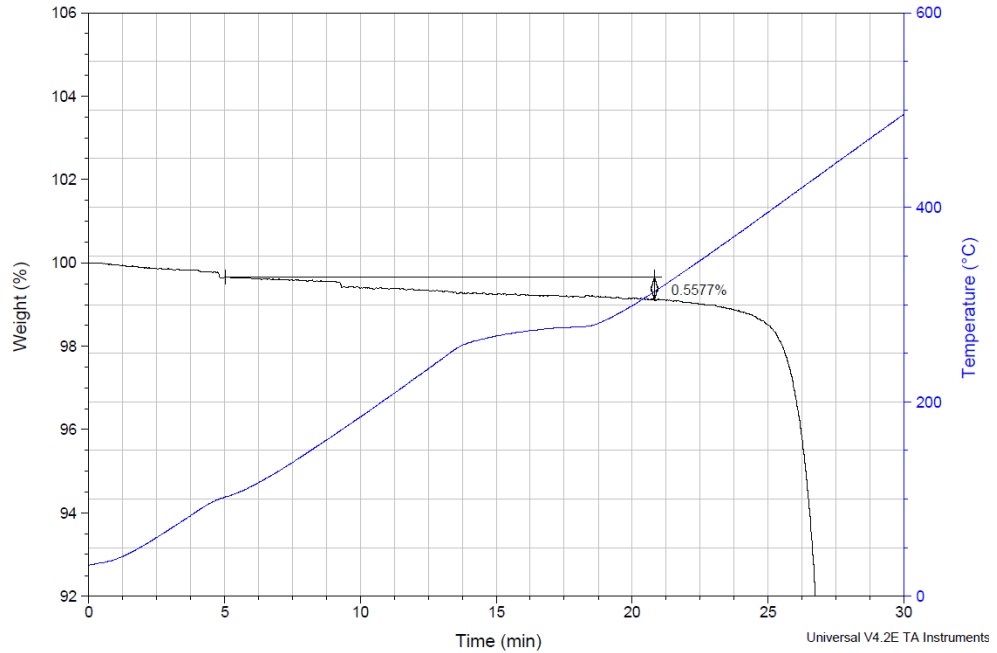
File: E:\...TGA\Casey\2 Feb2012\LLDPE-T-0.5-2
Operator: CDean
Run Date: 01-Feb-2012 12:57
Instrument: 2950 TGA V5.4A



Sample: LLDPE-T-0.5-Dip-2
Size: 4.7990 mg
Method: Casey TGA
Comment: LLDPE-T-0.5-Dip-2

TGA

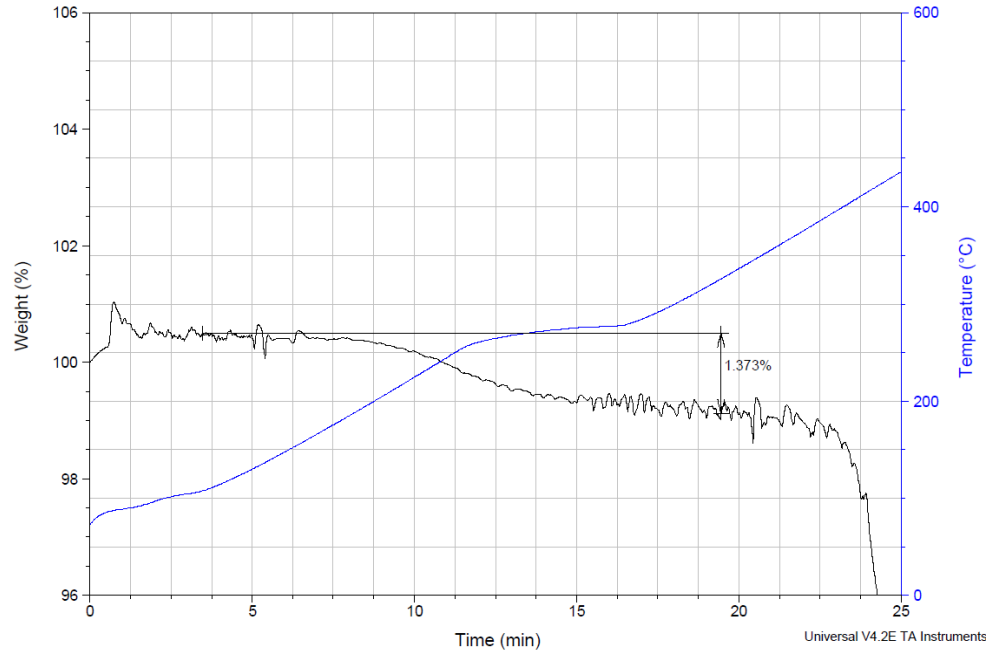
File: E:\...Casey\2 Feb2012\LLDPE-T-0.5-Dip-2
Operator: CDean
Run Date: 02-Feb-2012 10:54
Instrument: 2950 TGA V5.4A



Sample: LLDPE-T-1.5-3
Size: 4.3750 mg
Method: Casey TGA
Comment: LLDPE-T-1.5-3

TGA

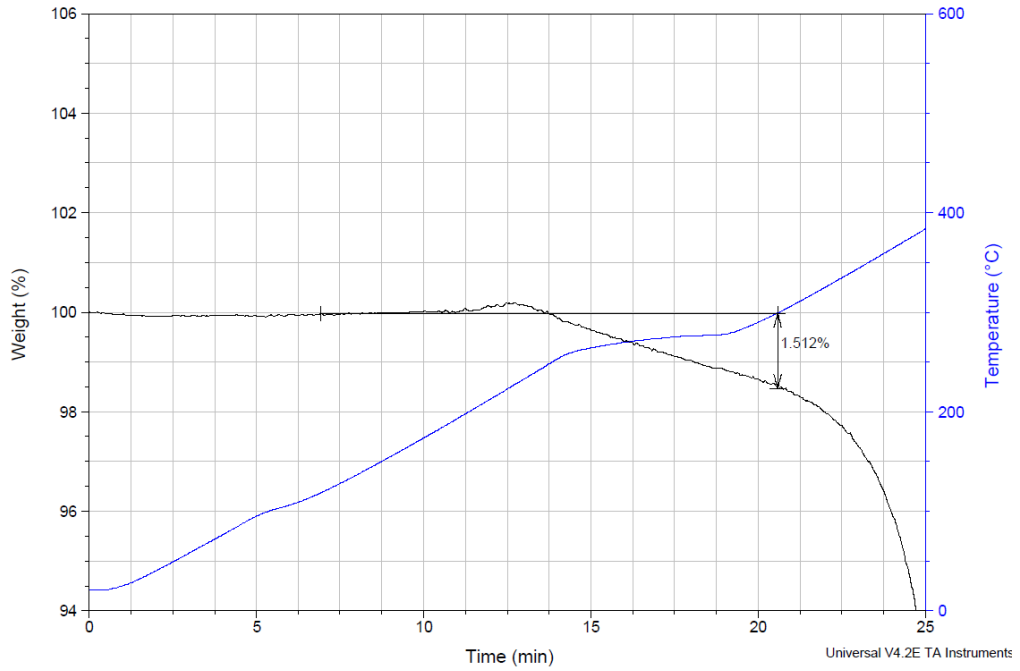
File: E:\...TGA\Casey\2 Feb2012\LLDPE-T-1.5-3
Operator: CDean
Run Date: 02-Feb-2012 14:25
Instrument: 2950 TGA V5.4A



Sample: LLDPE-T-1.5-Dip-1
Size: 4.3830 mg
Method: Casey TGA
Comment: LLDPE-T-1.5-Dip-1

TGA

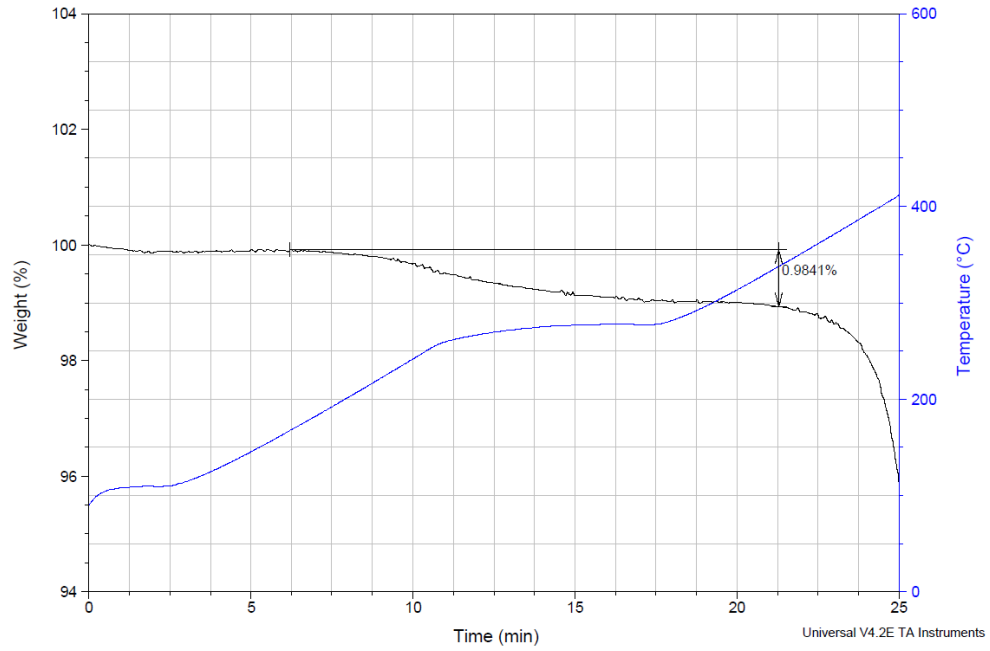
File: E:\...Casey\2 Feb2012\LLDPE-T-1.5-Dip-1
Operator: CDean
Run Date: 03-Feb-2012 08:39
Instrument: 2950 TGA V5.4A



Sample: LLDPE-T-2.5-1
Size: 4.2520 mg
Method: Casey TGA
Comment: LLDPE-T-2.5-1

TGA

File: E:\...TGA\Casey\2 Feb2012\LLDPE-T-2.5-1
Operator: CDean
Run Date: 03-Feb-2012 11:08
Instrument: 2950 TGA V5.4A



Sample: LLDPE-T-2.5-3
Size: 4.4740 mg
Method: Casey TGA
Comment: LLDPE-T-2.5-3

TGA

File: E:\...TGA\Casey\2 Feb2012\LLDPE-T-2.5-3
Operator: CDean
Run Date: 03-Feb-2012 12:39
Instrument: 2950 TGA V5.4A

